

ELECTIVE IRRADIATION OF THE NECK:

A three-dimensional CT definition
of the target for conformal radiotherapy

ELECTIEVE BESTRALING VAN DE HALS:

Een drie-dimensionale CT definitie
van het doelvolumen voor conformatie-radiotherapie

PROEFSCHRIFT

ter verkrijging van de graad van doctor
aan de Erasmus Universiteit Rotterdam
op gezag van de rector magnificus

Prof. Dr P.W.C. Akkermans M.A.

en volgens besluit van het College voor Promoties.
De openbare verdediging zal plaatsvinden op

woensdag 3 december 1997, om 15.45 uur

door

Peter Johannes Catharina Martinus Nowak

geboren te Sittard

PROMOTIECOMMISSIE

Promotoren: Prof. Drs C.F. van der Klauw
Prof. Dr P.C. Levendag

Overige Leden: Prof. Dr P. van den Broek
Prof. Dr C.D.A. Verwoerd
Prof. Dr J. Voogd

This thesis was financially supported by:

Scanditronix Medical AB

Siemens

Sinmed

Varian-Dosetek

Wigant Media

Design:

Joe Hoey, Studio Xtension

Printed by:

Karstens drukkers/designers

CONTENTS

Contents

1	Introduction	9
2	The clinically negative neck – scope of the problem	13
2.1	Clinical aspects	15
2.2	Diagnostic aspects	16
2.3	Clinical management – general aspects	17
2.4	Clinical management – radiotherapeutic aspects	18
2.4.1	<i>Target definition</i>	18
2.4.2	<i>Dose-response</i>	18
2.4.3	<i>Side effects</i>	20
2.4.4	<i>Treatment techniques – conformal radiotherapy</i>	21
2.4.5	<i>Quality assurance</i>	25
2.4.6	<i>Summary</i>	27
3	Elective neck irradiation – conventional techniques	29
3.1	Introduction	31
3.2	Conventional portals in elective neck irradiation	31
4	Three-dimensional CT target definition	35
4.1	Introduction	37
4.2	Target definition – procedures and results	37
4.2.1	<i>Anatomical studies</i>	37
4.2.2	<i>Surgical definition – levels</i>	38
4.2.3	<i>Target borders on anatomical slices</i>	39
4.2.4	<i>Target borders on CT slices</i>	39
4.2.5	<i>Radiotherapy definition – regions</i>	39
4.3	Verification of the three-dimensional target definition	50
5	Elective neck irradiation – conformal techniques	53
5.1	General	55
5.1.1	<i>Beam intensity modifiers</i>	55
5.1.2	<i>Margins</i>	55
5.1.3	<i>Comparison of treatment plans</i>	56
5.2	Three-dimensional treatment planning of the elective neck	57
5.2.1	<i>Contouring</i>	57
5.2.2	<i>Treatment techniques</i>	57
5.2.3	<i>Dose distributions</i>	59

6	Visual justification	65
6.1	CD-i introduction	67
6.2	Content and design of the CD-i	68
6.2.1	<i>Menu</i>	68
6.2.2	<i>Definition target</i>	70
6.2.3	<i>Magnified target</i>	74
6.2.4	<i>Beam's eye view</i>	75
6.2.5	<i>Radiation therapy</i>	76

References	81
-------------------	-----------

Addendum A	87
-------------------	-----------

Addendum B	103
-------------------	------------

Addendum C	117
-------------------	------------

Addendum D	129
-------------------	------------

Abbreviations	139
----------------------	------------

Summary – Samenvatting	143
-------------------------------	------------

Acknowledgments	149
------------------------	------------

Curriculum Vitae	153
-------------------------	------------

CHAPTER 1

INTRODUCTION

1 Introduction

When no lymph node metastases are detected clinically in patients with head and neck cancer, the neck is staged as N0 (42). The elective treatment of the N0 neck, by either surgery or radiotherapy, results in excellent local control rates (2,4, 7,29). This thesis specifically deals with the use of radiotherapy as a single modality treatment for the clinically negative neck. Given the risk of radiation-induced side effects, elective neck irradiation is advocated in many institutions only if the probability of subclinical disease is considered to be more than 10-20% (31). The major side effects of the elective irradiation of the neck are the dry mouth syndrome (xerostomia) and dental caries due to damage to the major and minor salivary glands.

A major advance in radiotherapy in the last decade has been the development and clinical implementation of conformal radiotherapy. With the introduction of three-dimensional CT-based radiotherapy planning systems, it has become feasible to conform the high dose region to the target volume. In case of elective neck irradiation for example, high doses of radiation can be delivered to the neck with sparing of the salivary glands and other normal tissues such as the spinal cord. The main objective of this thesis is to provide a three-dimensional CT definition of the target of the N0 neck which will indeed allow the design of conformal radiotherapy techniques for elective neck irradiation. It is defined and presented in such a way that it can be studied and verified interactively on CD-i.

The second goal of this thesis is the development of conformal radiotherapy treatment plans and subsequently, to demonstrate the potential for reducing the side effects of elective neck irradiation by using such conformal techniques. The coverage of the three-dimensional N0 neck target and the amount of sparing of the parotid (and submandibular) salivary glands can subsequently be studied interactively with a CD-i, using all CT-, MRI- and anatomical slices obtained from a human cadaver.

In Chapter 2, clinical aspects relevant to the treatment of the N0 neck are summarized. In addition, the basic radiobiological postulates pertinent to the subject of subclinical disease and also the rationale and treatment principles of conformal radiotherapy are discussed in detail.

In Chapter 3, the outcome of a nationwide survey in The Netherlands on the elective neck target volume is reported. Treatment fields for the N0 neck were planned, using conventional techniques according to institutional preferences, for tumors located in the mobile tongue and supraglottic larynx by a number of Dutch radiation oncologists. The results highlight the need for better guidelines on the definition of neck nodal regions.

In Chapter 4, detailed proposals for a CT definition of the three-dimensional neck target are presented; this data and the way they were obtained were incorporated into the CD-i.

Subsequently, in Chapter 5, three-dimensional treatment planning aspects regarding conformal radiotherapy of the N0 neck are presented. Dose distributions of conventional and three-dimensional conformal treatment plans are shown and compared interactively on CD-i.

Chapter 6 describes how the data which was presented in Chapters 4 and 5 were implemented on CD-i. The purpose of making available the thesis data on CD-i was to provide the tools for the study of the three-dimensional CT target definition of the neck in a user-friendly self-assessment program, in an interactive manner. In addition the tools were provided for the reproduction of the three-dimensional CT target definition, to verify the definition given in Chapter 4.

The work for this thesis is part of an on-going project at the Daniel den Hoed Cancer Center in Rotterdam involving the development of conformal radiotherapy techniques on a MM50 Racetrack Microtron. The dual gantry MM50 Racetrack Microtron, which has been in operation in our institution since March 1994, is a fully computer-controlled treatment unit and is eminently suited for advanced conformal radiotherapy techniques. Photon beams can be produced between 10 to 50 MV, in steps of 5 MV. Electron beams are available from 7.5 to 50 MeV with a step size of 2.5 MeV. The system is equipped with double focused multileaf collimators. For both electron and photon beams, flat beam profiles are created by scanning of elementary beams according to fixed scanning patterns. Due to the beam scanning, flattening filters for photon beams can be omitted (or limited to very thin filters), yielding extremely flat beam profiles at all depths. For electron beams, the applied scattering foils are very thin. The combination of beam scanning, thin scattering foils and the presence of helium in the treatment head enables the use of high energy electron beams in isocentric irradiation techniques, with the multileaf collimator acting as a beam shaping device. Intensity modulated beams can be generated by computer-controlled superposition of multileaf collimator-defined fields, by the scanning of elementary beams according to individualized scanning patterns, and by dynamic multileaf collimation.

CHAPTER 2

THE CLINICALLY NEGATIVE NECK

—

SCOPE OF THE PROBLEM

2 The clinically negative neck – scope of the problem

2.1 Clinical aspects

Curability of patients with tumors in the head and neck is dependent on factors such as patient characteristics, tumor biology and the specifics of the treatment technique. In patients with head and neck cancer, the development of lymph node metastases in the neck (and thus the presence of subclinical disease) has proven to be an extremely important prognostic parameter for predicting loco-regional failure and/or development of distant metastases (11,38,40,46). The risks for subclinical disease in a clinically negative neck can be derived from the reported incidence of pathologically positive nodes found after elective neck dissection for particular tumor sites (and stages) and/or estimated from the conversion rate of a untreated clinically negative neck into a positive neck, that is, a neck with metastatic deposits in the regional lymph nodes (see Table 2-1).

Table 2-1. Incidence of lymph node metastases in a clinically negative neck with no neck treatment (after Mendenhall et al.) (29).

Site	Conversion Rate [%]
Floor of Mouth	20-35
Gingiva	17
Hard Palate	22
Buccal Mucosa	16
Oral Tongue	38-52
Nasopharynx	19-50
Retromolar Trigone	10-15
Soft Palate	16-25
Tonsillar Fossa	22
Supraglottic Larynx	33

A high risk for lymph nodal involvement has been found to be associated with histology (e.g. undifferentiated squamous cell carcinoma) and size (e.g. advanced T-stage) of the primary tumor (26). The relative density of capillary lymphatics at the site of the primary tumor site also plays an important role in the potential for dissemination of the cancer cells to the regional lymph nodes. For example, the nasopharynx and piriform sinus have the most profound capillary lymphatic networks in contrast to the middle ear, paranasal sinuses and vocal cords which have very few capillary lymphatics. This is in agreement with the high- and low incidence, respectively, of lymph node metastases found at presentation when the primary tumor is confined to these tumor sites (29). Finally, pathological examination of neck dissection specimen has shown an orderly and predictable progression of lymph nodal involvement (39). The neck nodes are usually divided into the submental nodes, the submandibular nodes, the junctional nodes, the subdigastric nodes, the middle- and lower jugular nodes, and the posterior neck nodes; or, as is most frequently the case in the surgical literature, into levels I-VI (see Figure 2-1) (37).

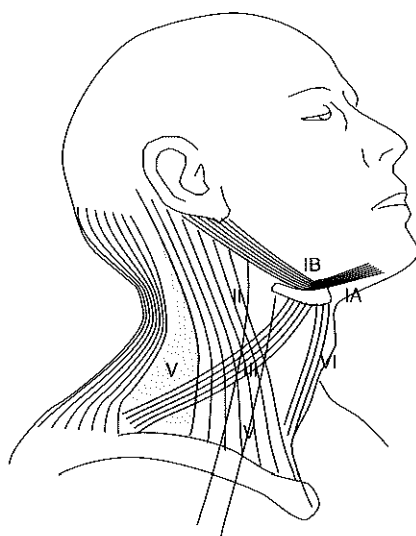


Figure 2-1. Lymph node levels in the neck after Shah et al. (37).

2.2 Diagnostic aspects

The detection of lymph node metastases in the neck is crucial for the appropriate management of the disease. There are several ways to examine the neck; clinical palpation, CT scanning, magnetic resonance imaging (MRI), ultrasound (US) and ultrasound fine needle aspiration cytology (USFNAC). Although not completely reliable, because of its simplicity palpation is still an important and certainly the most used diagnostic procedure. In recent years, the combination of US and fine needle aspiration cytological examination of suspected lymph nodes has dramatically improved the assessment of lymph node metastases in the neck. For example, in Table 2-2, the accuracy, sensitivity and specificity for the different diagnostic means as reported by van den Brekel et al., is presented (45). Micrometastases may, however, still be missed because of sampling errors. For instance, Brennan et al. identified, using molecular analysis techniques for p53 mutations, tumor cells in 6 out of 28 lymph nodes that were initially found to be negative by pathological examination (6).

Table 2-2. Accuracy of diagnostic procedures in staging of the neck.

Method	Accuracy [%]	Sensitivity [%]	Specificity [%]
USFNC	93	90	100
MRI	82	82	81
CT	78	83	70
US	75	75	75
Palpation	69	67	73

2.3 Clinical management – general aspects

Controversy still exists with regards to the optimal treatment of the clinically negative neck. An important aspect of elective neck treatment is the small (or non-existing) tumor-load present at the time the treatment, and thus, a high regional control rate can be expected from either surgery or radiotherapy. This has indeed been substantiated by many publications, where well over 90% regional control rates have been reported for the two modalities (2,4,7,29). Patients without lymph node metastases are treated unnecessarily. This is of particular relevance since both surgery and radiotherapy are not without side effects. On the other hand, if neck nodes show up after a wait and see policy, only about 60% (somewhat depending on the primary tumor site) will be controlled by a subsequent therapeutic neck dissection. In other words, not all patients are salvaged after a policy of watchful waiting (24). Moreover, it has been argued that failure to treat the neck electively may lead to an increased risk for dissemination to distant sites (21,29). Other disadvantages of a wait and see policy are the need for a more extensive follow up and the psychological uncertainty about the ultimate outcome for patients, and also their doctors.

Table 2-3. Relation between types of neck dissection (ND) and the removal (yes or no) of the submandibular gland(s) for different head and neck tumor sites.

Type of neck dissection	Resection of the submandibular gland(s)	
	Larynx	All other sites
Functional ND	no	yes
Radical ND	yes	yes
Supra-omohyoida! ND	no	yes
Selective ND	no	yes / no
Anterior ND	no	no

The choice whether to irradiate the neck electively or to perform an elective neck dissection is also dependent on a number of factors. Next to subjective arguments such as institutional (doctors) preferences, the decision depends also on the treatment modality used for the primary cancer. For reviews on the matter the reader is referred to Nahum et al. and to Baatenburg de Jong et al. (1,33). Elective neck dissection almost always constitutes resection of one or both submandibular glands (see Table 2-3). This will result in a significant decrease in salivary flow rate, with approximately one third of the patients developing xerostomia, particularly at nights and dental carious lesions (20). Despite the drawbacks, radiotherapy still plays an important role in the clinical management of the N0 neck and is usually recommended if the estimated risk of neck disease exceeds 10-20%. The aim of this thesis is to improve on the radiotherapy techniques used for elective neck irradiation, i.e. to decrease the associated normal tissue toxicity, in particular with regard to the problem of xerostomia. Moreover, by reducing the associated morbidity neck irra-

diation, being non-invasive, will continue to remain one of the mainstays in the elective neck treatment armament.

2.4 Clinical management – radiotherapeutic aspects

2.4.1 Target definition

In the treatment of cancers of the head and neck by ionizing radiation, one aims for loco-regional control of the disease with minimal damage to the surrounding normal tissues. In order to achieve an optimal result a precise definition of the target volume is mandatory. In this thesis, the ICRU-50 recommendations for the target definition are adopted (19). These are summarized in Figure 2-2.

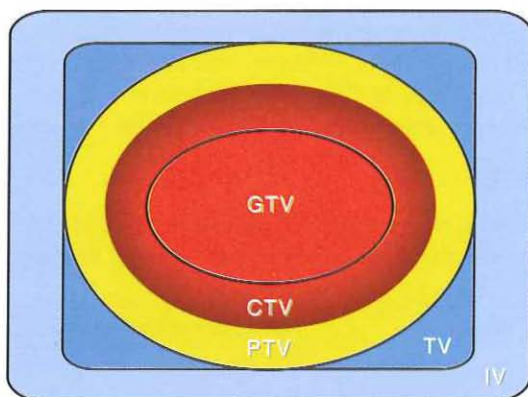


Figure 2-2. Definition of the target volumes according to the ICRU-50 guidelines. (19) GTV: gross tumor volume, CTV: clinical target volume, PTV: planning target volume, TV: treated volume, IV: irradiated volume.

The gross tumor volume (GTV) denotes the visible or palpable tumor. The clinical target volume (CTV) stands for the GTV and an estimated margin for subclinical spread of the disease. The volume of the neck considered to be at risk for subclinical disease is also called CTV. The planning target volume (PTV) is a geometrical concept and consists of the CTV and a margin to account for (daily) variations of the CTV in size, shape, and position relative to the treatment beam(s). The PTV may even extend outside the body of a patient. The treated volume is the volume that receives a radiation dose that is considered important for loco-regional control or cure. The irradiated volume is the volume that receives a dose which is considered important in relation to normal tissue tolerance.

2.4.2 Dose-response

Radiobiological data indicates that radiation cell kill is basically exponential; i.e. a given dose results in the kill of a proportion of tumor cells. Of particular relevance are the surviving tumor cells which are capable of regenerating the tumor, i.e. clono-

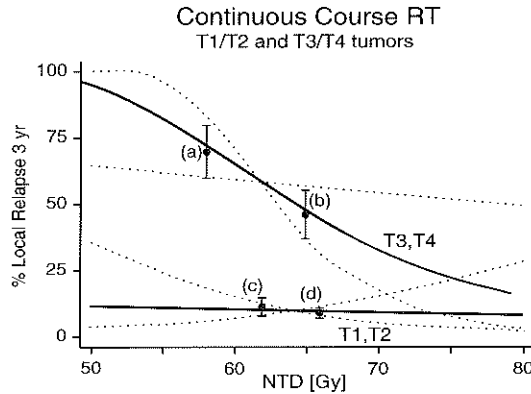


Figure 2-3. Dose-response relationship in head and neck tumors treated by radiotherapy only using a continuous course technique. Figure 2-3 was taken from original publication (see also Addendum A, this thesis)

genic cells. For a given tumor size, the probability of eradicating all clonogenic cells increases with higher doses (so-called dose-response curve). Many reports highlight the existence of these dose-response relationships (35,41). For example, a retrospective study of 1493 head and neck cancer patients was performed to test this radiobiological postulate at the Daniel den Hoed Cancer Center / University Hospital Rotterdam (DHCC/UHR). Primary squamous cell carcinomas of the head and neck which were irradiated to a dose of at least 50 Gy, were analyzed. In Figures 2-3 and 2-4 the probability of local relapse at 3 years is shown as a function of normalized treatment dose (NTD) for T1/T2 versus T3/T4 tumor stages, treated by continuous course radiotherapy (CC-RT; Figure 2-3) or split course radiotherapy (SC-RT; Figure 2-4), respectively. With the exceptions of a small subset of T1/T2 CC-RT patients, the data summarized by both figures indeed generate evidence for the

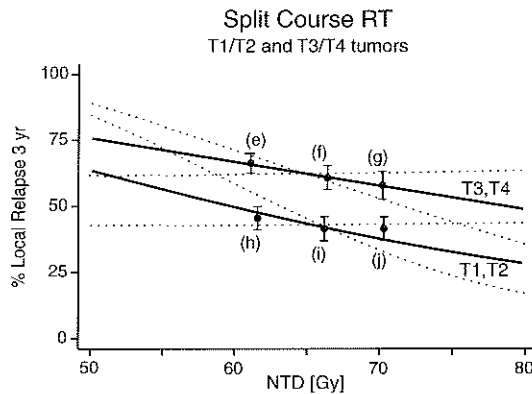


Figure 2-4. Dose-response relationship in head and neck tumors treated by radiotherapy only using a split course technique. Figure 2-4 was taken from original publication (see also Addendum A, this thesis)

existence of a dose-response relationship in gross disease. A more detailed analysis of the results is given in the paper as reported in Addendum A.

Table 2-4. Control rates for subclinical disease in the neck (13,25,30).

Dose / Treatment Duration	Regional Control Rates
30 Gy / 3 weeks	70 %
40 Gy / 4 weeks	80-90 %
45-50 Gy / 5 weeks	95 %

As mentioned previously, the diagnostic procedures to detect lymph node metastases in the neck are far from being accurate. Moreover, even the pathological examination of neck dissection specimens can miss lymph node metastases. Consequently, the tumor-load of patients with occult neck disease may be more than "microscopic". Nevertheless, the maximum number of clonogenic cells and, consequently, the dose needed to obtain regional control, will certainly be less than in case of a gross tumor volume (e.g. the primary tumor). In 1971, Berger et al. proposed a dose of 45-50 Gy in to be delivered in 5 weeks for effective elective irradiation of (parts of) the neck (4). In many institutions, this is still the recommended dose range for elective neck irradiation. In fact, as is the case for gross disease, a sigmoidal dose response curve for subclinical disease in the neck is apparent from data in the literature. Table 2-4 indicates the approximate regional control rates for elective neck irradiation as a function of dose.

2.4.3 Side effects

The side effects of the irradiation of healthy tissues can be divided into two categories: acute and late injuries. Generally there is no correlation between these two types of injuries, and the severity of the acute reactions does not necessarily predict for the severity of the late sequelae.

In head and neck cancer, acute effects mostly result from damage to the skin and mucous membranes, and are usually of a temporary nature. Depending on treatment techniques (e.g. dose to the skin, field size, overall treatment time) and patient factors (e.g. site, degree of pigmentation of the skin), the skin reactions range from erythema, dry desquamation to moist desquamation. Healing is almost always complete within 2-4 weeks after treatment. The mucosal side effects manifest 1 week after start of the treatment with erythema. Mucositis is present at the end of the second week and is accompanied by a sore throat which is usually most severe 2½ to 3 weeks after the start of the treatment. The mucous membranes normally heal 2½ to 3 weeks following radiotherapy. The loss of taste generally begins in the second week of a course of radiotherapy, and rapidly progresses after 20 Gy. Taste acuity will recover to a large extent after the end of radiotherapy, and recovery is usually complete between 60 to 120 days post treatment. However, a subjective loss of taste with little or no tendency for improvement is sometimes reported by patients. The latter is believed to be at least partially due to xerostomia.

Xerostomia is a late side effect which causes severe discomfort to the patients because of the dry mouth per se and because of a difficulty in swallowing. The reduction in salivary flow also decreases taste acuity and contributes to dental decay. Salivary gland dysfunction has its onset during the course of radiotherapy and is usually permanent and complete after doses of more than 40 Gy have been applied. Since the reduction of this extremely troublesome clinical problem is pertinent to the goal of this thesis, a few relevant reports of the literature on this subject are discussed in more detail. For example, Leslie and Dische reported a volume response and a dose response relationship in the changes of the parotid flow during the first months after the end of the treatment (23). Doses exceeding 40 Gy produced a complete loss of salivary flow. In contrast, if 50% or less of the parotid glands were included in the irradiated high dose volume, the loss of flow rate 8 weeks after the end of radiotherapy was less than 50% of the pre-treatment flow rate. Mira et al. showed that doses of 30 to 40 Gy to all salivary gland tissue were capable of inducing minimal flow rates with no recovery seen at 1 to 17 months after treatment (32). In the first 12 months post treatment, Makkonen et al. observed partial recovery of salivary flow rates after doses of 31 to 46 Gy to the salivary glands (27). However, the authors noted that in their cases, the upper (cranial) parts of the parotid glands were usually found to be outside the radiation portals. Many authors have claimed that the parotid glands are responsible for most of the saliva production. Ferguson showed that this is particularly true for the stimulated salivary gland flow (12). During sleep and in rest, however, it is believed that the submandibular glands contribute most to the total flow produced by the salivary glands (20). In fact, it is not uncommon for patients to wake up at night because of a severe dry mouth. Therefore, special attention is given in this thesis to the geographical position of both the parotid- and the submandibular glands in relation to the irradiated volume.

Finally, high-dose irradiation to gross disease can produce late sequelae like subcutaneous fibrosis, fibrosis of muscles and even ulceration or necrosis of soft tissues and bone. Other critical structures, that can be injured by high dose irradiation are the thyroid gland, ear, spinal cord, brain, cranial nerves (including the visual pathways) and pituitary gland. However, as the doses used in elective irradiation of the neck typically vary between 40 to 50 Gy, i.e. well below the tolerance levels of many of these tissues, a detailed account of all such side effects is beyond the scope of this thesis. This thesis will highlight the late sequelae due to the irradiation of the major salivary glands.

2.4.4 Treatment techniques - conformal radiotherapy

The most commonly used technique in head and neck cancer utilizes parallel opposed portals, with or without an abutted low anterior portal. This can have major disadvantages, regarding side effects (e.g. xerostomia, see Chapter 2.4.3) and target coverage. With respect to target coverage (that is too low a dose to the target - see also Chapter 2.4.2), major emphasis is given at present to three-dimensional conformal radiotherapy techniques. With the development of sophisticated multiple beam treatment plans, the three-dimensional target can be adequately treated to high doses of irradiation whilst minimizing the dose to normal tissues.

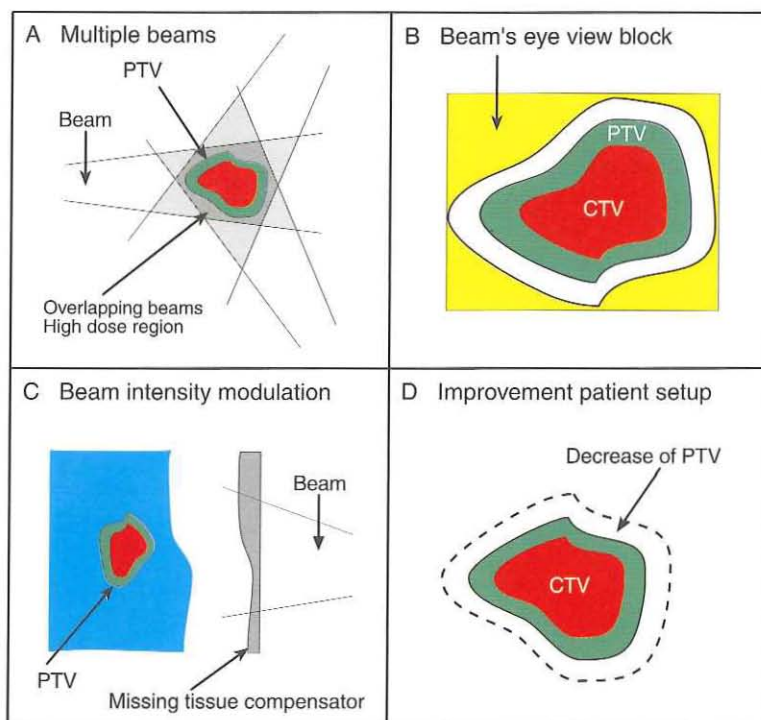


Figure 2-5. Basic principles of conformal radiotherapy. A: multiple non-opposing fields, B: beam's eye view-blocks (multileaf collimator) , C: beam intensity modulation (e.g. dynamic multileaf collimator, missing tissue compensator), D: minimizing patients setup errors. See text for explanation.

The current literature on conformal radiotherapy focuses mainly on the use of sophisticated conformal radiotherapy treatment techniques for the primary (gross) tumor volume, i.e. for relatively limited target volumes. In the majority of patients, however, it is not desirable (or even feasible) to irradiate the primary tumor and neck as separate entities. Therefore, the premise for developing a sophisticated elective neck irradiation technique in order to spare critical structures such as (part of) the major salivary glands, implies that a conformal treatment technique (portals) should adequately cover the primary (gross) tumor volume as well, and vice versa. The intricate relationship between the primary cancer and the neck is an obvious limitation for treatment techniques, in particular those which are conventional techniques. However, with conformal radiotherapy techniques a number of improvements can be anticipated in this regard (see also Chapter 5).

In conformal radiotherapy, a treatment plan is designed using a three-dimensional target defined on CT slices. For elective neck irradiation, the contours of the primary tumor as well as of the node negative neck (CTV) have to be delineated on every CT slice. In order to conform the high dose radiation area to the three-dimensional target volume with optimal sparing of the normal tissues, some basic principles of conformal radiotherapy are important.

Firstly, radiation fields produce a high dose in the overlapping field region. The use of multiple non-opposing, non co-planar portals smears out the dose outside the PTV sparing the normal tissues, as schematically illustrated in Figure 2-5A.

Next, beam's eye view graphics and use of customized blocks or a multileaf collimator make it feasible to choose and shape portals such that the irradiation of critical normal structures can be avoided (Figure 2-5B).

Thirdly, it is also possible to change the beam intensity profile with so called beam intensity modifiers (Figure 2-5C; see also Chapter 5). This may allow to choose beams that avoid critical structures, and still be able to cover the target homogeneously.

Finally, by the obligatory need for accurate treatment setup techniques and by limiting the day-to-day variations in patient positioning, margins around the CTV can be decreased. The resulting smaller PTV allows for the use of smaller fields (Figure 2-5D).

An example of the potential benefits of conformal radiotherapy in primary head and neck cancers, is seen in the findings of a failure analysis performed on 109 patients with squamous cell carcinoma of the piriform sinus (PS), who were treated between 1973-1984 in the DHCC/UHR (see also Addendum B). The incentive for the failure analysis per se was the apparent poor results obtained in PS cancer treated by radiotherapy only, i.e. a 5-year loco-regional relapse free survival of only 40% was observed. However, when a PS cancer treatment plan using conventional radiotherapy techniques (Figure 2-6) was compared with a plan of the same tumor mass treated by conformal radiotherapy using beam intensity modifiers (Figure 2-7), at least three findings are obvious. Firstly, with the conventional parallel-opposed

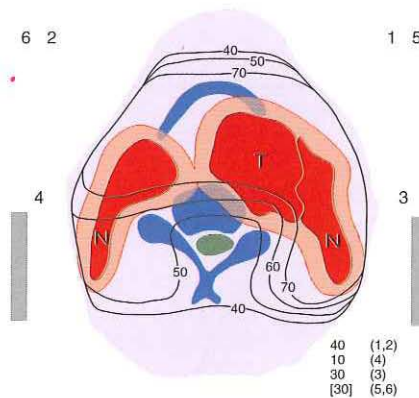


Figure 2-6. Conventional technique (as used in study period 1973-1984): The target volume is irradiated by two parallel opposed wedged fields, using 4 MV photons (fields 1 and 2); the lower neck (nodes) by an abutted anterior photon portal (not depicted in the diagram). The posterior part of the piriform sinus lies in close proximity to the vertebra/cord. After a dose of 40 Gy, the spinal cord is shielded and the primary tumor is taken to 70 Gy (fields 5 and 6). An ipsilateral low energy electron field (10 MeV) is added to the parallel opposed (blocked) photon fields to boost the posterior part of the primary tumor to a dose of 70 Gy (field 3); in a number of patients the posterior contralateral neck was carried (electively) to a cumulative dose of 50 Gy (field 4). Figure 2-6 was taken from original publication (see also Addendum B, this thesis).

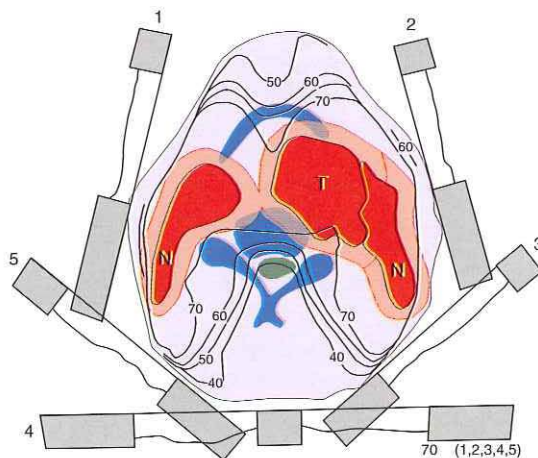


Figure 2-7. Example of stage I/II piriform sinus cancer using three-dimensional conformal radiotherapy technique (future technique). Same tumor as depicted in Figure 2-6 was hypothetically irradiated by a 5-field technique using beam intensity modifiers. As is demonstrated in this schematic diagram, the target volume (primary tumor) can be easily taken to a cumulative dose of 70 Gy without overdosing the normal tissues. Figure 2-7 was taken from original publication (see also Addendum B, this thesis).

treatment techniques used at the time of the study period, some parts of the primary tumor mass were underdosed. Secondly, dose escalation would have been difficult without significantly exceeding the tolerance of the cord. Finally, xerostomia was inevitable with the conventional technique because of the high doses delivered to large parts of the parotid glands.

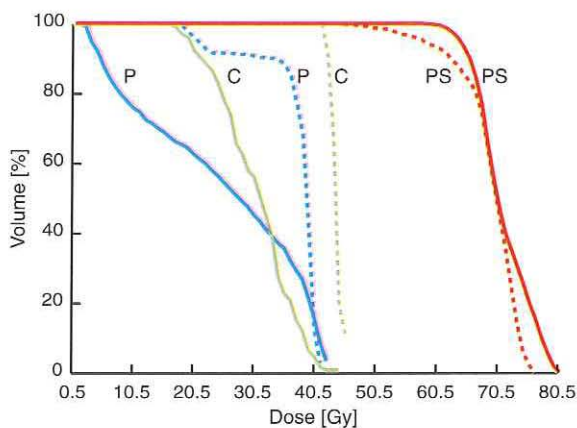


Figure 2-8. Dose volume histograms for primary piriform sinus (PS) cancer, parotid gland (P) and cord (C), comparing conventional treatment technique dotted lines; see Figure 2-6) and conformal radiotherapy using a 5-field technique with beam intensity modifiers (solid lines; see Figure 2-7). Figure 2-8 was taken from original publication (see also Addendum B, this thesis).

In summary, the authors proposed that by using a multiple beam arrangement with beam intensity modifiers, increased loco-regional control rates could be achieved with reduced morbidity due to the sparing of the parotid glands (Figure 2-8). A full account of the study is given in Addendum B.

2.4.5 Quality assurance

Conformal radiotherapy requires highly accurate techniques, both in the preparation phase and during the course of treatment. In general, errors that occur in the preparation phase will lead to systematic errors during the treatment, whereas errors originating during the treatment can both be systematic and/or random. Treatment setup errors may occur in the preparation phase or during a course of radiotherapy. With the use of tighter margins and beam intensity modifiers in conformal radiotherapy an error in beam positioning during treatment preparation can influence treatment outcome significantly.

In order to evaluate the impact of such errors, the simulation accuracy for maxillary sinus tumors has been studied in the DHCC/UHR. Five patients were planned as if they were to be treated for a maxillary sinus tumor. A three beam CT scan-based computer calculation was performed for each patient. The position of the central beam axis of each beam, relative to bony anatomical landmarks, was measured. Patients were then simulated using the bony references to position the radiation beams. Subsequently, the simulation procedure was repeated with the use of a noninvasive external localization frame, with a known accuracy and reproducibility of < 2 mm (34). When defining the clinical target volume as the tumor with a 1 cm margin, three of the five patients would have suffered a geographical miss throughout the entire radiation treatment course due to erroneous beam positioning at the simulation stage (Table 2-5).

Table 2-5. Beam positioning errors expressed in mm at the time of simulation of a maxillary sinus tumor, detected by a noninvasive external localization frame. CC: cranio-caudal, AP: antero-posterior, SD: standard deviation. Table 2-5 was taken from original publication (see also Addendum C, this thesis).

	Left Beam		Right Beam		Anterior Beam	
	CC	AP	CC	AP	CC	LL
Patient 1	-8	7	-8	16	-8	3
Patient 2	-10	6	-10	-8	-10	10
Patient 3	14	3	14	0	14	11
Patient 4	-10	5	-10	-2	-10	0
Patient 5	13	-5	3	3	13	6
Mean (1-5)	-0.2	3.2	-0.2	1.8	-0.2	6
SD (1-5)	11.2	4.3	11.2	8.0	11.2	4.1

With regards to the normal tissues, the contra-lateral eye lens would have been irradiated to a considerable dose (expressed in a large normal tissue complication

probability (NTCP) value) in the two patients with the largest beam positioning errors. In contrast, the right eye lens (which would have received a full dose when irradiating according to the computer plan) was found to receive doses well below its tolerance level in the patients with the largest beam positioning errors (Table 2-6).

Table 2-6. Tumor control probability (TCP)- and normal tissue complication probability (NTCP) values for patients with maxillary sinus tumors when simulated and treated according to treatment plan (Intended plan: using the noninvasive external localization frame) or with simulation errors (Patient 1-5: simulating by anatomical landmarks). Table 2-6 was taken from original publication (see also Addendum C, this thesis).

	TCP [%]	NTCP [%]		
		ipsilateral eye lens	contralateral eye lens	spinal cord
Intended plan	77.6	100.0	7.2	0.0
Patient 1	41.3	61.8	0.7	0.0
Patient 2	22.5	1.6	0.2	0.1
Patient 3	8.8	100.0	99.7	1.3
Patient 4	47.2	7.0	0.1	0.0
Patient 5	15.9	100.0	96.6	0.4
Mean (1-5)	27.1			

These data clearly demonstrate that beam positioning errors during simulation are of particular clinical relevance and should be taken into serious consideration when defining a planning target volume if anatomical landmarks are to be used during simulation. The additional treatment margins needed for this reason have still to be decided upon and will probably vary according to tumor site, the treatment technique used, and whether or not correction protocols are implemented. A more detailed account of the study is given in the paper as reported in Addendum C.

Portal films can be made in order to evaluate the positioning errors during a radiotherapy course. In a prospective study in the DHCC/UHR using portal films on tumors in the head and neck, the standard deviation of random positioning errors appeared to be 3 mm (18). The introduction of fast on-line electronic portal imaging systems however, allows for improvement of patient set-up accuracy during the treatment course, minimizing both systematic and random positioning errors (8, 10,28,47,50). The major disadvantage of such procedures is the considerable increase in treatment time. Bel et al. described a verification procedure to correct systematic deviations of patient set-up at an early stage during treatment, yielding a high overall set-up accuracy with a minimal workload (3). Using this procedure, the systematic errors in patient set-up become small compared to the random positioning errors during a radiotherapy course. In summary, the need for an additional margin around the CTV to account for systematic errors can probably be eliminated with portal imaging using a verification procedure. Random day-to-day patient positioning errors during treatment are measured with portal imaging, to verify that an adequate margin around the CTV was used during treatment planning.

2.4.6 Summary

Chapter 2 describes the literature findings of elective treatment of the neck, in particular the treatment techniques and side effects of these treatments. From this review it is apparent that the use of conformal radiotherapy techniques might improve the therapeutic ratio. In order to implement conformal radiotherapy in elective neck irradiation one needs an adequate description of the three-dimensional target of the neck on CT. This data is as yet unavailable; see also Chapter 3.

CHAPTER 3

ELECTIVE NECK IRRADIATION

—

CONVENTIONAL TECHNIQUES

3 Elective neck irradiation - conventional techniques

3.1 Introduction

Standard treatment techniques have been used for elective neck irradiation over many years. For the conventional elective irradiation of both sides of the neck, two types of treatment techniques are in use. One consists of two lateral parallel opposed fields, and the other of lateral opposed fields with a matched anterior lower neck portal down to the clavicles. When using these techniques, the target (i.e. the node negative neck) is defined on simulation films. In defining the target, one (in principle) delineates the projection of a three-dimensional target on X-ray (simulation) films. Although the control rates after using such conventional techniques are reported to be excellent, these are achieved with side-effects, and in particular xerostomia (see also Chapter 2). Since these side effects are related to the (excessive) amount of normal tissues irradiated, the question then arises as to whether the two-dimensional demarcations on simulation films really conform to the projections of the three-dimensional target. In other words, is there a good two-dimensional target definition? To answer this question a study was performed to analyze the variations in applied treatment portals for elective neck irradiation in The Netherlands.

3.2 Conventional portals in elective neck irradiation

The variation among radiation oncologists in the choice of treatment portals for elective neck irradiation, and its consequences for the incidence of side effects, were analyzed by a nation-wide survey in The Netherlands. Two typical primary tumor sites were selected: a T2 mobile tongue carcinoma (MT), and a T3 cancer of the supraglottic larynx (SL), both without clinically detectable disease in the neck (N0). The patients were to be treated in supine position on a 6 MV linear accelerator to a total dose of 46 Gy in fractions of 2 Gy, 5 times per week. The demarcating borders of the portals correspond to the 50% isodose line. Copies of lateral and anterior simulation films of a single patient, who was previously treated in the DHCC/UHR, were sent to 16 radiation oncologists in 11 Radiation-Oncology departments in The Netherlands. On these films, the radiation oncologists were asked to delineate their "routine" portals for elective neck irradiation of both primary tumor sites. A CT scan for planning purposes of the patient was only available to us (slices were taken every 5 mm in treatment position, using a Siemens Somatom Plus scanner).

The delineated treatment portals were digitized in the DHCC/UHR and entered into the CADPLAN three-dimensional planning system (version 2.61, Varian Dosetek). The CT data were also transmitted to CADPLAN. For both primary tumor sites (MT & SL) the radiation oncologists were divided into 2 groups, one using lateral opposed fields only, the other using a combination of lateral opposed fields and an anterior field for the lower neck. The data were analyzed by superimposing all treatment portals (delineated by the radiation oncologists) on beam's eye view images of the patient, including the parotid- and submandibular glands. With

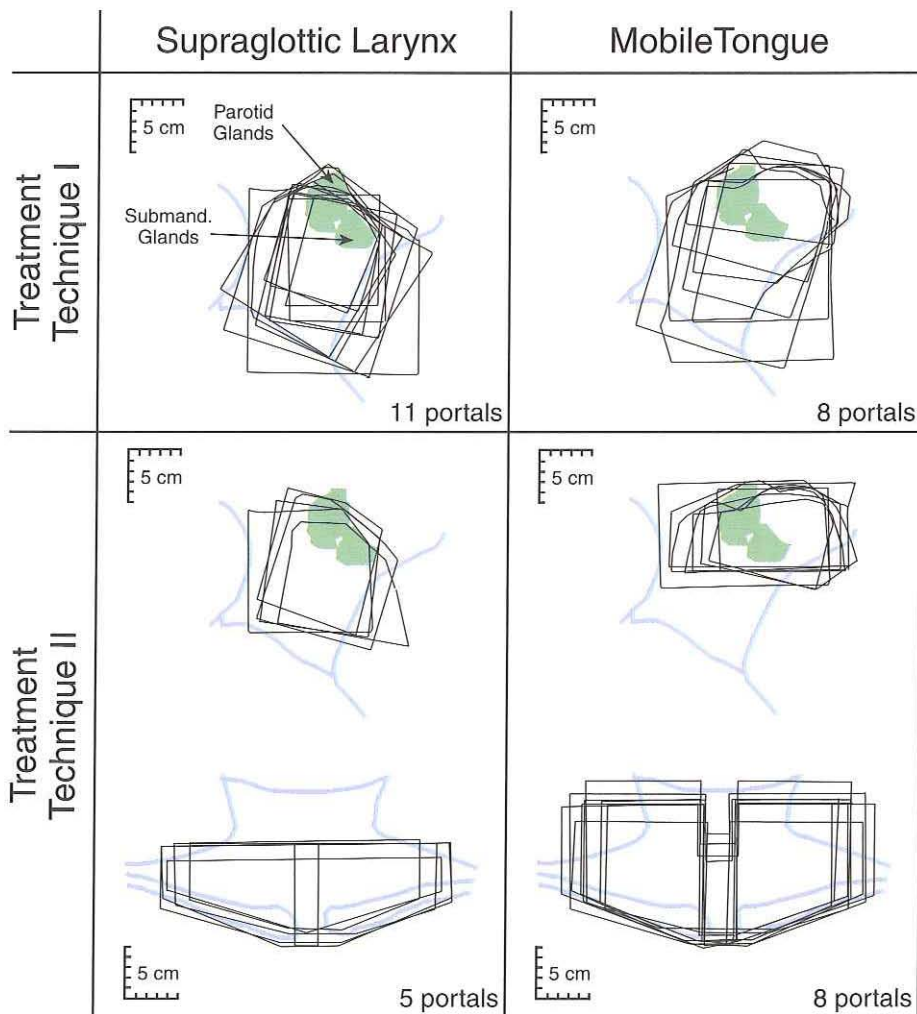


Figure 3-1. A nationwide survey on treatment portals: the delineated treatment portals for a T2N0 mobile tongue cancer and a T3N0 cancer of the supraglottic larynx of all participating radiation oncologists superimposed in beam's eye view on the patient anatomy, i.e. the patient outline and the submandibular- and parotid glands for the lateral portals and the patient outline and the clavicles for the anterior portals. Technique I: lateral parallel opposed portals only; Technique II: lateral parallel opposed portals in combination with an anterior portal. The scale (5 cm) relates to a distance of 100 cm from the focus. Figure 3-1 was taken from original publication (see also Addendum D, this thesis). For further explanation, see text.

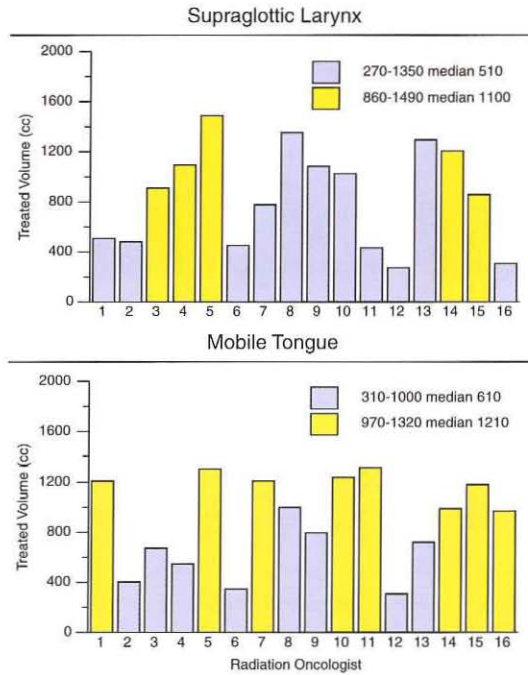


Figure 3-2. Treated volumes, i.e. volumes receiving more than 95% of the prescribed dose for Techniques I (blue) and II (yellow), in combination with minimum, maximum and median values. Figure 3-2 was taken from original publication (see also Addendum D, this thesis). For further explanation, see text.

CAPLAN dose distributions were calculated for all treatment plans using 6 MV photon beams (according to the treatment technique and portals selected by each individual radiation oncologist). The treated volume (see Chapter), defined as the volume enclosed by the 95% isodose line, was calculated for every treatment plan.

In addition, dose volume histogram analysis was performed for the parotid- and submandibular glands, together with an analysis of the NTCP values. In Figure 3-1, beam's eye view images of elective neck irradiation portals for cancer of the MT and SL are shown. The large variation in the size of the portals is apparent and indicates a lack of standardization. These differences can also be seen in the treated volumes (Figure 3-2).

There are two possible explanations for the variation in treatment portals. Firstly, some radiation oncologists conceptually treat different lymph nodal groups in the neck for the same primary tumor stage. Secondly, there is disagreement on the geographical borders of these lymph nodal groups even if radiation oncologists intend to irradiate the same lymph nodal groups. The vast differences in the posterior border are indicative for the second argument in particular. The beam's eye view images also demonstrate that roughly one-half to two-thirds of the parotid glands are within the radiation fields; for a few portals both parotid glands are incorporated totally in the treated volume. The impact of the parotid gland volume included in

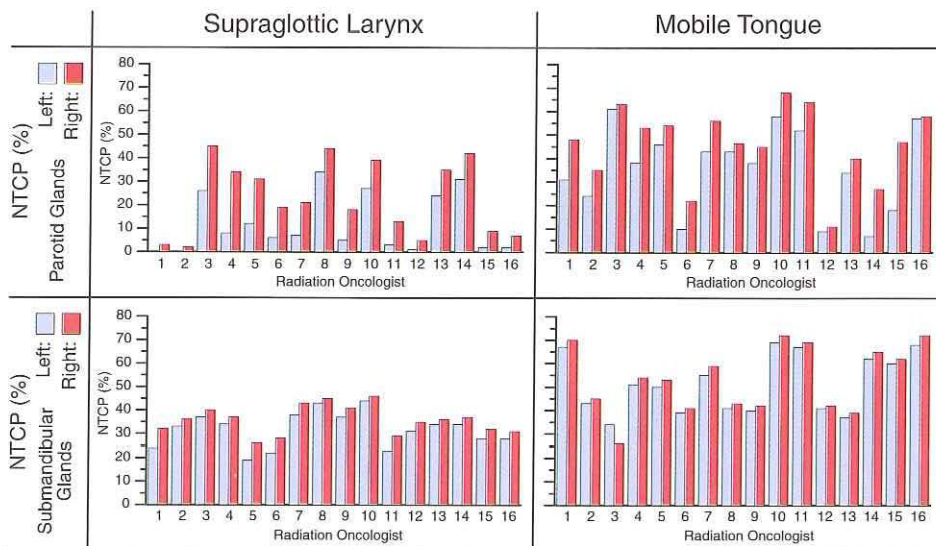


Figure 3-3. Normal tissue complication probability (NTCP) values of the left (blue) and right (red) parotid gland for a prescribed dose of 46 Gy to the neck. Figure 3-3 was taken from original publication (see also Addendum D, this thesis). For further explanation, see text.

the irradiated volume can also be appreciated from the NTCP values shown in Figure 3-3.

A detailed description and analysis of this study is presented in Addendum D. In summary: there appears to be no consensus between radiation oncologists as to the areas of the neck that need to be electively irradiated for (at least) the primary tumor sites studied. A translation of the three-dimensional target, i.e. the potential lymph nodal “areas” (regions) of the neck, into a two-dimensional target (delineation on simulation films) is mandatory. Following this step, radiation oncologists will need to decide (preferably by consensus) on the neck regions which require irradiation’s for any particular clinical indication. This latter aspect of elective neck irradiation is, however, a subject beyond the scope of this thesis.

CHAPTER 4

THREE-DIMENSIONAL CT TARGET DEFINITION

4 Three-dimensional CT target definition

4.1 Introduction

In order to define a three-dimensional CT definition of the elective neck, the following requirements were postulated. Firstly, the clinical target volume in surgery should in principle be similar to the CTV in radiotherapy, as elective neck dissection results in the same regional control rates as is the case with elective neck irradiation. Secondly, contouring of the target volume and critical structures on multiple CT slices should be fast with minimal risk for errors. This requires that the landmarks used be easily recognizable during the process of delineation of the target on CT, and this will also enhance reproducibility. Thirdly, the definition of the target should be given in treatment position of the neck. For elective neck irradiation, this refers to a supine position without rotation of the head, and is therefore somewhat distinct from the situation with surgery. Furthermore, it is postulated that subclinical disease respects natural borders like muscle compartments, bone and cartilage.

The accuracy of the CT target definition should be easily verified. It was felt that the best way to achieve this goal, was to implement the CT target definition on CD-i together with the anatomical information that was obtained from a human cadaver study. The target definition in this chapter was given for CT as almost all three-dimensional treatment planning systems only work with CT images. As these systems are rapidly evolving, and as it is to be expected that the target and critical structures in the near future will be delineated on CT and MRI, a matched MRI image for every CT image was included on the CD-i as well.

4.2 Target definition - procedures and results

4.2.1 Anatomical studies

In order to be able to correlate the surgical borders of the levels (I-VI) with structures seen on CT and MRI, two anatomical studies were performed using fixed (phenol, formaldehyde) human cadavers.

Firstly, a modified radical neck dissection was performed by an ENT surgeon on a human cadaver. The sternocleidomastoid muscle and the spinal accessory nerve were spared. Borders of the levels I-VI were demarcated using plastic tubes filled with liquid fat. CT slices were obtained every 3 mm with a Siemens Somatom Plus scanner. Using the laser lights in the gantry of the CT scanner, the position of the first slice was marked. This position was reproduced when MRI scans were acquired (slices every 3 mm), using a Magnetom scanner (Siemens). This way matched transverse CT- and MRI slices were obtained.

The second human cadaver was immobilized on a wooden support using a polyurethane construction foam. Matched CT- and MRI slices (every 3 mm) were again obtained. Besides the CT- and MRI images, simulation films were also taken as is performed for conventional radiotherapy technique; i.e. two lateral opposed fields and an anterior portal for the lower neck. The cadaver was then frozen to minus 80° Celsius and sectioned into slices of 5 mm thickness, using an immobile

bandsaw. This cryosectioning procedure has been described by Entius et al. in detail (9). Directly following the cryosectioning, the slices were rinsed with cold water. After alignment with the previously added special demarcations, photographs were taken (35 mm color films). The photographs were digitized and stored on a photo-CD. The transversal CT-, MRI- and anatomical slices (photographs of the slices) were matched. From the matched CT- and MRI data, a matched CT- and MRI volume was reconstructed. Both volumes were then “software sectioned” to obtain matched frontal and sagittal CT- and MRI slices. The image editing was performed using the AVS visualization system (version 5.02 Advanced Visual Systems Inc.).

Table 4-1. Lymph node classification system according to the level definition of the Memorial Sloan-Kettering group (37).

Level	Lymph nodes	Borders
IA	Submental	The anterior belly of the digastric muscles and the hyoid bone
IB	Submandibular	The anterior and posterior bellies of the digastric muscle and the body of the mandible
II	Upper jugular	Superior: skull base Inferior: carotid bifurcation (or hyoid bone) Anterior: lateral border sternohyoid muscle Posterior: posterior border sternocleidomastoid muscle
III	Middle jugular	Superior: carotid bifurcation (or hyoid bone) Inferior: omohyoid muscle (or cricothyroid notch) Anterior: lateral border sternohyoid muscle Posterior: posterior border sternocleidomastoid muscle
IV	Lower jugular	Superior: omohyoid muscle (or cricothyroid notch) Inferior: clavicle Anterior: lateral border sternohyoid muscle Posterior: posterior border sternocleidomastoid muscle
V	Posterior triangle	Inferior: clavicle Anterior: posterior border sternocleidomastoid muscle Posterior: anterior border trapezius muscle
VI	Anterior	Superior: hyoid bone Inferior: suprasternal notch Lateral: medial borders carotid sheath

4.2.2 Surgical definition - levels

The backbone for the current three-dimensional CT definition was an official report of the American Academy of Otolaryngology-Head and Neck Surgery, which was released in 1991 (36). With respect to the level definition, the most important objectives of the Subcommittee for Neck Dissection Nomenclature were to define the clinical and surgical borders of each of the lymph nodal groups to be removed with the neck dissection specimen, and to develop a classification that correlates with current oncological principles in the head and neck. The lymph nodal groups

were classified according to the level system as originally described by the Memorial Sloan-Kettering Group (37). The level classification was designed for surgical procedures and is defined by using many soft tissue landmarks (muscles, carotid bifurcation etc.), as summarized in Table 4-1. Unfortunately, many of the listed anatomical structures are not easily distinguishable on CT and, therefore, are not particularly suitable for translation into a CT target definition.

4.2.3 Target borders on anatomical slices

Using the data from the first anatomical study, for every anatomical slice the cranial-, caudal-, ventral-, dorsal-, medial- and lateral borders of levels, corresponding to the surgical borders of the level definition of the Memorial Sloan-Kettering group, were demarcated, in close cooperation with the otolaryngologist and the radiologist. The demarcated tissue boundaries (Table 4-2) correspond exactly to the original level definition, except for the cranial border of level II; that is, for the cranial border of level II the transverse process of vertebra C-II in stead of base of skull was chosen.

4.2.4 Target borders on CT slices

The second anatomical study was used to find the borders on corresponding CT slices; after some adjustments, the delineated CT slices were subsequently implemented on a CD-i. The adjustments of the borders had to be made in order to arrive at the CT target definition. Because of the albeit slight adjustments, the lymph node levels in the neck are designated as "regions". With respect to the target of the N0 neck, only fatty tissue in between CT landmarks, including vessels and nerves, will be considered as the clinical target volume. Moreover, in contrast to the level definition, the carotid artery and jugular veins are included into the CTV. The cranial border of region 2 is the most cranial CT slice on which vertebra C-I is still visible; this is in agreement with the level definition of the Memorial Sloan-Kettering Group. Since the flow of the major lymph nodal chain (jugular chain) is almost perpendicular to the transversal CT scan slices, the caudal- and cranial border of region 2 (level II) and region 3 (level III), and of region 3 (level III) and region 4 (level IV), respectively are depicted on one CT slice. In other words, the caudal border of region 2 (Figure 4-3) is the same as the cranial border of region 3 (Figure 4-4). Furthermore, the hyoid body is taken as the border between region 1 (level I) and region 6 (level VI), and is considered to correspond to one CT slice. Also some minor modifications were made for the dorsal border of regions 2, 3 and 4, and the ventral and dorsal border of region 5, because of the different treatment position of the head at the time of surgery (rotated head) compared to the position at the time of radiotherapy (see Tables 4-2 and 4-3).

4.2.5 Radiotherapy definition - regions

Table 4-3 summarizes the definition of the borders of the CT target volume for the elective neck with respect to all six regions. As can be seen from this table, if it

Table 4-2. Lymph node classification system according to the level definition of the Memorial Sloan-Kettering group. (37) The borders of the levels for the surgical

Target	Level I	Level II	Level III
Cranial	Mylohyoid muscle / Hyoglossus muscle	Transverse process C-II	Hyoid bone
Caudal	Platysma / Hyoid bone	Hyoid bone	Omohyoid muscle
Ventral	Mandible	Posterior belly digastric muscle	Sternohyoid muscle / Omohyoid muscle
Dorsal	IA Hyoid bone IB Posterior belly digastric muscle	Posterior border sternocleidomastoid muscle	Posterior border sternocleidomastoid muscle
Lateral	IA Anterior belly digastric muscle IB Mandible	Sternocleidomastoid muscle	Sternocleidomastoid muscle
Medial	IA <i>Not present</i> IB Anterior belly digastric muscle	Pharyngeal wall / Carotid artery / Deep cervical muscles	Larynx / Pharyngeal wall / Carotid artery / Deep cervical muscles

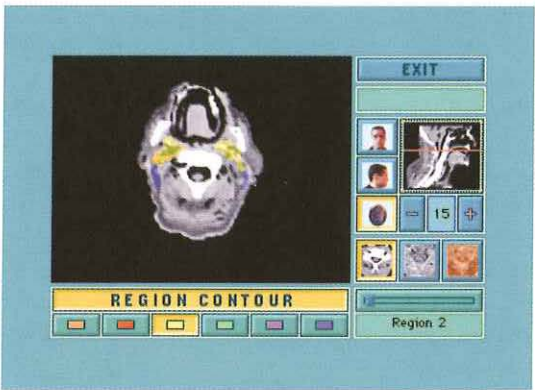


Figure 4-1. Screen of the module "Definition Target" on CD-i. The CT-target for the elective neck can be studied by clicking "Contour" and one of the colored buttons at the bottom. Every color is associated with a region as indicated in the text window at the bottom right. The target is defined by comparing matched anatomy and CT slices using the "slider".

approach are translated into borders for transversal anatomical sections.

Target	Level IV	Level V	Level VI
Cranial	Omohyoid muscle	Mastoid	Hyoid bone
Caudal	Clavicle	Clavicle	Suprasternal notch
Ventral	Sternohyoid muscle	Sternocleidomastoid muscle	Sternohyoid muscle
Dorsal	Sternocleidomastoid muscle	Trapezius muscle	Vertebra
Lateral	Sternocleidomastoid muscle	Platysma / Skin	Carotid sheath
Medial	Thyroid gland / Carotid artery	Deep cervical muscles	<i>Not present</i>

was not possible to identify a clear landmark, a distance is calculated (cm) in reference to a well defined and easily recognizable structure on CT (see, for example, the dorsal border of region 2 and Table 4-2). Starting with the cranial CT slices will facilitate the process of finding the borders of the regions on all CT slices. On every CT slice, lateral, medial, ventral, and dorsal borders are defined. A specific border can be found by approaching that border from the ipsilateral side, and looking for the first structure, mentioned in the list of that border in Table 4-3.

An audio-visual description of the entire three-dimensional elective target of the neck has been implemented on CD-i. For example, select the button "Definition Target" in the main menu on the CD-i. Figure 4-1 shows the screen of the target definition module (see also Chapter 6). Selecting a transversal CT, MRI or anatomy slice, and "Contour" will show the region definitions on the respective slices. Clicking one of the colored buttons will give an audio-visual representation of the region that corresponds to the color as indicated in the text window.

Cranial and caudal borders of the target and critical structures are hard to depict on transversal slices. Therefore, frontal and sagittal CT- and MRI images were implemented on CD-i. For example, after selecting "CT", and "Frontal" or "Sagittal", the

Table 4-3. Definition of lymph node regions for elective neck irradiation on transverse CT slices. The upper parts of regions 2 and 5 coincide: the junctional nodes. The caudal parts of regions 4 and 5 also coincide. The borders are defined delineat-

Target	Region 1 submental (1A) and submandibular (1B)	Region 2 high-jugular	Region 3 mid-jugular
Cranial	1A Caudal CT slice symphysis mandible 1B CT slice middle part of ramus mandible / Floor of mouth muscles	Cranial CT slice C-I	Caudal CT slice hyoid body
Caudal	1A CT slice hyoid body 1B CT slice hyoid body	CT slice hyoid body	CT slice caudal to thyroid cartilage
Ventral	1A Innerside mandible / Platysma / Skin 1B Innerside mandible / Platysma / Skin	1/3 of ramus mandible / 2 cm ventral to vertebra / Hyoid body	Hyoid body / Platysma / Skin
Dorsal	1A Floor of mouth muscles / Hyoid body 1B Digastric muscle / Medial pterygoid muscle / 1 cm ventral to vertebra	2 cm dorsal to ventral border of vertebra	Dorsal border vertebral body
Lateral	1A Line depicted by symphysis mandible and medial border parotid gland / Digastric muscle 1B Innerside mandible / Platysma / Skin	Medial pterygoid muscle / Parotid gland / Sternocleidomastoid muscle / Platysma / Skin	Sternocleidomastoid muscle / Platysma / Skin
Medial	1A <i>Not present</i> 1B Lateral border IA	Pharyngeal wall / medial border carotid artery / Deep cervical muscles	Larynx / Pharyngeal wall / medial border carotid artery / Deep cervical muscles

ing the target on the CT slices in a cranio-caudal direction. The “/” indicates that the border is either one of the structures mentioned, that is the first structure in the list found on the CT slice is the border.

Target	Region 4 low-jugular	Region 5 posterior triangle	Region 6 anterior
Cranial	CT slice caudal to thyroid cartilage	Cranial border region 2	CT slice Hyoid body
Caudal	Cranial CT slice with origin sternocleidomastoid muscle (approximately 2 cm cranial to sternoclavicular joint)	Caudal border region 4	Caudal border region 4
Ventral	Platysma / Skin / Sternocleidomastoid muscle / Clavicle	Dorsal border regions 2, 3 and 4	Skin
Dorsal	Dorsal border vertebral body / Transverse process / Rib	1 cm ventral to spinous process vertebra / most ventral part trapezius muscle / lung / ventral border rib	Vertebra
Lateral	Most lateral part sternocleidomastoid muscle / Platysma / Skin	Most ventral part trapezius muscle / most medial part clavicle / Platysma / Skin	Carotid sheath / Thyroid gland
Medial	Thyroid gland / medial border carotid artery / Esophagus	Vertebra / Deep cervical muscles	<i>Not present</i>

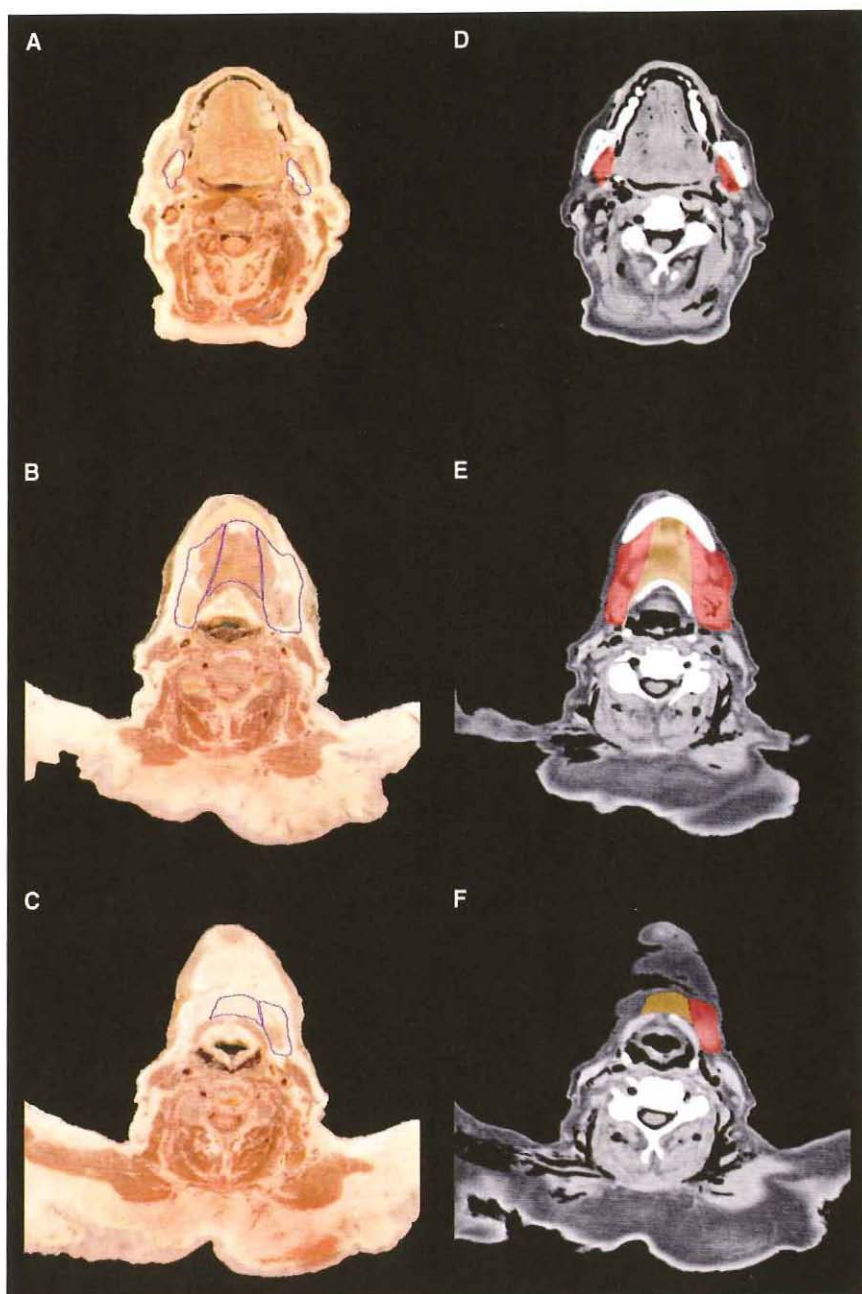


Figure 4-2. Region 1: borders are in blue-outline on the anatomy slices (left) and in orange (region 1A) and in red (region 1B) colorwash on the CT slices (right). The upper and lower borders of region 1A were on two consecutive slices of the human cadaver.

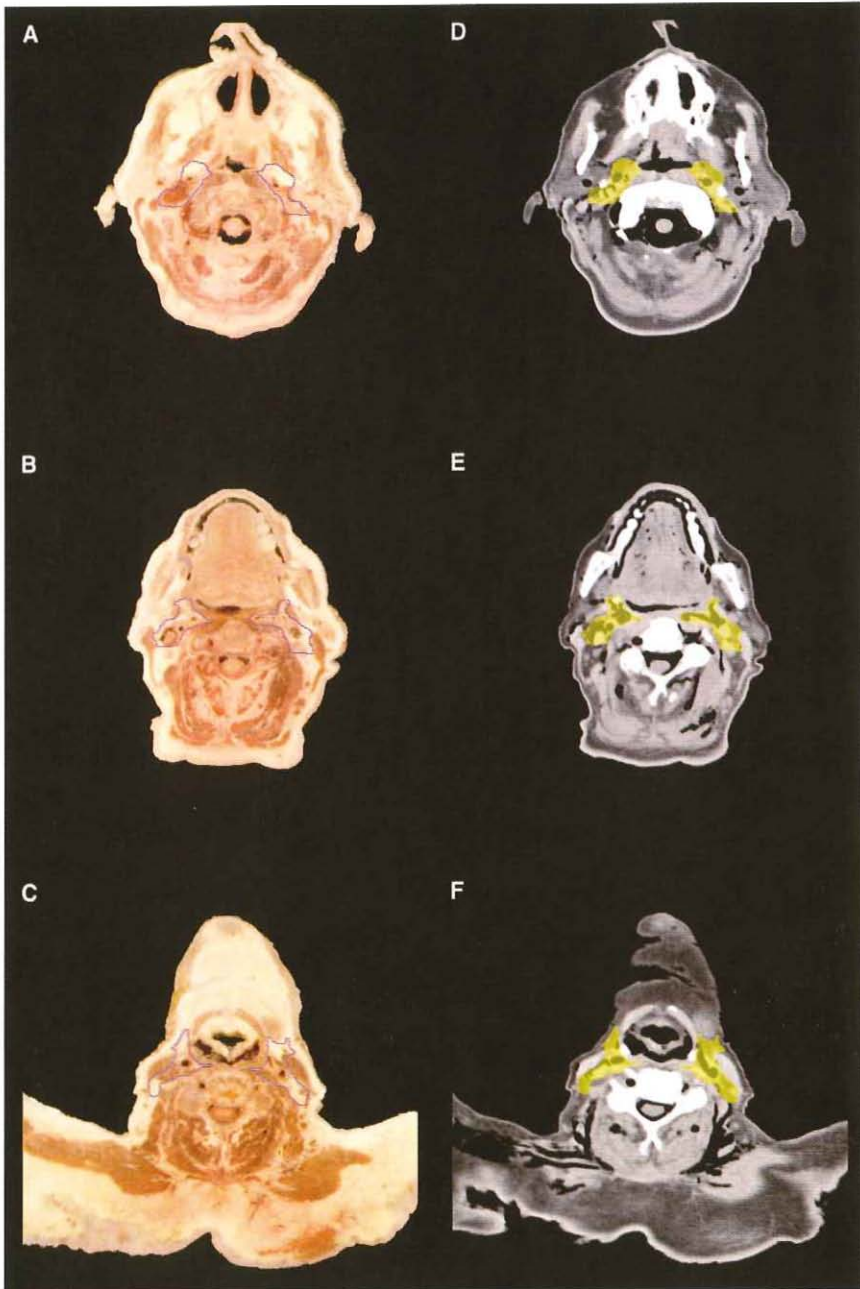


Figure 4-3. Region 2: borders are in blue outline on the anatomy slices (left) and in yellow color-wash on the CT slices (right).

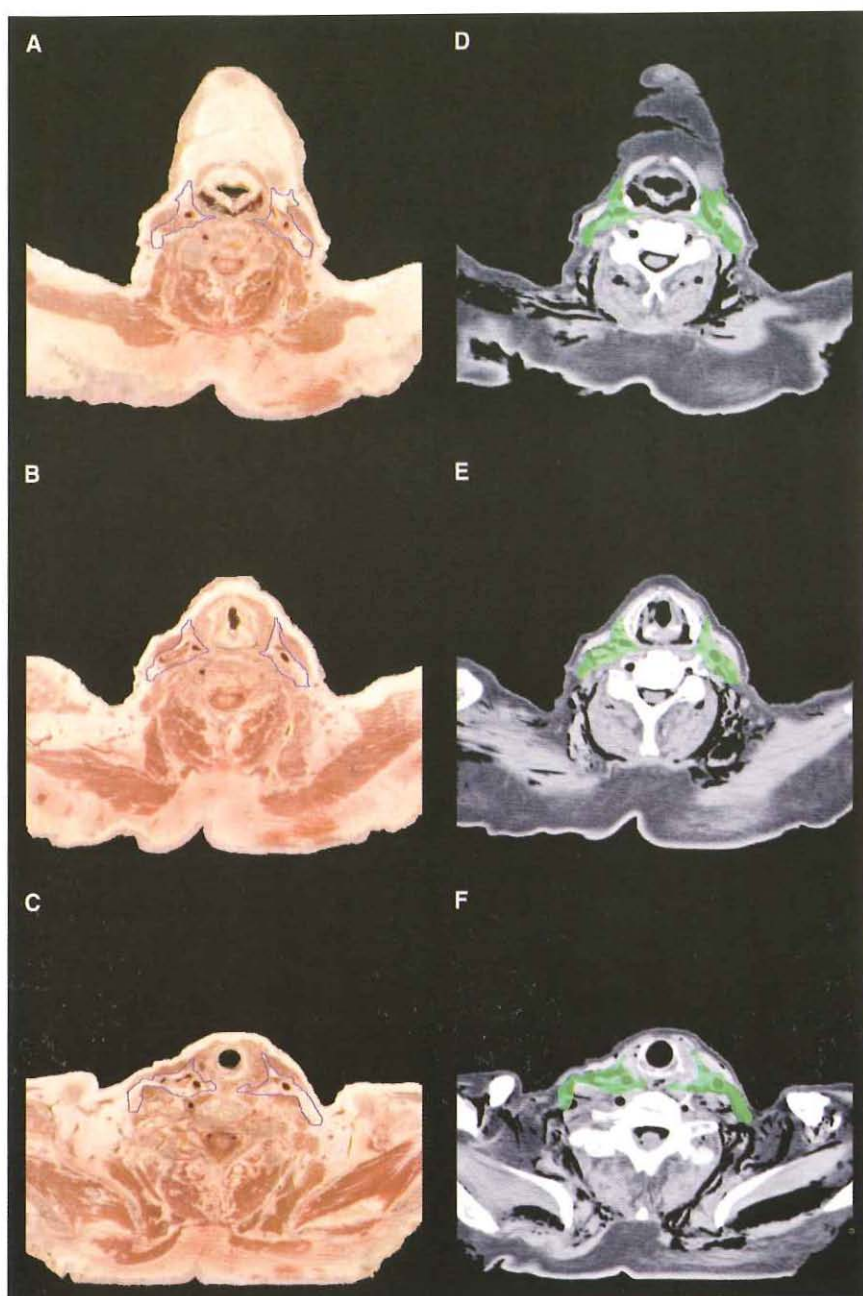


Figure 4-4. Region 3: borders are in blue outline on the anatomy slices (left) and in green color-wash on the CT slices (right).

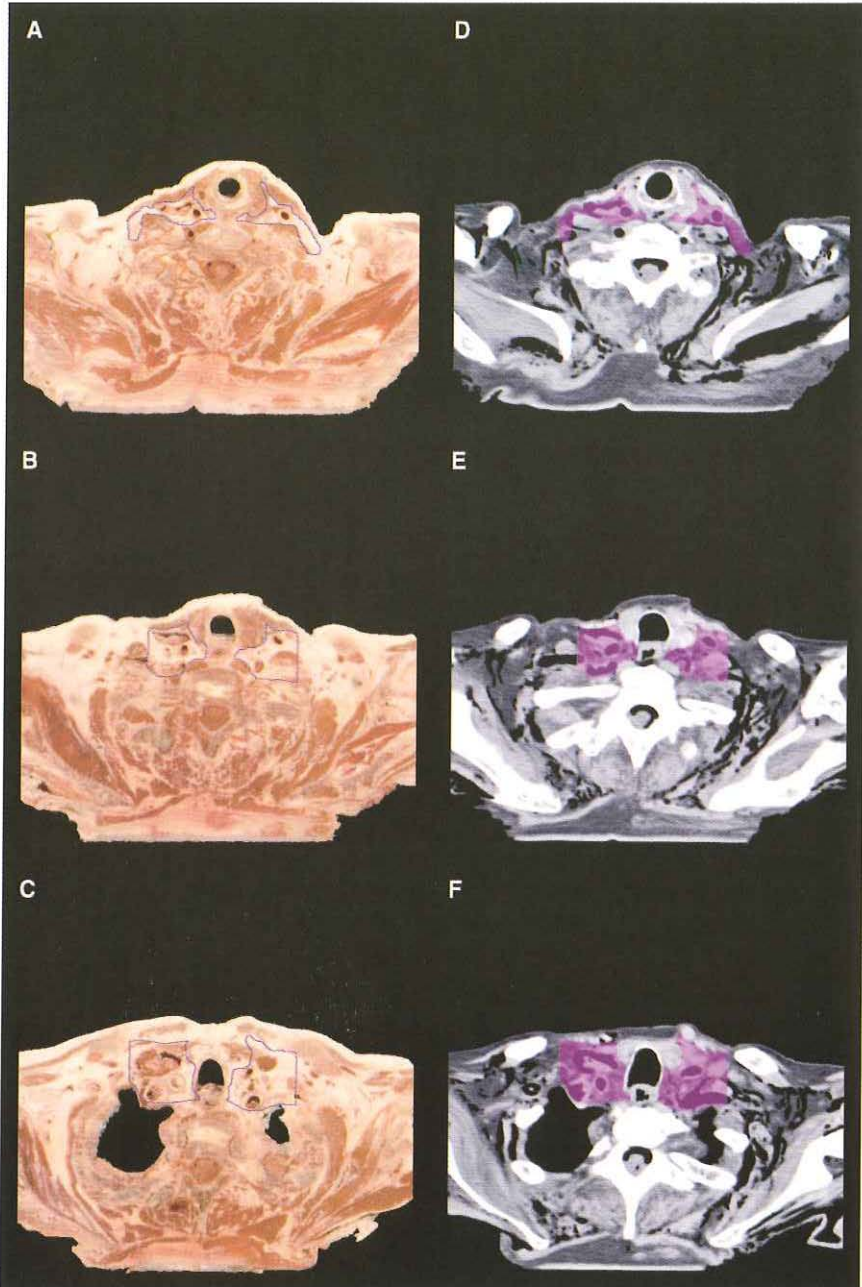


Figure 4-5. Region 4: borders are in blue outline on the anatomy slices (left) and in purple color-wash on the CT slices (right).

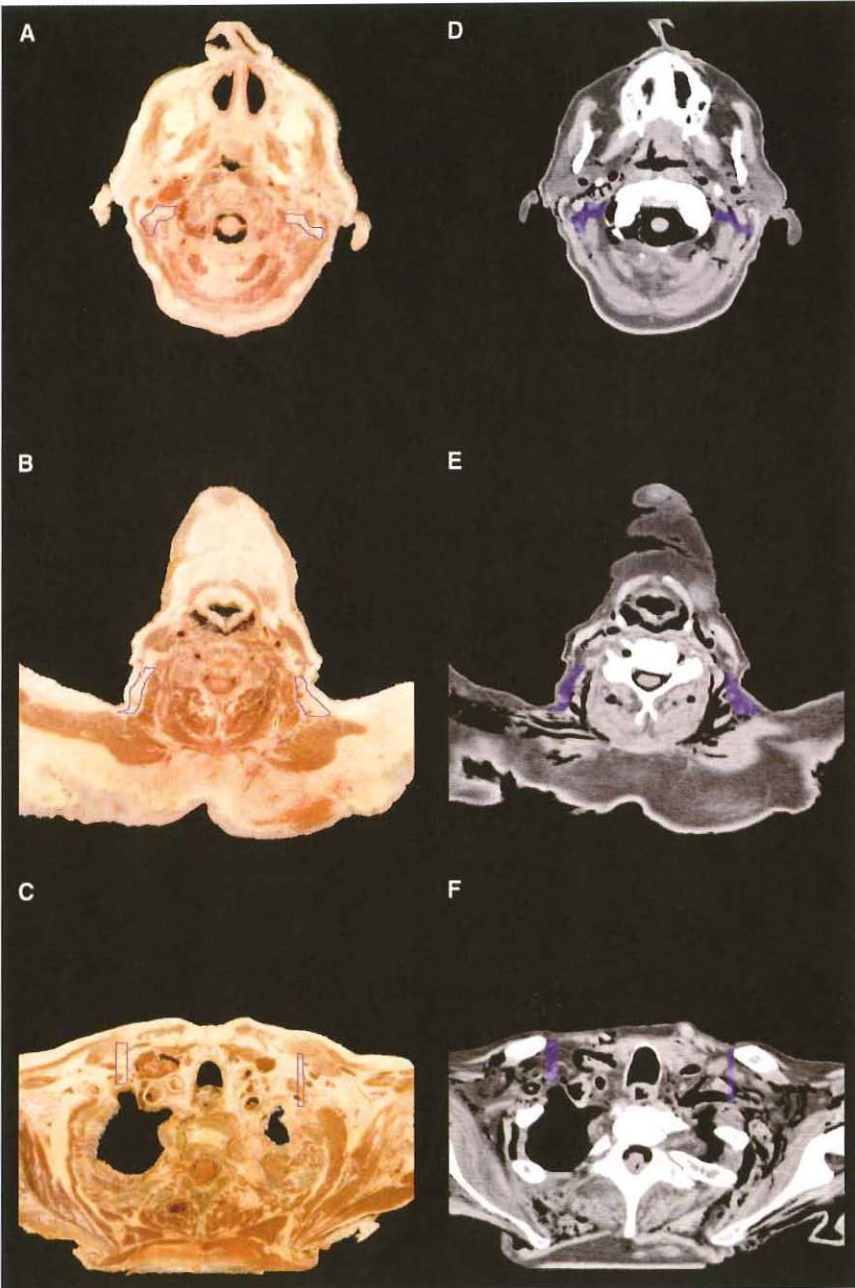


Figure 4-6. Region 5: borders are in blue outline on the anatomy slices (left) and in blue colorwash on the CT slices (right).

contours on all frontal or sagittal CT slices (if any defined for the selected image) can be studied on the CD-i.

In the module "Magnified Target", a summary is given of the target definition. Borders are defined on full screen anatomy and CT images. Three levels of each region are shown; two represent the cranial and caudal border of that region, and an other slice is located in between.

The description of the outlines of the regions is represented by Figure 4-2 through 4-6. The borders of each region are shown in a yellow outline on the anatomy images (left side of the figures), and in colorwash on the CT slices (right side of the figures). The colors correspond to the colors of the regions on CD-i.

Region 1 is always treated as a single entity. On the other hand it is easier to describe this region by splitting it into two sub-regions 1A and 1B, like the surgical definition of level I. Moreover, both sub-regions correspond to different anatomical sites; region 1A encloses the submental lymph nodes, and region 1B the sub-mandibular lymph nodes. For these reasons in Table 4-3 and on CD-i region 1 was divided into regions 1A and 1B. Due to the position of the head of the human cadaver only two consecutive slices represent region 1A (Figure 4-2). The borders of region 1A are the mandible, the hyoid bone, the skin (platysma), the floor of mouth muscles (the mylohyoid- and the hyoglossus muscle), and the digastric muscle. If the digastric muscle can not identified clearly, the line connecting the symphysis mandible and the medial border of the parotid gland is used. The borders of region 1B (Figure 4-2) are the mandible, the hyoid bone, the skin (platysma), the floor of mouth muscles, the medial pterygoid muscle, and the digastric muscle (or the line running from the symphysis mandible to the medial border of the parotid gland). If the dorsal border can not be identified it will be situated 1 cm ventral to the vertebral body. Region 1 corresponds to levels IA and IB without any adjustments.

The borders of region 2 in Figure 4-3 are delineated by distances from the ventral border of the vertebral bodies (2 cm ventral and dorsal), the medial borders of the medial pterygoid muscle and the parotid gland, the skin (platysma), the sternocleidomastoid muscle, the hyoid body, and the pharyngeal wall and deep cervical muscles. The distance between the ventral border of the vertebra and one third of the ramus mandible is also roughly 2 cm. The cranial border is in agreement with the Memorial Sloan-Kettering level definition. Given the different treatment position during radiotherapy compared to surgery (rotation of the head), the dorsal border was adjusted. In view of the close relationship of the lymphatics with the carotid artery and the jugular vein, these blood vessels were included in the target volume. The caudal border is the CT slice showing a major part of the hyoid body.

Figure 4-4 summarizes the definition of region 3. The borders of this region agree with the borders of region 2. The larynx will be a new medial border. The dorsal border is the width of the vertebral body (about 2 cm) dorsal to the ventral border of the vertebra. The cranial border of region 3 is the caudal border of region 2. The caudal border is the CT slice caudal to the thyroid cartilage.

Figure 4-5 depicts region 4. The borders are the skin (platysma), the sternocleidomastoid muscle, the clavicle, the transverse process of the vertebra, the rib, the thyroid gland, and the esophagus. The cranial border is the caudal border of region 3.

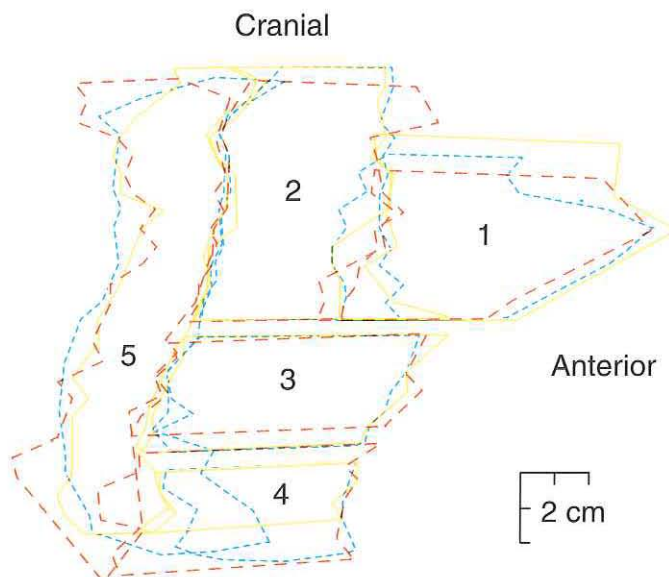


Figure 4-7. Delineation of the elective target in the neck by three radiation oncologists. Regions 1 through 5 were delineated on CT scans, and a beam's eye view reconstruction was made. Only minor deviations are seen in the beam's eye view images.

The caudal border ends at the insertion of the sternocleidomastoid muscle on the clavicle, which is cranial to the sternoclavicular joint.

The ventral border of region 5 in Figure 4-6 is the dorsal border of regions 2, 3, and 4. The cranial and caudal border are the cranial border of region 2 and the caudal border of region 4, respectively. A cranial adjustment of the dorsal border was made, being 1 cm ventrally to the spinous process of the vertebra. The most cranial part of region 5 coincides more or less with region 2. The common area encompasses the junctional lymph nodes. The caudal part of this region coincides more or less with region 4. The most difficult parts to delineate (and to describe) are the lateral and dorsal borders, because the lymphatics of the posterior neck triangle move from cranially, the lateral and dorsal part of the neck to caudally, the medial and ventral part of the neck. The dorsal border is always ventral to the most ventral part of the trapezius muscle, the lung and the ribs. The lateral border is always medial to the most medial part of the clavicle and the most ventral part of the trapezius muscle.

4.3 Verification of the three-dimensional target definition

The CT defined regions are based on the surgical levels as presented by the Memorial Sloan-Kettering Group, and which have proven to be consistent and valuable in clinical practice. As a first test of reproducibility, two independent head and neck radiation oncologists and a resident in radiation oncology delineated all

Elective Irradiation of the Neck Supraglottic Larynx

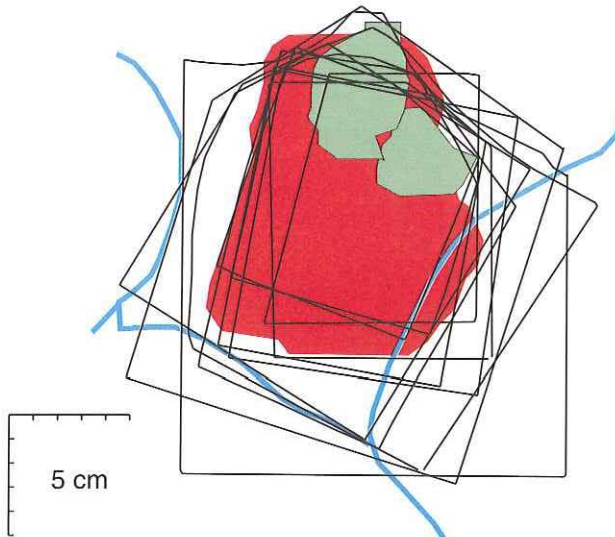


Figure 4-8 Comparison of conventional portals for a T3N0 supraglottic larynx carcinoma (see Chapter 2) and a beam's eye view reconstruction of the target delineated on CT slices. Red area: primary tumor and regions 2 and 3, delineated on CT, and reconstructed on simulation film (beam's eye view). Solid lines: conventional portals as drawn by the different radiation oncologists for a similar tumor. Green areas: projection of the parotid and submandibular glands on simulation film.

regions on CT scans of five different patients. With the help of beam's eye view images, the CT based portals were compared (Figure 4-7). Only minor differences were observed, particularly when comparing these discrepancies to the variations in outcome found in the national survey (Figure 4-8).

However, the best test of consistency would be to give any radiation oncologist the opportunity to define a three-dimensional N0 neck target and compare it with the definition as described here. With an interactive medium such as CD-i, this is possible and has been implemented.

In order to define the CT target on the CD-i, one has to choose "Definition Target" in the main menu (see Figure 4-1). A transversal CT slice is chosen, using the "transversal" and "next" or "previous" buttons. Selecting "Anatomy" will show the corresponding anatomy slice in the image window. The border of a level on this image can be chosen using Table 4-2. Using the slider, the location of this border is found on the CT. A structure on the CT slice corresponding to this location is identified. As mentioned previously this border may be corrected. The newly defined borders can finally be compared with the CT target definition given in this chapter.

CHAPTER 5

ELECTIVE NECK IRRADIATION — CONFORMAL TECHNIQUES

5 Elective neck irradiation - conformal techniques

5.1 General

5.1.1 Beam intensity modifiers

In elective neck irradiation, the three-dimensional target of the N0 neck is a very irregular- and large target volume, within an irregular body contour. Depending on the site of the primary tumor, air cavities can exist in close approximation to the target volume. These aspects make it difficult to obtain a homogeneous dose distribution in the target volume. Several authors have therefore advocated the use of intensity modulated beams to produce optimal dose distributions in these circumstances (16). Calculation of the required beam intensity profiles is possible using a variety of methods (e.g. feasibility search, simulated annealing, filtered back-projection) and constraints (e.g. prescription dose, tumor control probability, uncomplicated control) (5,17,48,49). In general, these procedures aim at optimization of the target dose homogeneity and, at the same time, sparing of the surrounding critical structures. In the three-dimensional planning system used in Rotterdam (i.e. CADPLAN), target dose optimization is implemented (so called "target compensation"). Sparing of critical structures is possible but it depends heavily on the expert input of the dosimetrist and/or physicist. A further constraint is that the dose homogeneity within the target should be better than 20% before starting the optimization program. The target compensation procedure has extensively been described by Ulsø et al. (43,44). The resulting intensity profiles usually exhibit large gradients. By smoothing the profiles, however, an acceptable beam intensity modifier is produced. By means of a milling machine, it is then possible to construct such a beam intensity modifier (i.e. tissue compensator), or one could reproduce the beam intensity profiles with a dynamic multileaf collimator.

5.1.2 Margins

The extra margin around the CTV to correct for patient positioning errors was 5 mm. This new volume (i.e. PTV) extends outside the body contour. In order to calculate a beam intensity modifier, the target compensation procedure requires that the PTV lies within the body contour (actually the build-up area of a beam). This adjusted PTV (PTV-a) was used for the calculation of dose-distributions, DVH and TCP values of the target, and the original PTV to define the portals. For further clarification, the slide show "Materials and Methods" in the "Introduction" submenu of the CD-i should be consulted. However, the dose to normal tissues may be underestimated as, arising from patient setup variations during multiple fractions, a larger part of the critical structures will be irradiated. Consequently, a second approximation was used to better estimate the dose to critical structures. Patient positioning errors during a course of radiotherapy were incorporated in the dose calculation algorithm in CADPLAN by convolution of the photon kernel with a gaussian distribution. A sigma of 3 mm was used, this being the standard deviation for positioning errors in head and neck cancer observed in a prospective study performed in the

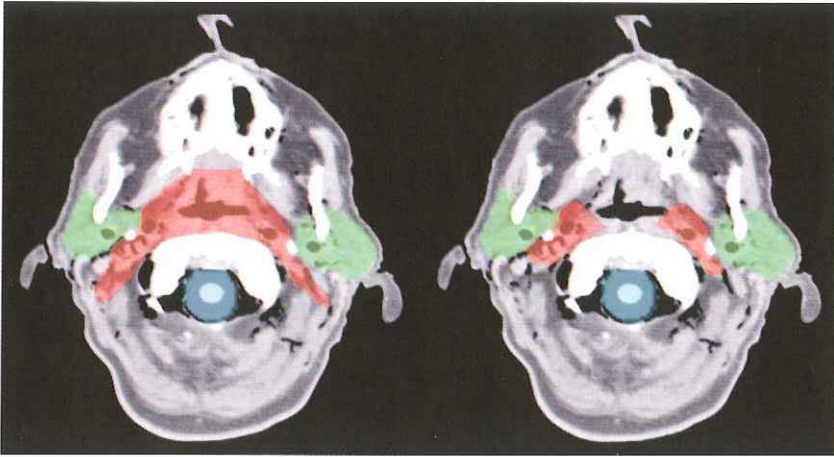


Figure 5-1 Clinical target volume (CTV) of an early stage nasopharyngeal cancer (left) and of a supraglottic larynx cancer (right) at the level of the parotid glands. The CTV is outlined in red-, the parotid glands in green- and the spinal cord in blue colorwash.

DHCC/UHR (18). As a result, a margin around the CTV is not necessary and treatment plans can be evaluated with respect to the CTV. However, this approximation assumes an infinite number of fractions. In order to better judge sparing of the salivary glands by conformal radiotherapy, both approximations were studied to calculate dose distributions.

5.1.3 Comparison of treatment plans

The best way to evaluate treatment plans is to inspect each individual dose distribution in multiple planes. However, this may be cumbersome, if not practically impossible, if the whole three-dimensional target including the critical organs for several treatment plans is to be studied. Several procedures are available, however,

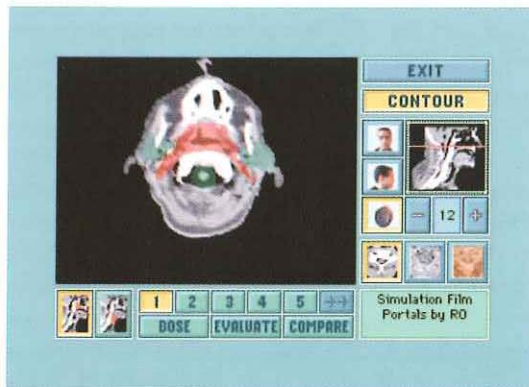


Figure 5-2. Screen of the "Radiation Therapy" module on CD-I. The image window shows a selected CT slice with the outlined clinical target volume of an early stage nasopharynx cancer (red) and the critical structures (green, see also Figure 5-1)

to facilitate this process. In general these methods reduce the information of the three-dimensional dose distribution to two- and even to one dimension. For example, cumulative dose-volume histograms (DVH) are two-dimensional representations. They tell what percentage of the target volume or volume of interest will receive at least a certain dose (or more than a certain dose), but information regarding the location is lost. Using bio-physical models it is even possible to give one-dimensional representations; i.e. figures of merit that estimate tumor control probability (TCP) and/or normal tissue complication probability (NTCP). Although allowing for reasonable approximations, the bio-physical models are imperfect and the comparison of treatment plans currently has still many limitations. The models used in order to calculate TCP and NTCP values, have been presented by Goitein and Kutcher (14,22).

5.2 Three-dimensional treatment planning of the elective neck

5.2.1 Contouring

To demonstrate the benefit of conformal radiotherapy in elective neck irradiation, two primary tumor sites were chosen: an early stage cancer of the nasopharynx (NP) and of the supraglottic larynx (SL). The regions for the NP to be treated were regions 2 through 5. For the SL, we elected to irradiate regions 2 and 3 in case of elective neck irradiation. Firstly, the CT slices from the second human cadaver were forwarded to CADPLAN. Body contours (automatically), and the contours of the two primary tumor sites (with a margin for subclinical disease, CTV-I), the elective neck regions (CTV-II), the PTV and PTV-a and the contours of the critical structures (parotid glands, submandibular glands, spinal cord) were delineated on every CT slice. Figure 5-1 depicts the CTV of both primary tumor sites on CT at the level of the parotid glands.

On the CD-i, the entire three-dimensional CTV of both primary tumors can be inspected. For example choose "Radiation Therapy" in the main menu (Figure 5-2). After selecting the primary tumor and "Contour", the target and critical structures can be seen and studied on every CT- and MRI slice as well as on the anatomical images by using the navigation buttons.

5.2.2 Treatment techniques

Some constraints were imposed upon the conformal radiotherapy technique. Firstly: theoretically the same or better loco-regional control rates should be obtained compared to conventional techniques, with at the same time sparing of the major salivary glands as much as possible. Secondly: care was taken not to surpass the tolerance dose of the spinal cord when increasing the dose to the primary tumor. Thirdly: the technique should be feasible in a regular (busy) radiotherapy department.

The prescribed dose was 46 Gy at the mean isodose percentage of the target volume. In accordance with ICRU-50 recommendations, the 95% isodose curves (surface) should encompass the whole target volume and the maximum dose within the

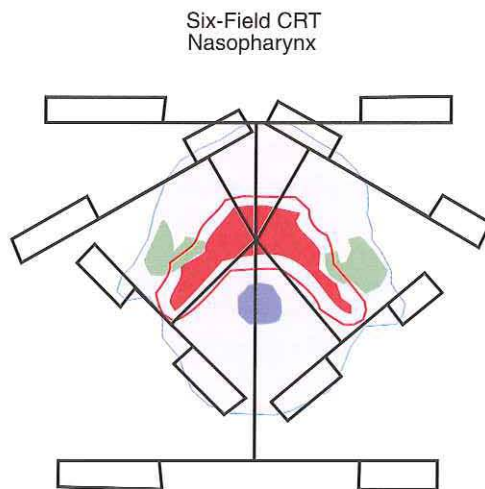


Figure 5-3.. Typical field arrangement for the described conformal radiotherapy of the nasopharynx and the supraglottic larynx. Red area: typical clinical target volume, red line: planning target volume, green area: parotid glands, blue area: cord. Six field with beam's eye view blocks are outlined.

target should be less than 107% of the prescription dose. Subsequently a six-field conformal radiotherapy treatment plan with one isocenter was developed using 6 MV photons generated in a KD-2 linear accelerator (Siemens) for both primary tumor sites. Figure 5-3 shows schematically the field arrangement which was essentially the same for both primary tumors (i.e. nasopharynx and supraglottic larynx). Before starting the compensator program the treatment plan was optimized in such a way that the dose to the parotid glands was minimized and that the 80% isodose curve/surface encompassed the planning target volume. This was achieved by adjusting the beam positions with the beam's eye view option of CADPLAN, by shielding part of the salivary glands and spinal cord in every beam with beam's eye view blocks, and by varying the beam weights. For example, for the oblique beams one parotid gland will not be irradiated at all. As a consequence also part of the target volume will not be irradiated, but this is compensated for by the other beams.

For the evaluation of conformal radiotherapy, three conventional techniques were planned. One involved portals drawn by the radiation oncologist directly on simulation films without knowledge of a three-dimensional target definition. These portals are comparable to the national survey study (see also Chapter 4). The second conventional technique is similar to first one, but it uses the three-dimensional CT definition. With the beam's eye view option of the planning system, customized blocks were placed around the target. In the third technique, the second technique was optimized, i.e. the lateral beams were rotated in such a way that the proximal shoulder of the human cadaver was outside the radiation fields. Dose prescription was the same as for the conformal radiotherapy technique. On CD-i, all beam's eye view images can be studied. For example to inspect the beams of the conformal radiotherapy technique of the NP choose "Beams Eye View" in the main menu of

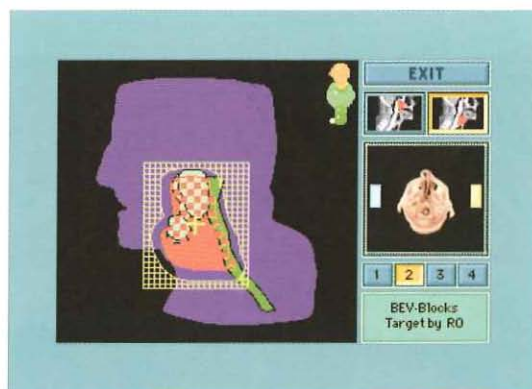


Figure 5-4. Screen of the "Beam's Eye View" module on CD-i. The "eye of the observer" is in the focus of the chosen beam looking in the beam direction to the patient. The red area of the image represents the target of the nasopharynx cancer or the supraglottic larynx cancer, the blue area the body outline of the patient, the two shades of green the critical structures (salivary glands light green, spinal cord dark green). The areas with red and green squares indicate an overlap of target and critical structures seen from this direction. The yellow hatched area is the shielded part of the beam.

the CD-i (Figure 5-4). After selecting the NP, every beam can be seen with the beam selector buttons.

5.2.3 Dose distributions

For both the NP and SL cancer, dose distributions were calculated for all treatment techniques on all transversal CT slices. Dose distributions were reconstructed with AVS for frontal and sagittal CT (and MRI) slices (see also Chapter 4). DVHs, TCPs and NTCPs were calculated for the PTV-a, CTV, salivary glands and spinal cord. The DVH and TCP of the primary tumors were calculated with and without convolution of the photon kernel for respectively the PTV-a and CTV.

In Figures 5-5 and 5-6 dose distributions of the optimized conventional technique using beam's eye view blocks and the conformal radiotherapy technique are compared at the level of the parotid and submandibular glands for both primary tumor sites.

Dose distributions of the conformal radiotherapy technique appear superior to the conventional technique. This was confirmed by comparing the DVHs (Figure 5-7) and the calculated TCPs and NTCPs (Tables 5-1 and 5-2) using both treatment techniques for the target volume and the parotid glands. To a somewhat lesser extent, sparing of the submandibular glands seems also better feasible with the conformal radiotherapy technique. The gain in NTCP value is, however, small.

A full presentation of the treatment techniques is provided on the CD-i. Dose distributions are presented on transversal CT and MRI as well on the anatomical slices. For example, in order to compare treatment techniques of the SL cancer choose, from the main menu "Radiation Therapy" (Figure 5-8)

Select the SL cancer and "Show Dose". After choosing "Compare" several treatment techniques can now be selected and the dose distributions of these techniques

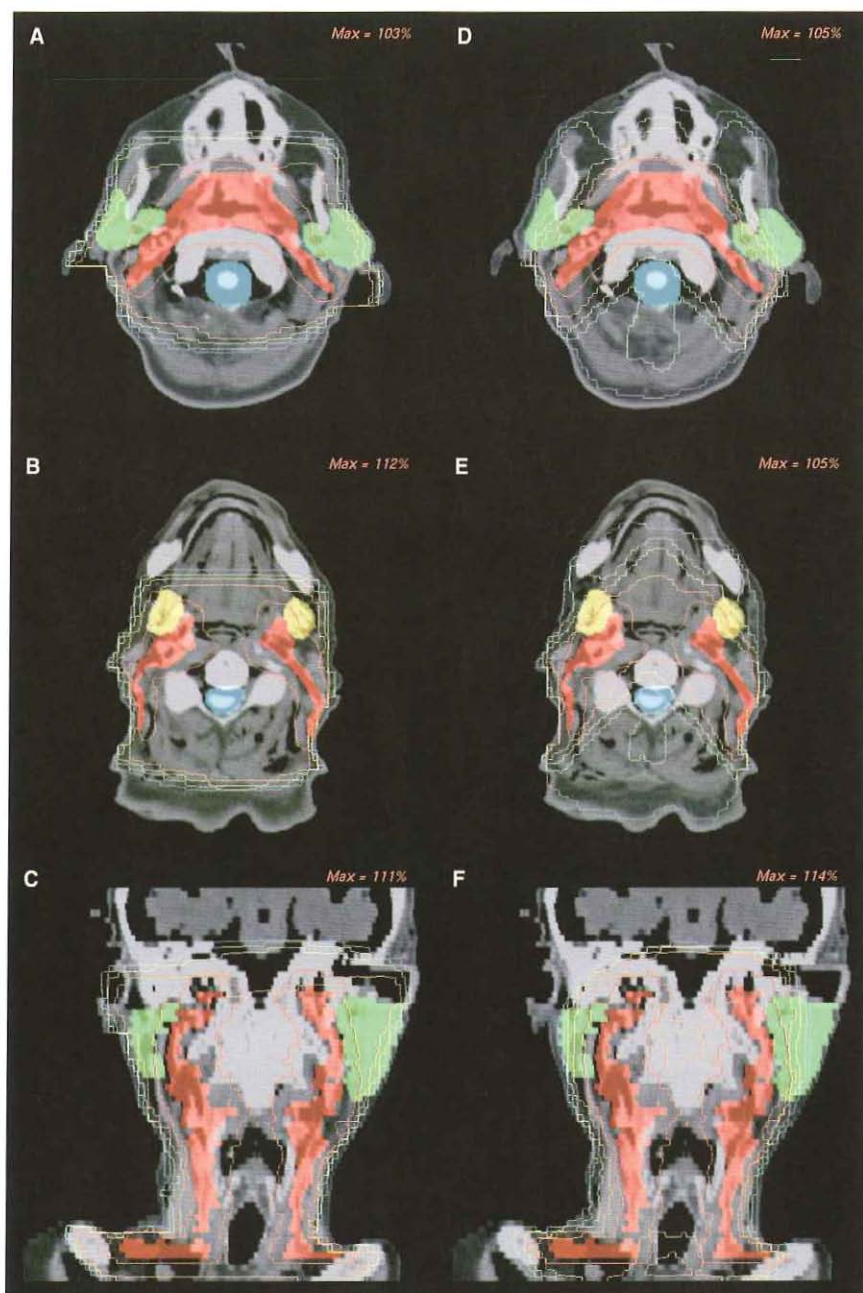


Figure 5-6. Comparison of dose distributions of the optimized conventional radiotherapy- (panels A-C) and the conformal radiotherapy technique (panels D-F) for an early stage nasopharynx cancer. Transversal slices are at the level of the parotid glands (panels A, D) and the submandibular glands (panels B, E). Frontal slices are at the level of the parotid glands (panels C, F).

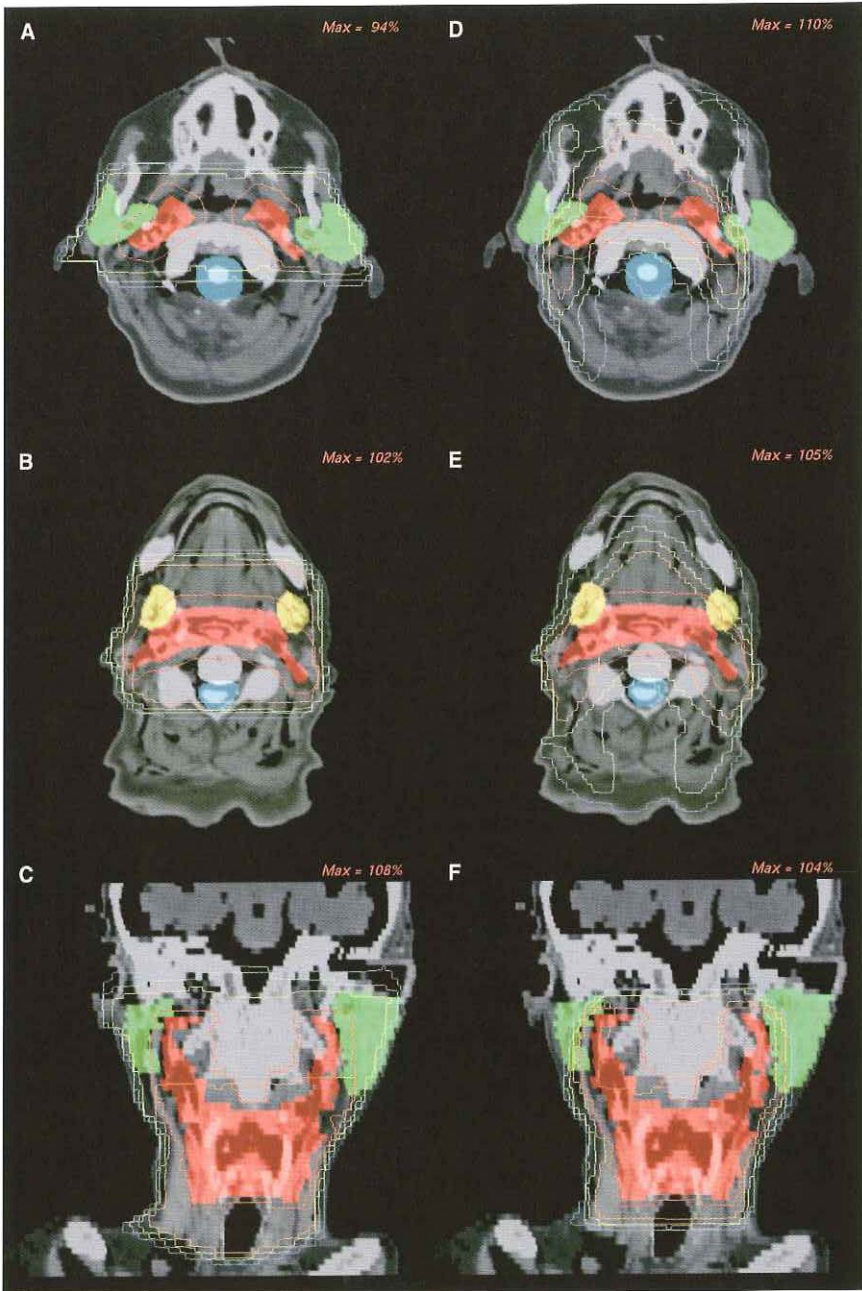


Figure 5-7. Comparison of dose distributions of the optimized conventional radiotherapy- (panels A-C) and the conformal radiotherapy technique (panels D-F) for an early stage supraglottic larynx cancer. Transversal slices are at the level of the parotid glands (panels A, D) and the sub-mandibular glands (panels B, E). Frontal slices are at the level of the parotid glands (panels C, F).

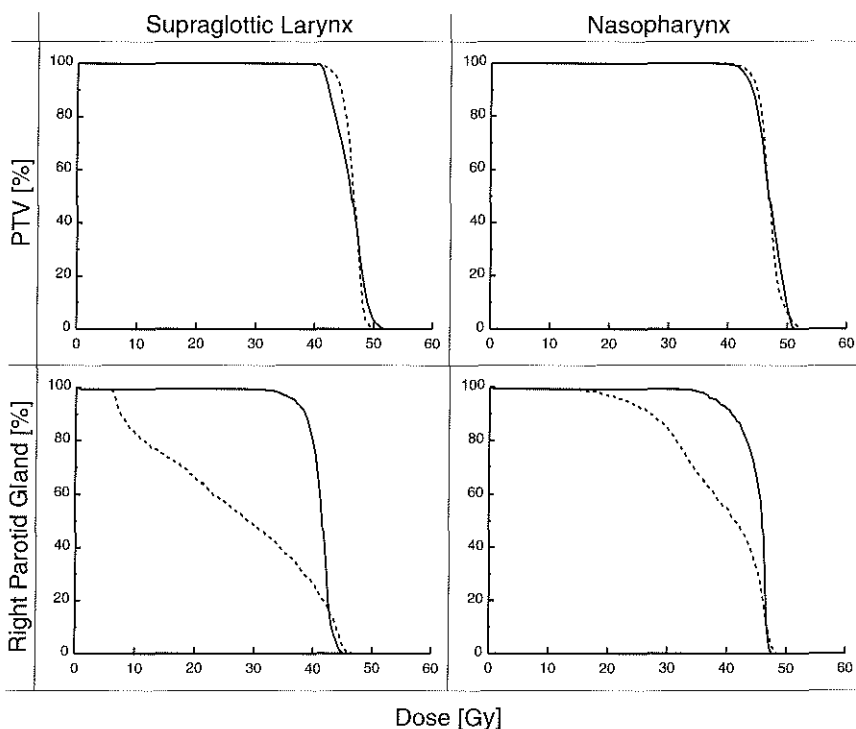


Figure 5-6. Dose volume histograms of the planning target volume (top) and right parotid gland (bottom) of an early stage supraglottic larynx cancer (left) and nasopharynx cancer (right). Solid line: optimized conventional technique, dashed line: six-field conformal technique.

can be compared to each other with the “Step” function. Selecting “Evaluate”, the same can be done for the DVH-, TCP- and NTCP values of the different treatment techniques.

Table 5-1. Tumor control probability (TCP) and normal tissue complication probability (NTCP) of the supraglottic laryngeal cancer for the different techniques (see text). RP and LP: right and left parotid gland respectively. RS and LS: right and left submandibular gland respectively. SC: spinal cord. CRT: conformal radiotherapy.

Technique	TCP [%]		NTCP [%]				
	PTV-a	CTV	RP	LP	RS	LS	SC
Simulation X-ray	58.9	88.4	29.5	40.6	50.7	56.0	2.2
beam's eye view	82.0	90.2	34.1	38.9	49.8	53.1	2.2
blocks							
beam's eye view	84.6	84.6	25.8	22.7	49.9	53.4	2.4
blocks optimized							
CRT	91.5	96.2	1.9	8.6	37.2	31.5	0.3
CRT $\sigma = 3$ mm	94.5	97.3	9.1	18.6	38.7	33.1	0.4

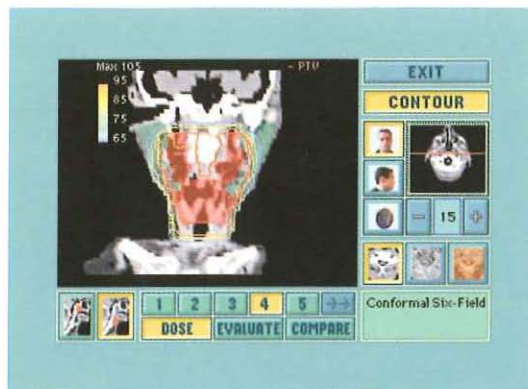


Figure 5-8. Screen of the "Radiation Therapy" module on CD-i. The image window shows a selected CT slice with the dose distribution belonging to the conformal radiotherapy technique of an early stage supraglottic larynx cancer.

From the figures, the tables, and by consulting the CD-i, it is apparent that theoretically conformal radiotherapy is able to spare the parotid and to a lesser extent the submandibular glands better than when using the conventional techniques with equal or even improved coverage of the target volume. Unfortunately, this goal is reached by smearing out the dose outside the target volume at the cost of more dose to oral cavity. Whether this conformal radiotherapy technique will produce less xerostomia can only be tested and objectivated in preferably a randomized trial, using also subjective scoring listings ("degree xerostomia") and saliva production measurements as parameter functions. These types of studies will in fact be initiated in the near future, but this subject is, however, beyond the scope of this thesis.

Table 5-2. Tumor control probability (TCP) and normal tissue complication probability (NTCP) of the nasopharyngeal cancer for the different techniques (see text and legend Table 5-1).

Technique	TCP [%]		NTCP [%]				
	PTV-a	CTV	RP	LP	RS	LS	SC
Simulation X-ray	54.1	85.1	44.8	48.9	67.6	71.9	5.1
beam's eye view	88.9	93.9	42.2	47.3	58.1	60.9	4.7
blocks							
beam's eye view	88.2	93.5	41.7	47.9	50.7	54.0	4.7
blocks optimized							
CRT	92.0	96.6	19.9	35.3	37.4	42.2	1.2
CRT $\sigma = 3$ mm	91.3	96.7	19.1	33.9	37.1	41.5	1.2

CHAPTER 6

VISUAL JUSTIFICATION

6 Visual justification

6.1 CD-i introduction

A three-dimensional CT definition of the target of the neck was presented in Chapter 4. Two primary cancers in the head and neck without detectable lymph nodes were illustrated: a T2N0 nasopharynx cancer and a T3N0 supraglottic larynx cancer. Using the CT target definition of the elective neck in Chapter 4, a conformal radiotherapy technique was developed for the combined primary tumor target and the neck target, demonstrating the potential benefit of conformal radiotherapy (see Chapter 5). The CT target definition of the elective neck and the procedures to arrive at this definition have been implemented in the modules "Definition Target" and "Magnified Target" on the CD-i. The conformal technique developed in Chapter 5 and the comparison with conventional techniques have been implemented in two modules on the CD-i. The "Beam's Eye View" module shows the beam arrangements of the conventional and conformal techniques. In the "Radiation Therapy" module, the dose distributions and DVH data belonging to the conventional and conformal techniques are compared. Slide shows, clarifying how these data were obtained and why this study was performed, were added. Also an introductory slide show was implemented showing the path from patient entry to actual treatment on a MM50 racetrack microtron in the DHCC/UHR. The reasons for the development of the CD-i can be summarized as follows.

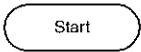
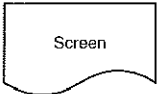
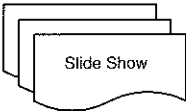
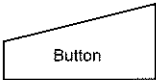
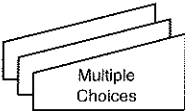


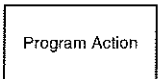

The CT definition of the three-dimensional target for elective neck irradiation results in huge amount of images. For verification purposes and for educational reasons it is necessary to show the entire CT definition of the regions in the neck on all (appropriate) images. An interactive medium like CD-i is perfectly suitable for this purpose. One of the main goals for the design of the CT definition module on the CD-i was to give the user the opportunity to reconstruct the CT definition procedure. This will provide him/her with the tools to create his/her own CT definition and then e.g. verify this with the available anatomical data. This is one of the best justifications of the appropriateness of the presented CT definition in Chapter 4. When delineating the regions according to the definition in Chapter 4, it can sometimes still be difficult to find the exact borders. However, the radiation oncologist can search for a matching image and this way the CD-i provides helpful information to arrive at the precise CT definition. The interface of the CD-i should therefore allow the user rapidly to select a certain image and show the region of interest. In general, this module was also constructed as a teaching tool.

One way to evaluate the benefit of conformal radiotherapy for the elective neck irradiation over conventional radiotherapy techniques is by comparing dose-distributions of different plans side by side (15). In case of conformal radiotherapy, this should be done for the entire three-dimensional target volume, including frontal and sagittal slices. The objective for the CD-i interface was to implement an easy procedure to do so. Similarly it should be possible to compare DVH curves of all the treatment plans.

6.2 Content and design of the CD-i

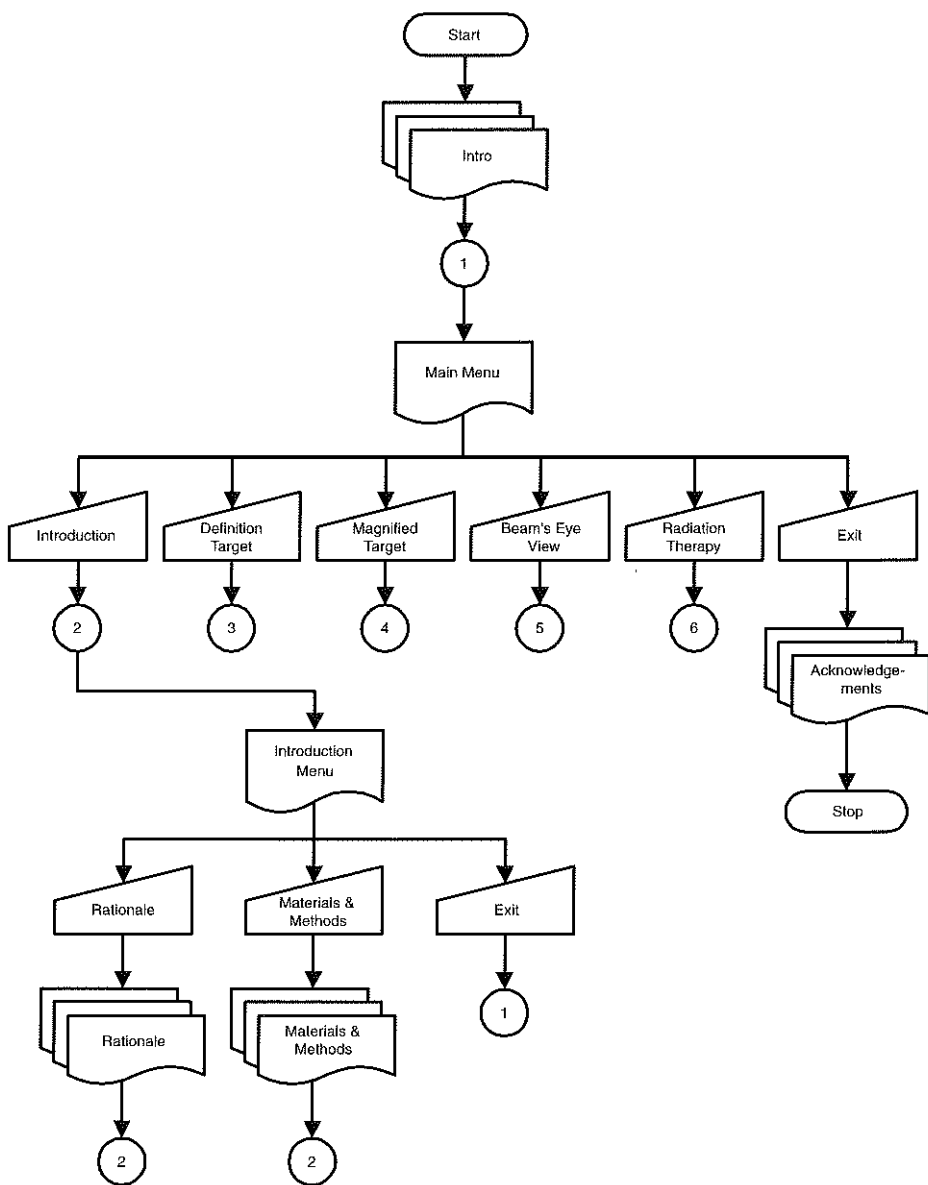
The design of the interface will be clear by studying the flowchart of the program. The flowchart itself is divided into eight parts (Flowchart 6-1 through 6-8). The explanation of the symbols used in the flowcharts is outlined in Table 6-1.

Table 6-1. Explanation of the symbols used in the flowcharts.

Symbol	Explanation
	Start/Stop CD-i program
	Visible interface on the television set
	Slide show
	Action that user performs (decision of the program)
	Group of buttons that will initiate the same kind of program action
	Image library on CD-i
	Flow of program depends on state of program, c.q. buttons
	Action that program performs
	Jump to other (part of) flowchart

6.2.1 Menu

Flowchart 6-1 shows the menus of the CD-i. When starting the program, an introductory slide shown is automatically started, showing the intake and treatment of a patient by radiotherapy in general and on the MM50 in particular. By clicking a



Flowchart 6-1. Module showing the main menu and the "Introduction" menu. For explanation see text.

mouse button, the slide show can be stopped. After this slide show the main menu shows up (Figure 6-1).

Six options are possible. The "Definition Target" button gives access to a module to study the three-dimensional CT target for elective neck irradiation as derived in Chapter 4. The "Magnified Target" button opens a menu that summarizes the target definition on a few enlarged images. The buttons "Beam's Eye View" and "Radiation

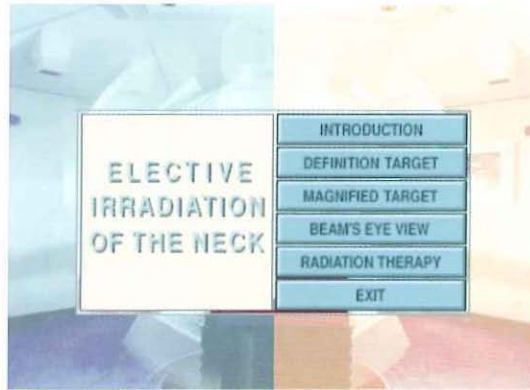


Figure 6-1. The main menu with five choices and an exit button.

Therapy” will bring up modules respectively to study beam positioning and dose distributions/DVH curves for elective neck irradiation of an early stage NP and SL cancer treated by conventional and conformal radiation techniques, as developed in Chapter 5. The “Exit” button starts a slide show with acknowledgments before the program stops. The “Introduction” button displays a submenu with another three options (Figure 6-2).

Two of them will display slide shows. “Rationale” explains why this study was performed and shows the underlying basis of the three-dimensional CT definition for elective neck irradiation. “Methods & Materials” shows how the data for the other modules were obtained. “Exit” displays the main menu again.

6.2.2 Definition target

This module gives the three-dimensional target definition of the elective neck on CT-, MRI- and anatomical slices (see Chapter 4). The procedure to arrive at the definition has also been implemented, allowing the user to create his “own” definition and compare it with the one given.

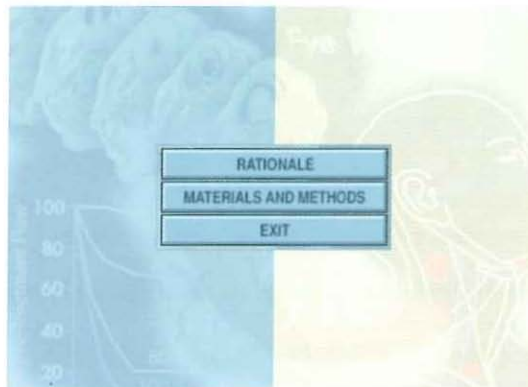


Figure 6-2. The “Introduction” menu, that gives access to two slide shows: “Rationale” and “Materials & Methods”.

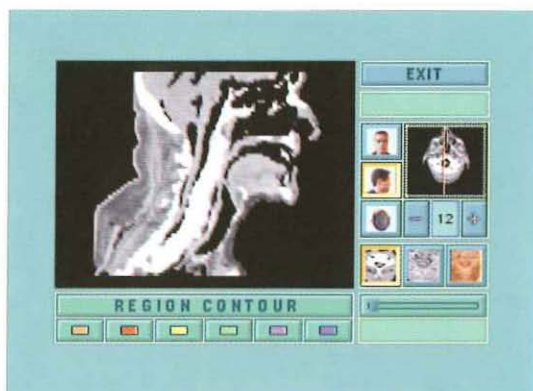


Figure 6-3. Opening screen of the "Definition Target" menu.

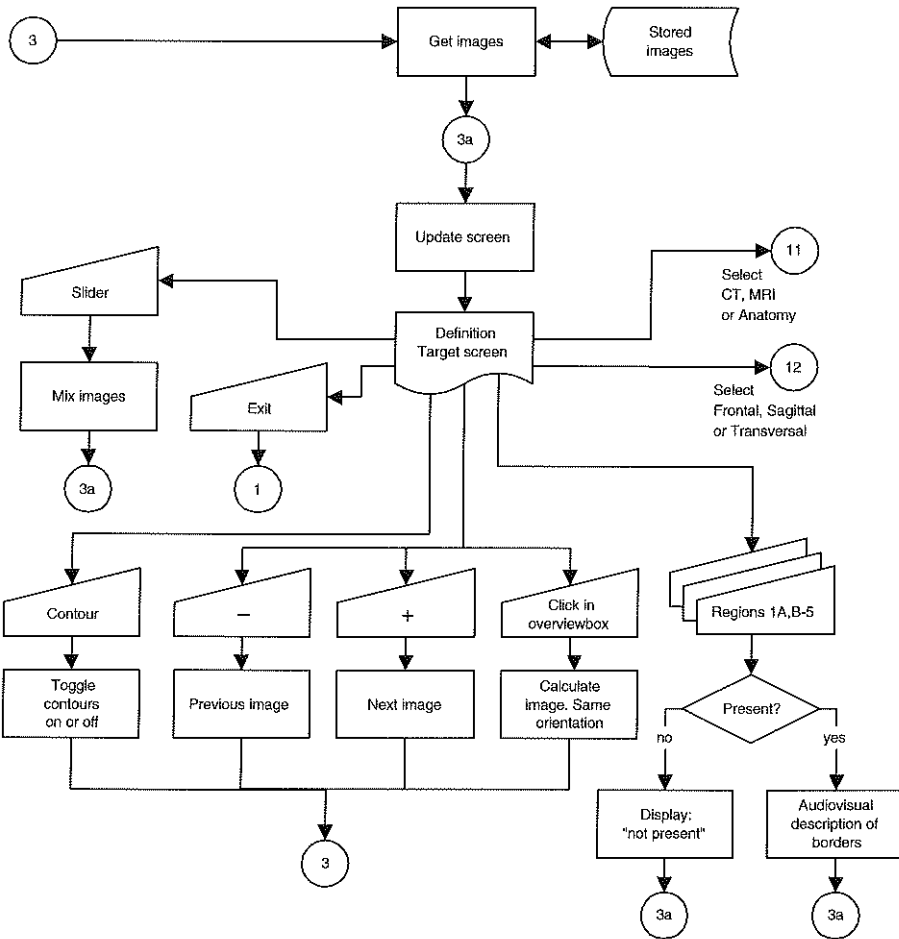
After pushing the "Definition Target" button the screen of Figure 6-3 is seen. The image window on the left may show transversal CT-, MRI slices or anatomical sections, or frontal or sagittal CT- or MRI slices. The panel on the right allows the user to choose an image. The panel at the bottom shows the contour buttons that give a audiovisual description or colorwash representation of the contours. The slider down-right is a crucial part of this interface as will be seen.

Flowcharts 6-2 and 6-3 explain all possible actions. After startup, a sagittal CT slice in the midline is shown. The matched MRI slice is also automatically loaded into memory (there are no sagittal anatomical sections) and can be seen by pushing the slider to the right. By holding the slider with the mouse, the slider can continuously be moved; depending on the position of the slider, CT- and MRI images are mixed and seen in the image window (Flowchart 6-2). If sagittal or frontal slices are chosen, only CT- and MRI images can be mixed. The anatomy icon/button is in that case disabled. If a transversal image is chosen, the CT-, MRI- and anatomy icons/buttons are all active. If one pushes a CT-, MRI- or anatomy button, the cursor is confined to the CT-, MRI- and anatomy button area. As indicated in the message box below the slider, by using one of the other two buttons combinations of images as outlined in Table 6-2 should be selected for comparison purposes (Flowchart 6-3).

Table 6-2. Possible and preferred combinations of images that can be compared in the "Target Definition" module.

Orientation	Slider	
	Left	Right
Transversal	CT	MRI
Transversal	CT	anatomy
Transversal	MRI	anatomy
Sagittal	CT	MRI
Frontal	CT	MRI

One can advance one slice forward or backward by pushing respectively the "+" or "-" button. The actual position is indicated by the line in the overview box above



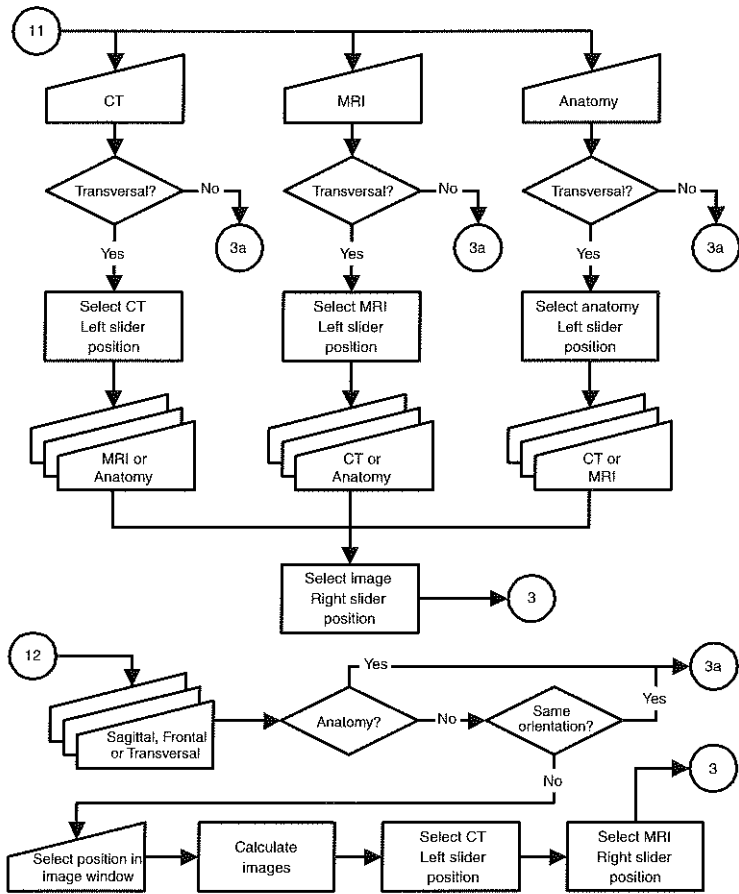
Flowchart 6-2. The "Definition Target" module. Branches 11 and 12 refer to Flowchart 6-3.

these buttons (and by the number of the slice in between these buttons). One advances fast forward or backward by clicking in the overview box, roughly at the desired location (Flowchart 6-2). By pushing the transversal-, frontal- or sagittal icons slices can be chosen in other orientations. Depending on the actual orientation, the icon/button belonging to this orientation is disabled. If, for instance, a sagittal slice is shown, the sagittal icon/button is disabled. Then pushing the transversal button will confine the cursor to the image area. The cursor itself changes into a horizontal line. The user may now choose in the sagittal image a transversal image at a particularly anatomical structure just by clicking the mouse at that spot. For the CT- and MRI images, all transitions are possible. If an anatomical image is chosen, visible or not, all the icons/buttons are disabled; only transversal images are implemented (Flowchart 6-3). The contour button acts as a toggle. If the button is active, contours will be shown on the selected image if any are defined on it. The contours will stay visible regardless any other action in this module, even if one temporarily exits the

module. Every region (region 1A, 1B, 2, 3, 4, and 5) has its own color as indicated by the colored buttons below the contour toggle. As explained in Chapter 4, region 1 has been split in two sub-regions (1A and 1B) purely to give an easier prescription to delineate region 1. When a region button is pushed and that region is present in the selected image an audiovisual description of the borders is given. During this time in the message box the name (number) of the region is shown (Flowchart 6-2).

The “Exit” button will bring back the main menu.

The creation a target definition can be summarized as follows (see also Chapter 4). The borders of a particular surgical level, i.e. anatomical structures, are outlined on the anatomy slices. With the slider corresponding borders are located on the CT slices. Often reproducible easy recognizable structures, corresponding to these borders, can not be found on the CT slices. New structures are then chosen on the CT slices. Some adjustments may also be needed as explained in Chapter 5.



Flowchart 6-3. Module belonging to Flowcharts to change to a transversal-, sagittal-, or frontal slice (upper part, 11), and to change to an anatomy-, MRI-, or CT image (lower part, 12). Branches 3 and 3a refer to Flowchart 6-2.

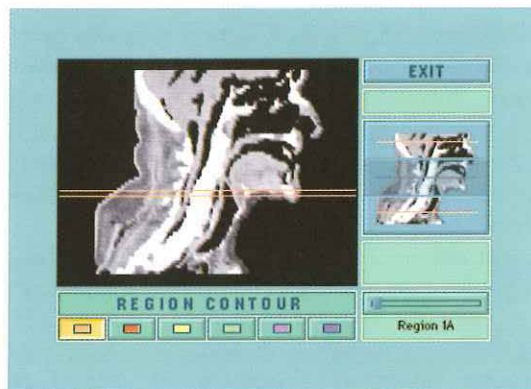
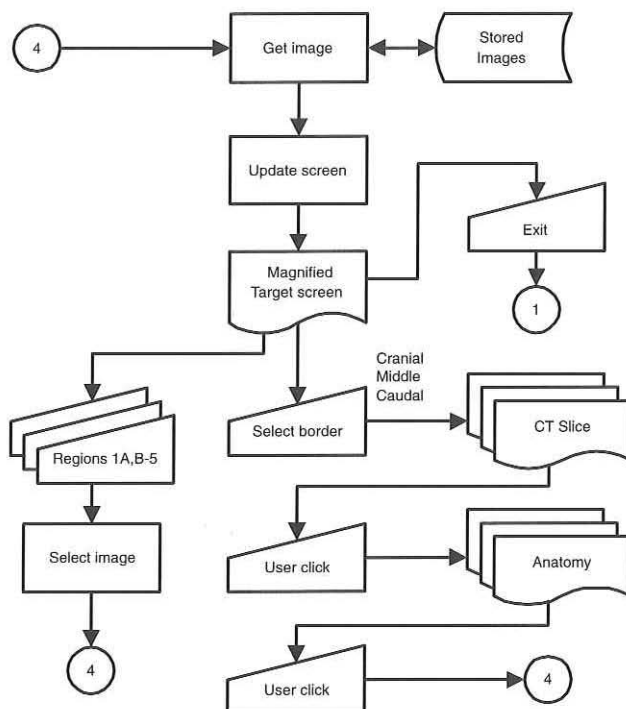


Figure 6-4. Opening screen of the "Magnified Target" menu.

6.2.3 Magnified target

The "Magnified Target" module is a summary of the "Definition Target" module. This module allows for the study of the target volume and the procedure of the definition more precisely on a few slices. For every region, full screen CT- and anatomy images are implemented at three different "levels". The "levels" are: either the images belonging to the cranial border of the region, or the images belonging to the



Flowchart 6-4. The "Magnified Target" module.

caudal border; and finally, an image "level" in between. For region 1A, the "level" in between is missing due to the position of the head of the specimen (see Figure 6-4). The borders of the regions on these anatomy images are delineated in a yellow outline, whereas the target volumes on these CT slices are given in colorwash. The colors correspond to the colors of the regions in the "Definition Target" module. They also match the colors of the buttons at the bottom of the "Magnified Target" screen (Figure 6-4). Flowchart 6-4 describes the program flow.

After pushing the "Magnified Target" button in the main menu, Figure 6-4 shows up. In the image window at the top-left a sagittal CT slice is seen. By clicking on one of the colored region buttons a specific region (Region 1a,b-5) may be chosen. The image window is updated with an image on which the cranial and caudal borders of the chosen region are indicated by lines. There is also a line in between. Also, the three buttons to the right of the image window are updated. They correspond to the lines ("levels"). By clicking on a button the CT slice belonging to that level is shown full screen. By clicking once somewhere on the screen, the corresponding anatomy image is seen full size. Clicking randomly again will bring the "Magnified Target" screen back.

Pushing the "Exit" button will display the main menu screen.

6.2.4 Beam's eye view

Figure 6-5 shows the screen after pushing the "Beam's Eye View" button. The flow of the program is illustrated in Flowchart 6-5.

This module shows the portals of all the treatment techniques discussed in Chapter 5. At the left side of the screen is the beam's eye view window. By pushing the nasopharynx or supraglottic larynx button at the top right, the primary tumor site can be chosen.

By pushing one of the numbered "technique" buttons, a particular technique may be chosen. Technique 1 consists of lateral parallel opposed portals, with or without an abutted anterior portal, as conventionally delineated by the radiation oncologist on a simulation film. Technique 2 consists of the same portals as tech-

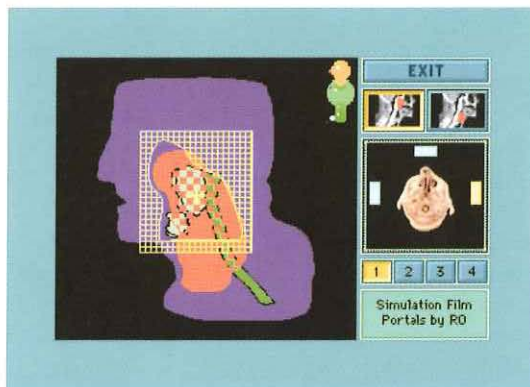
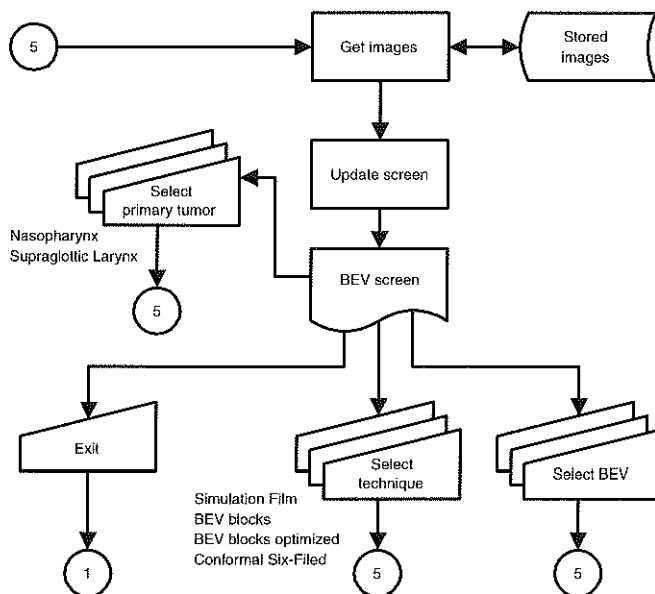


Figure 6-5. Opening screen of the "Beam's Eye View" menu.



Flowchart 6-5. The "Beam's Eye View" module.

nique 1, but the target (using the target definition of Chapter 4) has been delineated on CT slices, and then beam's eye view, customized blocks were made. Technique 2 has also been optimized to give technique 3. Portals were rotated to avoid the homo-lateral shoulder. Technique 4 is a six-field conformal technique (see Chapter 5). A short description of these techniques is given in the message box down right. The little bars in the beam setup window at the right side of the screen represent the beams belonging to the chosen technique. By clicking on such a bar, the beam's eye view of that beam is seen in the beam's eye view window.

The "Exit" button will bring back the main menu.

6.2.5 Radiation therapy

Clicking on the "Radiation Therapy" button enables the user to evaluate and compare the treatment techniques of Chapter 5. All possible actions are shown in Flowcharts 6-6, 6-7 and 6-8. The interface looks much alike the interface of the "Definition Target" module (Figure 6-6). The image area on the left shows besides the CT-, MRI- and anatomical images, DVH curves and TCP- and NTCP values to evaluate the plans. The navigation buttons to choose images act the same way as in the "Definition Target" module. One can choose transversal CT-, MRI- or anatomical slices, or frontal or sagittal CT- or MRI slices with the respective buttons, but comparison of the slices is not possible (Flowchart 6-7). Again there are a contour button (toggle), an advance forward and backward button, and a fast forward-backward option as in the "Definition Target" module, and a nasopharynx and supraglottic larynx button that work in the same way as in the "Beam's Eye View" module. When the contour button is activated, the CTV (primary tumor and elective neck) of the

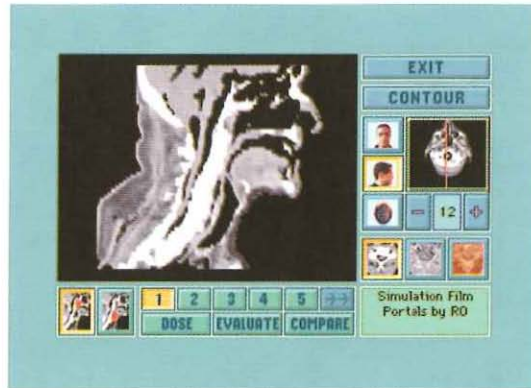
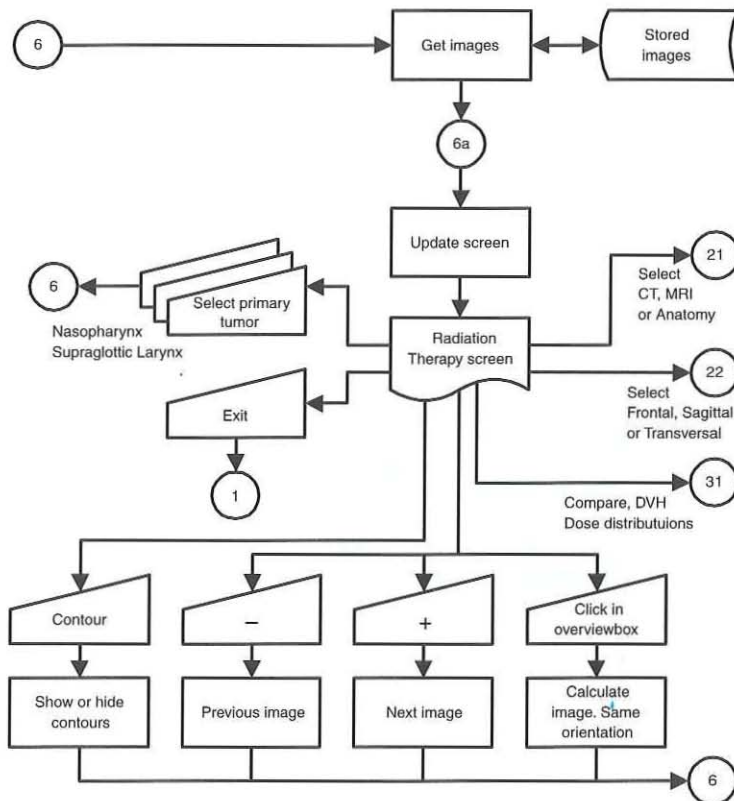
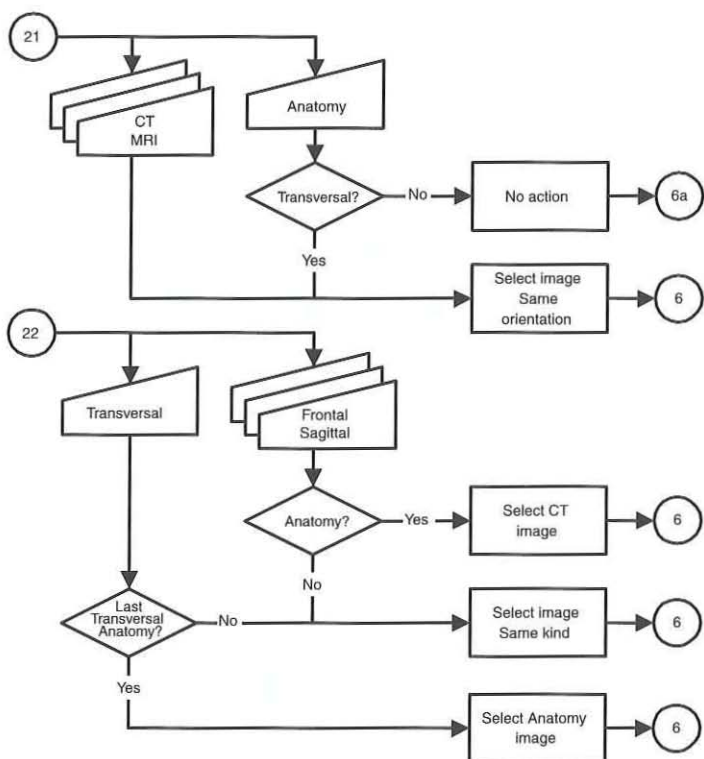


Figure 6-6. Opening screen of the "Radiation Therapy" menu.

chosen tumor site is shown in red-, the parotid glands, the submandibular glands and the spinal cord in green colorwash (Flowchart 6-6). There are now five technique buttons. The fifth technique is the same conformal radiotherapy technique as



Flowchart 6-6. The "Radiation Therapy" module.



Flowchart 6-7. Module belonging to Flowchart 6-6 to change to an anatomy-, MRI-, or CT image (upper part, 21), and to change to a transversal-, sagittal-, or frontal slice (lower part, 22). Branches 6 and 6a refer to Flowchart 6-6.

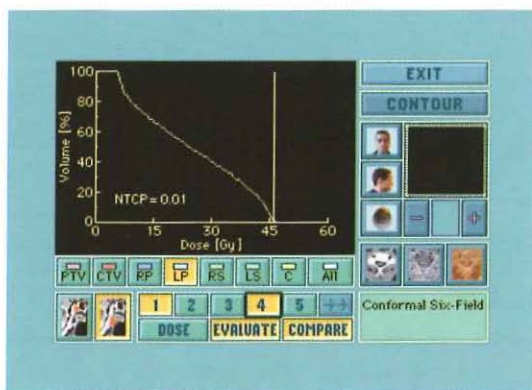
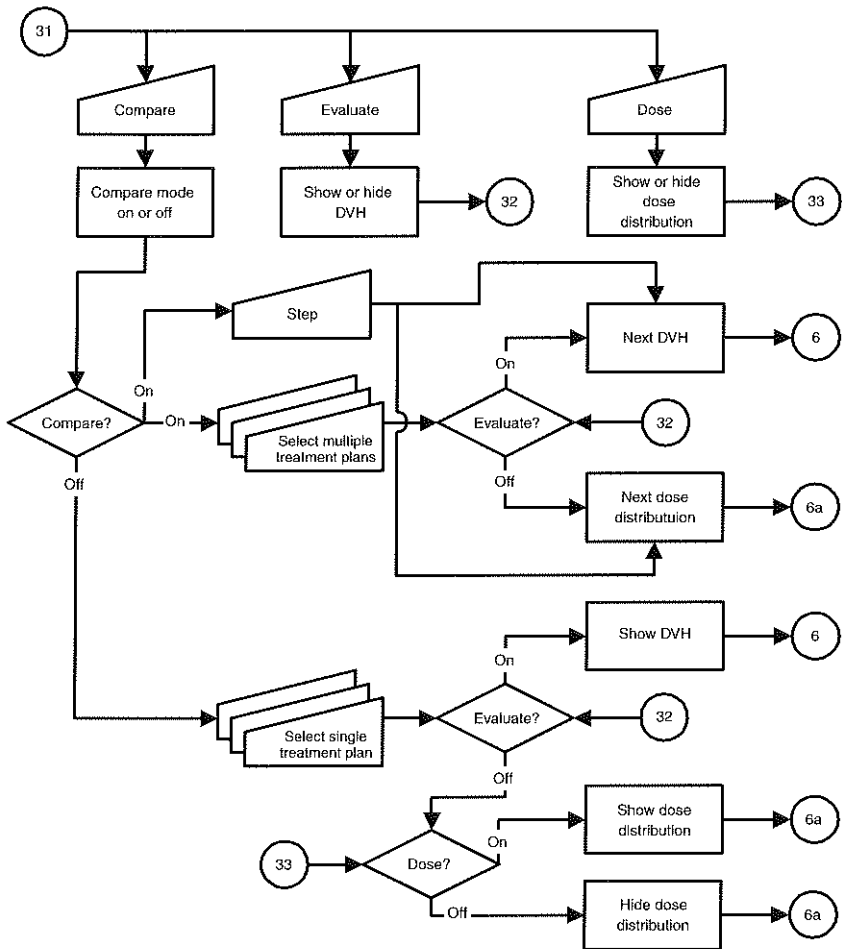


Figure 6-7. Compare and evaluate mode of the "Radiation Therapy" menu. Techniques 1 (simulation film) and 4 (conformal six-field) of an early stage supraglottic laryngeal cancer are compared. The DVH curve and NTCP value of the left parotid gland of technique 4 are shown.

shown by using button 4 (see also Chapter 6.2.4), but is calculated differently (for explanation, see Chapter 5).

Dose distributions are shown by clicking on the “Show/Hide Dose” button, which like the contour button, acts as a toggle. When this button is activated isodose curves representing 65%, 75%, 85% and 95% of the prescribed dose of the selected treatment plan are seen (Flowchart 6-8).

Special attention has been given to comparing treatment plans as illustrated in Flowchart 6-8. By clicking on the “Compare” button, which is also an on/off toggle, the program will enter a compare mode. The “Step” button is activated and it is then possible to select several or all treatment plans. By clicking the “Step” button, the dose distributions of the selected treatment plans are sequentially seen in the image window.



Flowchart 6-8. Module belonging to Flowchart 6-6 to show or hide dose distributions and DVHs, and to enter compare mode. In compare mode, dose distributions or DVHs of different treatment techniques can successively be studied by pushing only one button. Branches 6 and 6a refer to Flowchart 6-6.

Any shift of the isodose curves is easily seen without having to “remember” the precise location of these curves when comparing plans side by side. By clicking the “Evaluate” button, any image of the selected treatment plan, with or without dose distribution/contours, is replaced by the DVH curve, and TCP- and NTCP values of a volume of interest of the selected treatment plan. The volumes of interest are the CTV, the PTV, the left and right parotid glands, the left and right submandibular glands and of the spinal cord. The buttons in the image window below the DVH curve(s) allow to choose a single volume of interest, or all together. Again in the compare mode the DVH curves, and TCP- and NTCP values of the chosen treatment plans may be sequentially studied (see Figure 6-7).

The “Exit” button will bring back the main menu.

REFERENCES

References

1. Baatenburg de Jong RJ, Knegt P, Verwoerd CDA. Reduction of the number of neck treatments in patients with head and neck cancer. *Cancer* 1993;71:2312-2318.
2. Barkley HT Jr, Fletcher GH, Jesse RH, Lindberg RD. Management of cervical lymphnode metastases in squamous cell carcinoma of the tonsillar fossa, base of tongue, supraglottic larynx, and hypopharynx. *Am J Surg* 1972;124:462-467.
3. Bel A, van Herk M, Bartelink H, Lebesque JV. A verification procedure to improve patient set-up accuracy using portal images. *Radiother Oncol* 1993;29:253-260.
4. Berger DS, Fletcher GH, Lindberg RD, Jesse RH. Elective irradiation of the neck lymphatics for squamous cell carcinomas of the nasopharynx and oropharynx. *Am J Roentgenol Radium Ther Nucl Med* 1971;111:66-72.
5. Bortfeld T, Boyer AL, Schlegel W, Kahler DL, Waldron TJ. Realization and verification of three-dimensional conformal radiotherapy with modulated fields. *Int J Radiat Oncol Biol Phys* 1994;30:899-908.
6. Brennan JA, Mao L, Hruban RH, Boyle JO, Eby YJ, Koch WM, Goodman SN, Sidransky D. Molecular assessment of histopathological staging in squamous-cell carcinoma of the head and neck. *N Engl J Med* 1995;332:429-435.
7. Chow JM, Levin BC, Krivit JS, Applebaum EL. Radiotherapy or surgery for subclinical cervical node metastases. *Arch Otolaryngol Head Neck Surg* 1989;115:981-984.
8. De Neve W, van den Heuvel F, de Beukeleer M, Coghe M, Thon S, de Roover P, van Lancker M, Storme G. Routine clinical on-line portal imaging followed by immediate field adjustment using a tele-controlled patient couch. *Radiother Oncol* 1992;24:45-54.
9. Entius CAC, Kuiper JW, Koops W, de Gast A. A new positioning technique for comparing sectional anatomy of the shoulder with sectional diagnostic modalities: magnetic resonance imaging (MRI), computed tomography (CT) and ultrasound (US). *J Int Soc Plastification* 1993;7:23-26.
10. Ezz A, Munro P, Porter AT, Battista J, Jaffray DA, Fenster A, Osborne S. Daily monitoring and correction of radiation field placement using a video-based portal imaging system: a pilot study. *Int J Radiat Oncol Biol Phys* 1992;22:159-165.
11. Farr HW, Goldfarb PM and Farr CM. Epidermoid carcinoma of the mouth and pharynx at Memorial Sloan Kettering Cancer Center, 1965 to 1969. *Am J Surg* 1980;140:563-567.
12. Ferguson DB. Salivary glands and saliva. In: Lavelle CLB, ed. *Applied physiology of the mouth*. Bristol, England: John Wright and Sons, 1975:147.
13. Fletcher GH. Irradiation of subclinical disease in the draining lymphatics. *Int J Radiat Oncol Biol Phys* 1984;10:939-942.
14. Goitein M, Niemerko A, Okunieff P. The probability of controlling an inhomogeneously irradiated tumor. *Int J Radiat Oncol Biol Phys*
15. Goitein M. The comparison of treatment plans. *Semin Radiat Oncol* 1992;2:246-256.
16. Gustafsson A, Lind BK, Brahme A. A generalized pencil beam algorithm for optimization of radiation therapy. *Med Phys* 1994;21:343-356.
17. Holmes TW, Mackie TR, Reckwerdt P. An iterative filtered backprojection inverse treatment planning algorithm for tomotherapy. *Int J Radiat Oncol Biol Phys* 1995;32:1215-1225.
18. Huizenga H, Levendag PC, de Porre PMZR, Visser AG. Accuracy in radiation field alignment in head and neck cancer: a prospective study. *Radiother Oncol* 1988;11:181-187.
19. International Commission on Radiation Units and Measurements., *Prescribing, Recording, and Reporting Photon Beam Therapy (ICRU Report 50)*. Pergamon Press, New York; 1993.
20. Jacob RF, Weber RS, King GE. Whole salivary flow rates following submandibular gland resection. *Head & Neck* 1996;18:242-247.

21. Jesse RH, Barkley HT, Lindberg RD, Fletcher GH. Cancer of the oral cavity: is elective neck dissection beneficial? *Am J Surg* 1970;120:505-508.
22. Kutcher GJ, Burman C, Brewster C, Goitein M, Mohan R. Histogram reduction method for calculating complication probabilities for three-dimensional treatment planning evaluations. *Int J Radiat Oncol Biol Phys* 1991;21:137-146.
23. Leslie MD, Dische S. The early changes in salivary gland function during and after radiotherapy given for head & neck cancer. *Radiother Oncol* 1994;30:26-32.
24. Levendag PC, Hoekstra CJM, Eijkenboom WMH, Reichgelt BA, van Putten WLJ. Supraglottic larynx cancer, T1-4 N0, treated by radical radiation therapy - Problem of neck relapse. *Acta Oncol* 1988;27:253-260.
25. Levendag PC, Sessions RB, Vikram B, Strong EW, Shah JP, Spiro RH, Gerold F. The problem of neck relapse in early stage supraglottic larynx cancer. *Cancer* 1989;63:345-348.
26. Lindberg RD. Distribution of cervical lymph node metastases from squamous cell carcinoma of the upper respiratory and digestive tracts. *Cancer* 1972;29:1446-1449.
27. Makkonen TA, Edelman L, Forsten L. Salivary flow and caries prevention in patients receiving radiotherapy. *Proc Finn Dent Soc* 1986;82:93-100.
28. Meertens H, van Herk M, Bijhold J, Bartelink H. First clinical experience with a newly developed electronic portal imaging device. *Int J Radiat Oncol Biol Phys* 1990;18:1173-1181.
29. Mendenhall WM, Million RR, Cassisi NJ. Elective irradiation in squamous-cell carcinoma of the head and neck. *Head Neck Surg* 1980;3:15-20.
30. Mendenhall WM, Million RR. Elective neck irradiation for squamous cell carcinoma of the head and neck: analysis of time-dose factors and causes of failure. *Int J Radiat Oncol Biol Phys* 1986;12:741-747.
31. Mendenhall WM, Van Cise WS, Bova FJ, Million RR. Analysis of time-dose factors in squamous cell carcinoma of the oral tongue and floor of mouth treated with radiation therapy alone. *Int J Radiat Oncol Biol Phys* 1981;7:1005-1011.
32. Mira JG, Wescott WB, Starcke EN, Shannon IL. Some factors influencing salivary function when treating with radiotherapy. *Int J Radiat Oncol Biol Phys* 1981;7:535-541.
33. Nahum AM, Bone RC, Davidson TM. The case for elective prophylactic neck dissection. *Laryngoscope* 1977;87:588-599.
34. Niël CGJH. A reference frame designed to use external numeric references during simulation for tumours located in the head. *Br J Radiol* 1993;66:927-929.
35. Peters LJ, Thames HD. Dose-response relationship for supraglottic laryngeal carcinoma. *Int J Radiat Oncol Biol Phys* 1983;9:421-422.
36. Robbins KT, Medina JE, Wolfe GT, Levine PA, Sessions RB, Pruet CW. Standardizing neck dissection terminology. Official report of the academy's committee for head and neck surgery and oncology. *Arch Otolaryngol Head Neck Surg* 1991;117:601-605.
37. Shah JP, Strong E, Spiro RH, Vikram B. Neck dissection: current status and future possibilities. *Clin Bulletin* 1981;11:25-33.
38. Shah JP. Cervical lymph node metastases - diagnostic, therapeutic, and prognostic implications. *Oncology* 1990;4:61-69.
39. Shah JP. Patterns of cervical lymph node metastasis from squamous carcinoma of the upper aerodigestive tract. *Am J Surg* 1990;160:405-409.
40. Snow GB, Annyas AA, van Slooten EA, Bartelink H, Hart AAM. Prognostic factors of neck node metastasis. *Clin Otolaryngol* 1982;7:185-192.
41. Terhaard CHJ, Karim ABME, Hoogenraad WJ. Local control in T3 laryngeal cancer treated with radical radiotherapy, time dose relationship: the concept of NSD and LQ model. *Int J Radiat Oncol Biol Phys* 1991;20:1207-1214.
42. UICC, International Union Against Cancer. TNM classification of malignant tumours. Springer Verlag, Berlin; 1987.

43. Ulsø N, Brahme A. Computer-aided irradiation technique optimization. Proceedings of the Joint US/Scandinavian Symposium on Future Directions of Computer-aided Radiotherapy. San Antonio, CA, USA, August 13, 1988
44. Ulsø N, Christensen JJ. Performance evaluation of an algorithm for optimization with compensating filters. Proc. Eighth Int Conf Use of Computers in Radiation Therapy. IEEE, Toronto, Canada, July 9-12, 1984.
45. Van den Brekel MW, Castelijns JA, Stel HV, Meyer CJ, Snow GB. Modern imaging techniques and ultrasound-guided aspiration cytology for the assessment of neck node metastases: a prospective comparative study. *Eur Arch Otorhinolaryngol* 1993;250:11-17.
46. Vikram B, Strong EW, Shah JP, Spiro R. Failure at distant sites following multimodality treatment for advanced head and neck cancer. *Head Neck Surg* 1984;6:730-733.
47. Visser AG, Huizenga H, Althof VGM, Swanenburg BN. Performance of a prototype fluoroscopic radiotherapy imaging system. *Int J Radiat Oncol Biol Phys* 1990;18:43-50.
48. Wang XH, Mohan R, Jackson A, Leibel SA, Fuks Z, Ling CC. Optimization of intensity-modulated 3D conformal treatment plans based on biological indices. *Radiother Oncol* 1995;37:140-152.
49. Webb S. Optimization by simulated annealing of three-dimensional, conformal treatment planning for radiation fields defined by a multileaf collimator: II. Inclusion of two-dimensional modulation of the x-ray intensity. *Phys Med Biol* 1992;37:1689-1704.
50. Wong JW, Binns WR, Cheng AY, Geer LY, Epstein JW, Klarmann J, Purdy JA. On-line radiotherapy imaging with an array of fibre-optic image reducers. *Int J Radiat Oncol Biol Phys* 1990;18:1477-1484.

ADDENDUM A

LOCAL TUMOR CONTROL IN RADIATION THERAPY OF CANCERS IN THE HEAD AND NECK

American Journal of Clinical Oncology (CCT). 1996;19:496-477.

Peter C. Levendag, M.D., Ph.D.,^a Peter J.C.M. Nowak, M.D.,^a Maurice J.C. van der Sangen, M.D.,^a
Peter P. Jansen, M.D.,^a Wilhelmina M.H. Eijkenboom, M.D., Ph.D.,^a André S.Th. Planting, M.D.,^b
Cees A. Meeuwis, M.D., Ph.D.,^c and Wim L.J. van Putten, M.Sc.^d

From the Departments of ^aRadiation Oncology, ^bMedical Oncology, ^cHead and Neck Surgery, and
^dMedical Statistics, Dr Daniel den Hoed Cancer Center/University Hospital Rotterdam Dijkzigt,
Rotterdam, The Netherlands.

Local tumor control in radiation therapy of cancers in the head and neck.

Background: A retrospective study of 1493 head and neck cancer patients was designed to test current radiobiological thinking, postulating the detrimental effect of protracted overall treatment times (OTT) and/or split course (SC) regimes in radiation therapy on local tumor control.

Methods: Primary squamous cell carcinomas of the oral cavity (OC), oropharynx (OP), hypopharynx (HP), nasopharynx (NP), and larynx radiated with a dose of at least 50 Gy, were analyzed. Those patients treated by brachytherapy and/or primary surgery were excluded. A detailed analysis of the 997 cancers of the larynx was recently published. This paper focuses on the relationship between local tumor control and treatment characteristics for the 496 tumors originating from the OC, OP, HP, and NP. Total doses of radiation ranged from 50 to 79 Gy, with a mean of 64 Gy.

Results: A local failure (LF) was observed for 278 patients. Using Cox regression analysis, T stage and site were strongly related to LF. Corrected for T stage and with reference to OP, tumors in the NP, HP, and OC had a relative LF rate of 0.5, 1.6, and 1.8, respectively. Patients treated with continuous course (CC) and higher doses of radiation therapy fared best. No association was found with OTT and the use of chemotherapy.

Conclusions: The results observed for the OC, OP, HP, and NP are in line with the findings for the larynx. Analyzing all 1493 patients, for SC regimes lower local control rates were observed as opposed to the CC treatment series. Moreover, for the normalized total doses, a dose-effect relationship could be established. This study corroborates that disruption of the treatment per se and/or the use of suboptimal total doses of RT are detrimental; it is argued that these observations could be of relevance when designing combined modality protocols.

Keywords: Head and neck, Radiation therapy, Chemotherapy, Local control, Split course, Continuous course, Overall treatment time, Dose response

1 Introduction

In discussing how to improve cure rates in cancer of the head and neck by radiation therapy (RT), some reports highlight the existence of dose-response relationships and therefore propose the use of high(er) doses of RT (1,2). Others have stressed the importance of short overall treatment times (OTT) and/or of abandoning split course radiation therapy (SC-RT) regimes (3-10). Moreover, in the past decade, fractionation schedules based on tumor cell kinetics and intrinsic radiosensitivity have been advocated (11-15). Clinical investigators have also proposed to use the response of the (primary) tumor to a first series of RT or to a few courses of chemotherapy (CHT) as a predictor for radiocurability (16-19). The validity of some of these treatment approaches is, however, much debated because of potential accelerated repopulation of residual tumor cells during the (rest) period after the first (series of) RT or CHT courses (4,11,20-23).

Over many years, the Rotterdam head and neck Cooperative Group (Dr Daniel den Hoed Cancer Center/University Hospital Rotterdam-Dijkzigt), used a consistent RT policy, that is a SC regime (5). Recently, a detailed analysis was presented on the effects of total dose, fractionation, SC and continuous course (CC) RT, and OTT on local control in 997 patients with cancer of the larynx treated between 1965 and

1985 to a minimum dose of 50 Gy (3). This paper adds to the debate by studying similar RT treatment related factors as well as the influence of CHT on local control in an additional 496 patients with cancers in the oral cavity (OC), oropharynx (OP), hypopharynx (HP), and nasopharynx (NP). Finally, by multivariate Cox regression analysis all 1493 patients combined were analyzed.

2 Materials and Methods

Between 1965 and 1985, 496 patients were treated by RT with a minimum dose of 50 Gy for a primary squamous cell carcinoma in the OC, OP, NP, and HP. All patients were retrospectively staged according to the UICC (1987)/AJCC (1988) classification recommendations (24,25). Patient and tumor characteristics are summarized in Tables 1 and 2. Most tumors originated in the OP (36%) and HP (30%), with the remaining tumor sites equally divided between NP and OC. Regarding all tumor sites combined, 54% had stage T3/T4 and 59% had N+ disease at admission.

Table 1. Patient and tumor characteristics. N0/+ : number of patients without/with (clinically) detectable lymph nodes at admission.

Age, mean (range)	63 years (19-92)
Sex	
male	367
female	129
Site	
Oral Cavity (OC)	86
Oropharynx (OP)	178
Nasopharynx (NP)	85
Hypopharynx (HP)	147
T stage	
T1	61
T2	165
T3	175
T4	95
Nodal status	
N0	203
N+	293

2.1 RT techniques

Patients were treated in supine position. Radiotherapy was given by a linear accelerator using, in general, 4 to 8 MV photon energies in combination with high-energy electrons. Immobilizing head shells were used; after simulation, dose calculation was performed using computer planning. In the majority of cases, the target volume was treated by two lateral opposed fields with matched anterior lower neck portals down to the clavicles. Field reduction "off-cord" of the photon portals was introduced at 40 Gy. Details of the technique have been presented previously (3,5).

Table 2. Patient characteristics - distribution by T stage, nodal status, and site. OC: oral cavity; OP: oropharynx; NP: nasopharynx; HP: hypopharynx; n: total number of patients; %N+: percentage of patients with (clinically) detectable lymph nodes at admission.

T stage	Site									
	OC		OP		NP		HP		Total	
	n	%N+	n	%N+	n	%N+	n	%N+	n	%N+
T1	7	57	23	43	9	100	22	50	61	56
T2	31	32	43	60	38	74	53	38	165	51
T3	21	62	86	64	15	60	53	70	175	65
T4	27	52	26	62	23	74	19	74	95	64
Total	86	48	178	60	85	74	147	56	496	59

2.2 RT protocol

During the study period, 88% (437/496) of the patients were irradiated intentionally by a SC-RT regime. In the majority of cases, patients were treated five times per week with a conventional fraction size of 2 Gy/day. First, a series of 40 Gy was applied; subsequently after a variable split period, in case of a complete or partial response to 40 Gy or ineligibility for S (because of patient refusal or poor medical condition), a second series of RT was given. In this paper, only primary tumors irradiated with a minimum tumor dose of 50 Gy were analyzed; patients treated by brachytherapy and/or surgery (S) up front or by S for a primary cancer after a first series of 40 Gy, were excluded. Surgery for a primary cancer after a dose of 50 Gy or more was regarded as treatment for local failure (salvage); these patients were included in the present analysis. For node negative (N0) patients, elective irradiation of the neck was given in 116 of 202 (57%) patients; for T1,2 in 55% and for T3,4 in 60% of the cases. Clinically palpable neck nodes were generally treated by a booster dose of RT; however, in 36 patients the first series of 40 Gy was followed by a neck dissection.

According to running protocols during the study period, RT was frequently combined with chemotherapy (CHT) in case of advanced tumor stages (stage III/IV); that is, CHT was given in 37% (44/118) of the T1,2N+ patients and in 49% (132/270) of the T3,4 tumors. In 79 of 189 (42%) patients treated by CHT, the cytotoxic agents were given in a neoadjuvant setting; sporadically (n=6), CHT was given after completion of RT. The majority of the patients (55%; 104/189) received CHT in an intercalated fashion in between two series of RT; due to the anticipated normal tissue reactions (e.g., dose limiting severe mucositis), the total RT dose to the primary tumor in this group was limited up front to 60 Gy.

2.3 Data Analysis

Patient data were abstracted from the charts and coded on a dataform. The following data were collected: patient identification number, date of birth, sex, T and

N stage, date of diagnosis, site of disease, grade of differentiation, dates of first and last fraction of RT to primary, fraction size d_i in grays for each different fraction size applied in a particular patient series, number of fractions with fraction size d_i (nf_i ; i index for different sizes), number of fractions per day, split (split period in days of at least 7 days after a first series of 40 Gy), total dose to treated neck (node), date of end of RT, date of local relapse, date of failure in neck, survival status, date of last follow-up and/or date of death.

From the RT data additional parameters could be derived: Total physical dose in grays = $D = \sum_i nf_i \cdot d_i$, average fraction size d , sum of squared fraction doses = $dD = \sum_i nf_i \cdot d_i^2$, normalized total dose (NTD) in grays for $\alpha/\beta = 10$ and fraction size of 2 Gy {with $NTD = [(\alpha/\beta \cdot D + dD) / (\alpha/\beta + 2)]$ }, overall treatment time between first and last fraction inclusive (OTT), number of days without RT between first and last treatment (NTT).

The analysis is focused on the relationship between RT characteristics and the risk of local relapse, taking the effect of tumor characteristics into account with Cox multivariate regression analysis (26,27). Details of the data analysis methods have been described in the paper on local control and OTT regarding cancer of the larynx (3).

Table 3. First type of failure – actuarial probability at 3 years. Cancers originating in the oral cavity (OC), oropharynx (OP), nasopharynx (NP), and hypopharynx (HP). NED: no evidence of disease; N0: no lymph nodes at admission; N+: (clinically) detectable lymph nodes at presentation; LF: local failure; RF: regional failure. 262 patients presented with a LF as first type of relapse, 97 of which at some point in time also experienced a RF; 238/262 (91%) succumbed to disease. 65 patients presented with a RF as first type of relapse, 16 of which also experienced a LF at some point in time; 61/65 (94%) succumbed to disease. 32 patients presented with distant metastasis as first type of relapse and succumbed to their disease.

		Alive	Dead	Local	Regional	Dead with
	(n)	NED	NED	failure	failure	distant
		(%)	(%)	(%)	(%)	metastasis
						(%)
All	493	24	9	50	13	5
Site						
OC	86	17	11	61	9	2
OP	178	30	8	48	11	3
NP	85	35	4	30	17	14
HP	147	17	10	56	14	3
T stage						
T1/T2	226	30	10	39	15	6
T3/T4	270	18	7	60	11	4
N stage						
N0	203	30	8	54	6	2
N+	293	21	9	48	17	7

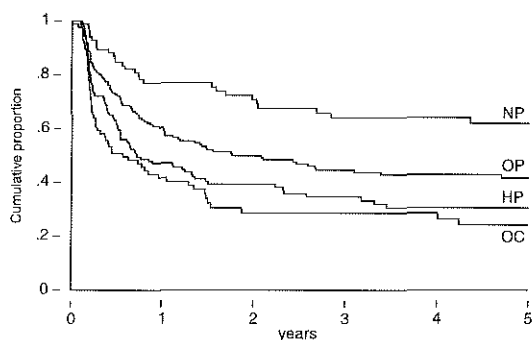


Figure 1. Patients with tumors in the oral cavity (OC), oropharynx (OP), nasopharynx (NP), and hypopharynx (HP), radiated with a minimum dose of 50 Gy. Actuarial local relapse-free probability by site.

3 Results

3.1 General aspects

At the date of last follow-up, 420 of 496 (85%) patients had died. Almost all patients with disease-related (that is, local, regional, and/or distant) failures appeared to have died within the first 3 years.

Two hundred seventy-eight (56%) patients experienced a local failure (LF); the median time to LF was 5 months, with 75% of the LF within 1 year and 95% within 3 years. Of those with a LF, 91% died of disease. Of the 218 patients remaining locally controlled, 166 (76%) eventually died; that is, 46% (77/166) after a relapse in the neck and/or with distant metastasis and 89 of 166 (54%) because of intercurrent events. Table 3 tabulates the actuarial probability of first failure type at 3 years for the different tumor sites, T stages and lymph nodal status at admission. From Table 3 it is apparent that death due to LF is more frequently seen in OC and HP tumors and in the more advanced (T3/T4) tumor stages in general. In NP, death due to distant failures is a prominent feature (Table 3).

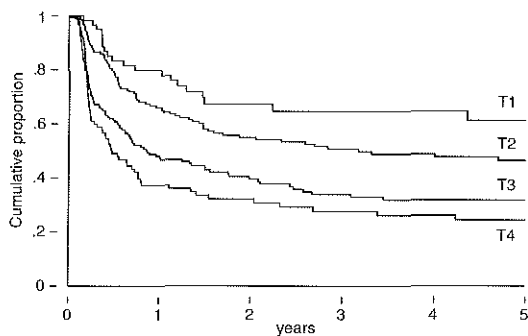


Figure 2. Patients with tumors in the oral cavity, oropharynx, nasopharynx, and hypopharynx, radiated with a minimum dose of 50 Gy. Actuarial local relapse-free probability by T stage.

Figures 1 and 2 show the actuarial local relapse-free survival (LRFS) for all tumors by site and T stage, respectively; Table 4 depicts the local relapse-free (LRF) and overall survival (OS) probabilities.

Table 4. Actuarial survival probabilities. Cancers originating in oral cavity (OC), oropharynx (OP), nasopharynx (NP), and hypopharynx (HP). N0/N+: no (clinically) detectable lymph nodes at admission; 3-year LRFS: local relapse-free survival at 3 years; 5-year OS: overall survival at 5 years; (% \pm SD): percentage \pm standard deviation.

Site	T stage	N0/N+	Number	3-year LRFS (% \pm SD)	5-year OS (% \pm SD)
OC	All stages		86	29 \pm 5	17 \pm 4
	T1/T2		38	34 \pm 9	24 \pm 7
	T3/T4		48	25 \pm 7	12 \pm 4
OP	All stages		178	45 \pm 4	28 \pm 3
	T1/T2		66	58 \pm 6	36 \pm 6
	T3/T4		112	34 \pm 5	23 \pm 4
NP	All stages		85	64 \pm 6	40 \pm 5
	T1/T2		47	73 \pm 7	48 \pm 8
	T3/T4		38	52 \pm 9	30 \pm 8
HP	All stages		147	35 \pm 4	15 \pm 3
	T1/T2		75	49 \pm 6	21 \pm 5
	T3/T4		72	18 \pm 6	8 \pm 3
All sites	All stages		493	42 \pm 2	24 \pm 2
	T1/T2		226	54 \pm 4	32 \pm 3
	T3/T4		270	32 \pm 3	18 \pm 2
		N0	203	43 \pm 4	28 \pm 3
		N+	293	42 \pm 3	21 \pm 2

3.2 Treatment characteristics

Table 5 shows the treatment characteristics for the SC-RT group as opposed to the patients treated by CC-RT. The SC-RT regime was given in 437 patients (88%), CC in 12%. The majority of fraction sizes ranged between 1.7 and 2.4 Gy; fraction sizes of 1.5-1.7 Gy were applied in 8% and those between 2.4-3.1 Gy in 10% of the cases. A close correspondence was found between the total physical dose and the normalized total dose (NTD10) ($r = 0.96$); in less than 20% the difference between total physical dose and NTD10 was more than 2 Gy, the maximum difference being 6 Gy. This difference is much smaller than the variation between patients, implying that in a regression analysis it is not possible to discriminate between these variables as covariates, that is, they are interchangeable.

The mean OTT of the SC patients was 76 days (43-121) versus 40 days (23-51 days) for the CC series. The number of days without radiation therapy between the first and the last fraction (NTT) for the SC as opposed to the CC was 47 versus 13 days (Table 5).

Table 5. Treatment characteristics. RT: radiation therapy; SD: standard deviation; dose: total physical dose; NTD: normalized total dose (see text); OTT: overall treatment time; NTT: no treatment time, that is number of days without RT between first and last fraction (see text). CC: continuous course; SC: split course.

	Split course RT, Mean (SD)	Continuous course RT, Mean (SD)	Range SC + CC
Number of patients	437	59	
Fractions	33 (4)	27 (4)	17 - 49
Fraction size (Gy)	2.0 (0.24)	2.3 (0.31)	1.5 - 3.1
Dose (Gy)	65 (5)	61 (4)	50 - 80
NTD (Gy)	65 (5)	62 (5)	49 - 80
OTT			
Days	76 (15)	40 (6)	
Range	43-121	23-51	23 - 121
NTT			
Days	47 (15)	13 (3)	
Range	23-167	7-19	7 - 167

With regard to the patients treated by a combined modality protocol, the mean OTT of the RT regime, defined as the time between the first and the last fraction, was not significantly different for the patients treated with or without CHT; that is, for the RT + CHT group, 75 days (range 42-120 days), for the RT-only group, 68 days (range 22-120 days).

No difference in LRFs was observed for the T1,2N+ or for the T3,4N0,+ category when comparing patients treated with or without CHT (Figure 3).

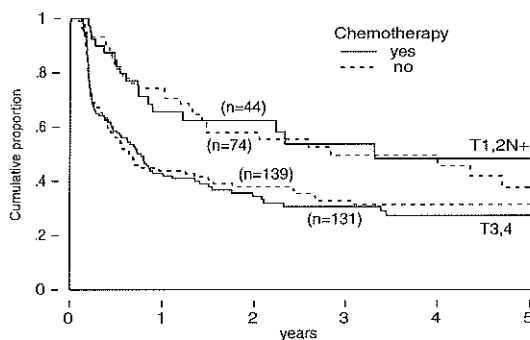


Figure 3. Patients with advanced cancers (stage III/IV) in the oral cavity, oropharynx, nasopharynx, and hypopharynx, treated by RT (minimum dose of 50 Gy), with or without chemotherapy. N0/+; patients without/with (clinically) detectable lymph nodes at admission. Actuarial local relapse-free survival for patients treated with (—) or without (---) chemotherapy for the T1,2 N+ (n=118) and T3,4 N0,+ (n=270) categories, respectively.

3.3 Prognostic factors

Local relapse-free (LRF) and overall survival (OS) rates are best in tumors originating in the NP and OP, followed by tumors of the OC and HP (Table 4). For each tumor site, T1,2 tumors fare better than locally advanced tumor stages (T3,4). A multivariate Cox regression analysis demonstrated the independent effects of T stage and site (Table 6). The relative local failure rate (RLFR) of tumors in the nasopharynx, with reference to the oropharynx, was 0.5, in the oral cavity tumors 1.8, and in the hypopharyngeal cancers 1.6. Nodal status, age, and sex were, as such, not correlated with LF when corrected for T stage and site.

Table 6. Multivariate Cox regression analysis - local relapse. Cancers in the oral cavity (OC), oropharynx (OP), nasopharynx (NP), and hypopharynx (HP). RLFR: relative locale failure rate; CI: confidence interval; CC: continuous course radiation therapy regime; SC: split course radiation therapy regime; NTD: normalized total dose (see text); OTT: overall treatment time.

	RLFR	95% CI	p
Site (vs OP)			0.000
OC	1.8	1.3-2.5	
NP	0.5	0.3-0.8	
HP	1.6	1.2-2.1	
T stage (vs T1)			0.000
T2	1.6	1.0-2.6	
T3	2.6	1.6-4.2	
T4	3.6	2.2-5.9	
NTD (+ 1 Gy)	0.97	0.95-1.0	0.02
OTT (+ 1 day)	0.99	0.98-1.0	0.13
Split (vs. CC)	1.38	0.91-2.1	0.13

The relationship between treatment characteristics (elective treatment of the neck, NTD, fraction size, OTT, CHT) and LF was also studied in a multivariate Cox regression analysis (not shown) and corrected for T stage and site; except for NTD ($p=0.02$), no significant association between any of these treatment characteristics and LF rate was observed (Table 6). Figure 4 (left panel) demonstrates the favorable outcome of T1/T2 patients treated by CC-RT, as opposed to the SC group ($p=0.04$). However, the difference in LRFS of the CC- vs SC-RT regime for T3/T4 patients was found to be not significant (Figure 4; right panel).

4 Discussion

Curability of tumors in the head and neck treated by RT is dependent on patient characteristics (e.g., age, sex, Karnofsky status), tumor specifics (e.g., tumor site, histology, differentiation grade, site, T stage, N stage), and treatment parameters (e.g., fractionation schedule, SC versus CC regimes, total dose, and OTT). We studied some of the prognostic factors retrievable from a large data base consisting of 1493

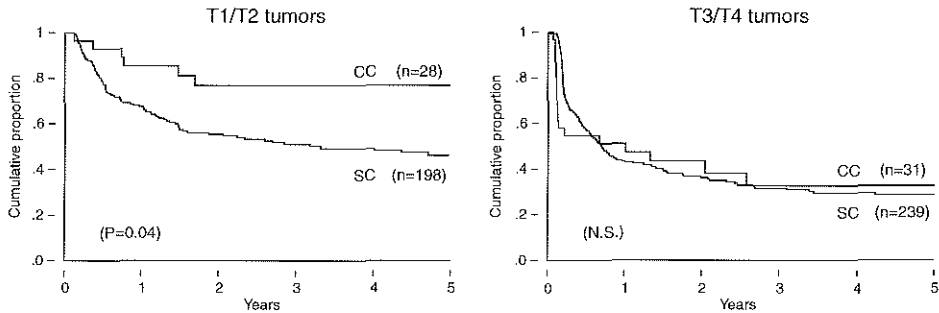


Figure 4. Patients (n=496) treated between 1965-1985 by split course (SC) or continuous course (CC) radiation therapy to a minimum primary tumor dose of 50 Gy for cancers originating in the oral cavity, oropharynx, nasopharynx, and hypopharynx. Panels display the local relapse-free probability by treatment regimes, that is split course (SC) versus continuous course (CC) RT, and T stage.

patients, treated between 1965 and 1985 by RT (with or without CHT) to a minimum dose of 50 Gy. As there is much concern in the current literature regarding the hazard of accelerated repopulation in SC regimes and/or RT schedules with long OTTs, and since SC designs are (still) not infrequently used in combined modality protocols, we have focused the analysis on this particular issue (6,7,8,9,11,22).

4.1 Tumors in the oral cavity, oropharynx, hypopharynx, and nasopharynx (n=496)

Table 4 demonstrates the poor OS rates at 5 years for the different tumor sites and T stages, varying from 8% for T3,4 hypopharyngeal (HP) tumors to 48% for T1,2 tumors originating in the nasopharynx (NP). The LRFS at 3 years varied between 18% and 73%. The LRFS is considerably better compared to the OS (Table 4), but the excess death rate due to a high number of intercurrent deaths compared to the age- and sex-matched (Dutch) standard population, is a well-established phenomenon in cancer of the head and neck (5).

Corrected for other prognostic factors and relative to the tumors in the oropharynx (OP), cancers of the NP fared best in terms of local control (RLFR 0.5; $p < 0.001$), whereas tumors of the oral cavity (OC) had a 1.8 ($p < 0.001$) and those of the HP a 1.6 ($p < 0.001$) times higher rate of relapse. Moreover, importantly, for all tumor sites with increasing dose, a significant decrease in the LF rate was observed (NTD; $p = 0.02$). Finally, OTT ($p = 0.13$), nodal status (N+ versus N0; $p = 0.95$), and sex (female vs male; $p = 0.55$) were not correlated with LF when corrected for T stage, tumor site, and split (Table 6).

At the time, RT was frequently combined with CHT for advanced tumor stages; overall, similar local control (LC) rates were observed for patients treated with CHT (39%; 74/189) as opposed to those treated without CHT (47%; 144/307). Moreover, the actuarial LRFS at 5 years showed no difference for the T1,2N+ and T3,4N0/N+ patients treated with or without CHT (Figure 3).

The multidrug CHT regimes used were cis-diaminedichloroplatinum based. In a substantial number of reports cisplatin has been shown to be a highly active agent in previously untreated patients with locally advanced head and neck cancer and may yield response rates up to 80%, with 30-40% of patients achieving a complete

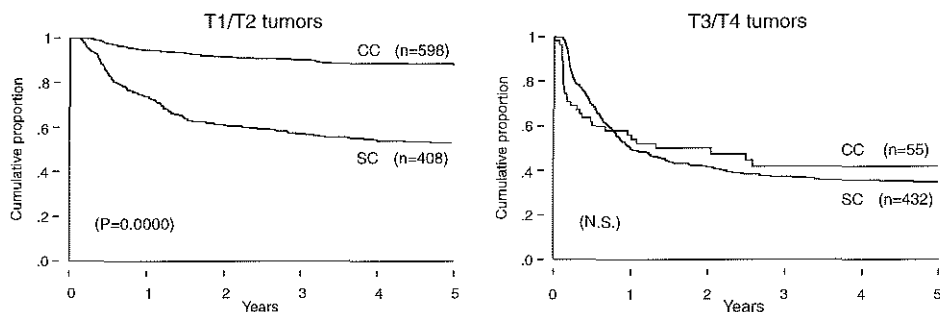


Figure 5. Patients (n=1493) treated between 1965-1985 by split course (SC) or continuous course (CC) radiation therapy to a minimum primary tumor dose of 50 Gy for cancers originating in the oral cavity, oropharynx, nasopharynx, hypopharynx and larynx. Panels display the local relapse-free probability by treatment regimes (SC vs. CC) and T stage.

response (28,29). However, the optimistic view on induction CHT has, in recent years, been considerably tempered (23). In fact, the outcome of randomized studies and the metaanalysis by Stell and Rawson even corroborated that the benefit of induction CHT is almost negligible (30). From phase II studies, the results obtained by concurrent CHT and RT (chemoradiation) seem to be more encouraging; however, normal tissue sequelae have been of major concern, thereby frequently leading to the design of studies using lower (suboptimal) doses of RT and/or introducing a rest (split) period in the treatment (31). In fact, a randomized study by Sanchiz et al. demonstrated that chemoradiation compared to adequate doses of RT alone gave similar results (32). In summary, as was recently stated by Kallman, at present, there is almost universal recognition that the effectiveness of drugs very strongly depends upon the schedule by which they are administered, as well as the intensity of the modalities used; these schedules should be studied preferably by randomized protocol designs (33).

In the multivariate Cox regression analysis, no significant impact of CHT on the LF rate in the patients of our study population could be substantiated. However, the different subsets of patients treated with CHT were small, and the study was done in a nonrandomized fashion. Moreover, the SC protocol and the combination of CHT with suboptimal doses of RT (e.g., 60 Gy for advanced tumor stages) are additional factors that might have adversely influenced the outcome.

Although the validity of using initial tumor response to RT as a predictor for either failure or control is now questionable, the large majority of our study population (88%) were treated consistently at the time by a SC-RT regime (4,20,21). From Figure 4 one can appreciate that the CC patients had a better LRFS as compared to the SC group. However, this difference in favor of the CC is only significant for the early (T1/T2) tumor stages ($p=0.04$). Moreover, after correction for T stage, nodal status, and site the difference between SC and CC for all 496 patients is no longer significant ($p=0.42$), probably due to the small total number of CC patients ($n=59$) (Table 6). Since some of these findings might lack statistical power because of too small numbers of patients in the different subsets, in the next section we have analyzed the influence of split, overall treatment time, and dose on LF for all 1493 head

and neck cancers, including the patients with cancer of the larynx published in detail by van Putten et al. in a recent paper (3).

4.2 All head and neck tumor sites combined (n=1493) with special reference to dose-response and split course irradiation

As can be seen from Figure 5, patients treated by CC-RT fare (much) better than those treated by a SC regime. In particular for the T1/T2 tumors, a significant difference was found ($p < 0.001$) (Figure 5, left panel). Due to the treatment philosophy at the time, especially in the advanced tumor stages (T3/T4), SC-RT was the preferred treatment; indeed, in the CC-T3/T4 category only 55 patients are available for analysis and (probably for that reason) the difference between SC versus CC was found to be not significant ($p=0.82$) (Figure 5, right panel).

In dose-effect relationships the effect of dose on LF is assumed to be a continuous effect in the sense that a higher dose implies more cell kill, and thus a lower LF rate. In Figures 6 and 7, the probability of local relapse at 3 years is shown as a function of normalized treatment dose (NTD) for T1/T2 versus T3/T4 tumor stages, treated by either CC-RT (Figure 6) or SC-RT (Figure 7). Except for the T1/T2-CC patients, the data summarized by both figures generate evidence for the existence of a dose-response relationship. For example, Figure 7 indicates that a 10 Gy decrease in total dose roughly corresponds with an 8% decrease in local control. However, as was also previously reported by the group of Parsons et al., with regard to the T1/T2 tumors, probably high doses of RT might not be so relevant for small tumors treated adequately in a CC fashion (Figure 6) (10).

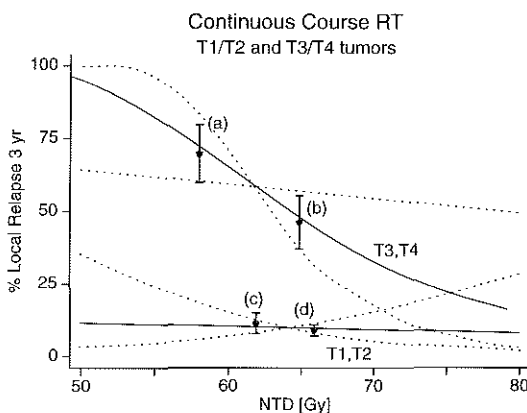


Figure 6. Patients with all head and neck tumor sites combined (oral cavity, oropharynx, nasopharynx, hypopharynx, and larynx; see text), treated with continuous course radiation therapy (n=653). The solid curves show the by Cox multivariate analysis fitted probability of local relapse at 3 years (LF-3) as a function of the normalized total dose (NTD) for T1,T2 and T3,T4 tumors, corrected for site. Each curve goes through a reference point defined by the mean NTD and the actuarial LF-3 probability of the group (T1,T2: mean NTD = 64.3 Gy, LF-3 = 9.9%; T3,T4: mean NTD = 61.9 Gy, LF-3 = 58.1%). The dotted curves are the boundaries of the 95% confidence region. In addition, the actuarial LF-3 probabilities with standard error bars are plotted in subgroups defined by NTD and T stage: (a) T3,T4, NTD \leq 60 Gy (n=24); (b) T3,T4, NTD $>$ 60 Gy (n=31); (c) T1,T2, NTD \leq 64 Gy (n=239); and (d) T1,T2, NTD $>$ 64 Gy (n=359). These points are plotted at the mean NTD of each subgroup.

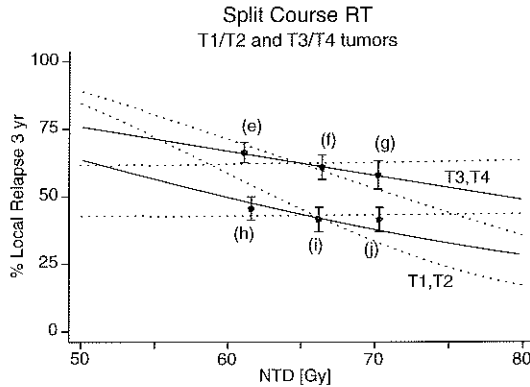


Figure 7. Patients with all head and neck tumor sites combined (see also legend Figure 6), treated with split course radiation therapy (n=840). Actuarial LF-3 probabilities with standard error bars in subgroups: (e) T3,T4, NTD \leq 64 Gy (n=200); (f) T3,T4, NTD 64-69 Gy (n=136); (g) T3,T4, NTD $>$ 69 Gy (n=96); (h) T1,T2, NTD \leq 64 Gy (n=148); (i) T1,T2, NTD 64-69 Gy (n=124); and (j) T1,T2, NTD $>$ 69 Gy (n=136).

The OTT is strongly correlated with the length of the disruption (= split duration) of the treatment, so (not shown) an analysis was performed regarding the effects of OTT. However, in a multivariate analysis, no effect could be substantiated.

5 Summary

This review has implicit, well-known limitations because of its retrospective nature; for example, selection bias during the long-term cohort of the study with (many) changes in physicians over time can not be totally excluded.

Concurrent with radiobiological thinking is the establishment of a dose-response relationship. That is, with higher doses of RT fewer local failures were observed, a finding which seems to be even more important for the more advanced tumor stages, with a higher clonogenic tumor load to be killed. Introduction of a split in the treatment also leads to more local failures (if not compensated for by the use of higher doses of RT). No difference in local relapse-free survival was observed for patients treated with or without chemotherapy. It was concluded that for local control, the use of optimal high total doses of radiation and the elimination of SC regimes are important and can be envisaged to be of relevance when designing combined modality protocols, for example, for advanced cancers in the head and neck.

We could not unequivocally demonstrate an effect of OTT. One speculation could be that interruption of the treatment per se (split) is an overriding discrete effect.

Acknowledgments: The authors greatly acknowledge P. van Assendelft, C.J.M. Hoekstra and J. van den Doel for helping evaluating the data set; the members of the Rotterdam Head and Neck Oncology Group for their expertise in patient care; and Ms. I. Dijkstra for her excellent secretarial work in preparing this manuscript.

References

1. Peters LJ, Thames HD. Dose-response relationship for supraglottic laryngeal carcinoma. *Int J Radiat Oncol Biol Phys* 1983; 9:421-422.
2. Terhaard CHJ, Karim ABMF, Hoogenraad WJ. Local control in T3 laryngeal cancer treated with radical radiotherapy, time dose relationship: the concept of NSD and LQ model. *Int J Radiat Oncol Biol Phys* 1991; 20:1207-1214.
3. Van Putten WLJ, Van der Sagen MJC, Hoekstra CJM, Levendag PC. Dose, fractionation and overall treatment time in radiation therapy - the effects on local control for cancer of the larynx. *Radiother Oncol* 1994; 30:97-108.
4. Levendag PC, Ravasz LA, Terhaard CHJ, Hordijk GJ. T3 squamous cell carcinoma of the larynx treated by a split-course radiation protocol. A multiinstitutional study. *Am J Clin Oncol* 1993; 16:509-518.
5. Hoekstra CJM, Levendag PC, Van Putten WLJ. Squamous cell carcinoma of the supraglottic larynx without clinically detectable lymph node metastases: problem of local relapse and influence of overall treatment time. *Int J Radiat Oncol Biol Phys* 1990; 18:13-21.
6. Bentzen SM, Johansen LV, Overgaard J, Thames HD. Clinical radiobiology of squamous cell carcinoma of the oropharynx. *Int J Radiat Oncol Biol Phys* 1991; 20:1197-1206.
7. Bentzen SM, Thames HD. Clinical evidence for tumor clonogen regeneration: interpretations of the data. *Radiother Oncol* 1991; 22:161-166.
8. Maciejewski B, Withers HR, Taylor JMG, Hliniak A. Dose fractionation and regeneration in radiotherapy for cancer of the oral cavity and oropharynx: tumor dose-response and repopulation. *Int J Radiat Oncol Biol Phys* 1989; 16:831-843.
9. Maciejewski B, Withers HR, Taylor JMG, Hliniak A. Dose fractionation and regeneration in radiotherapy for cancer of the oral cavity and oropharynx. Part 2. Normal tissue responses: acute and late effects. *Int J Radiat Oncol Biol Phys* 1990; 18:101-111.
10. Parsons JT, Bova FJ, Million RR. A reevaluation of split-course technique for squamous cell carcinoma of the head and neck. *Int J Radiat Oncol Biol Phys* 1980; 6:1645-1652.
11. Withers HR, Taylor JMG, Maciejewski B. The hazard of accelerated tumor clonogen repopulation during radiotherapy. *Acta Oncol* 1988; 27:131-146.
12. Trott KR, Kummermehr J. What is known about tumor proliferation rates to choose between accelerated fractionation or hyperfractionation? *Radiother Oncol* 1985; 3:1-9.
13. Tucker SL, Chan KS. The selection of patients for accelerated radiotherapy on the basis of tumor growth kinetics and intrinsic radiosensitivity. *Radiother Oncol* 1990; 18:197-211.
14. Fowler JF. Brief summary of radiobiological principles in fractionated radiotherapy. *Semin Radiat Oncol* 1992; 2:16-21.
15. Begg AC, Hofland I, Van Glabbeke M. Predictive value of potential doubling time for radiotherapy of head and neck tumor patients: results from the EORTC cooperative trial 22851. *Semin Radiat Oncol* 1992; 2:22-25.
16. Terhaard CHJ, Wiggenraad RG, Hordijk GJ, Ravasz LA. Regression after 50 Gy as a selection for therapy in advanced laryngeal cancer. *Int J Radiat Oncol Biol Phys* 1988; 15:591-597.
17. Ensley JF, Jacobs JR, Weaver A. Correlation between response to cis-platinum combination chemotherapy and subsequent radiotherapy in previously untreated patients with advanced squamous cell cancers of the head and neck. *Cancer* 1984; 54:811-814.
18. Pfister DG, Strong E, Harrison L. Larynx preservation with combined chemotherapy and radiation therapy in advanced but resectable head and neck cancer. *J Clin Oncol* 1991; 9:850-859.

19. Veterans Affairs Laryngeal Cancer Study Group. Induction chemotherapy plus radiation compared with surgery plus radiation in patients with advanced laryngeal cancer. *New Engl J Med* 1990; 324:1685-1690.
20. Sobil S, Rubin P, Keller B, Poulter C. Tumor persistence as a predictor of outcome after radiotherapy of head and neck cancers. *Int J Radiat Oncol Biol Phys* 1976; 1:873-880.
21. Suit HD, Lindberg R, Fletcher GH. Prognostic significance of extent tumor regression at completion of radiation therapy. *Radiology* 1965; 84:1100-1107.
22. Tubiana M. Repopulation in human tumors - a biologic background for fractionation in radiotherapy. *Acta Oncol* 1988; 27:83-88.
23. Rosenthal DI, Pistenmaa DA, Glatstein E. A review of neoadjuvant chemotherapy for head and neck cancer: partially shrunken tumors may be both leaner and meaner. *Int J Radiat Oncol Biol Phys* 1994; 28:315-320.
24. International Union Against Cancer. TNM classification of malignant tumours. Berlin/Heidelberg: Springer Verlag, 1987.
25. American Joint Committee on Cancer. Manual for Staging of Cancer. Philadelphia: Lippincott, 1988.
26. Cox DR. Regression models and life tables. *J R Stat Soc* 1972; B 34:187-220.
27. Berry G. The analysis of mortality by the subject-years method. *Biometrics* 1983; 39:173-184.
28. Zidan J, Kuten A, Cohen Y. Multidrug chemotherapy using bleomycin, methotrexate and cisplatin combined with radical radiotherapy in advanced head and neck cancer. *Cancer* 1987; 59:24-26.
29. Ervin TJ, Clark JR, Weichselbaum RR. An analysis of induction and adjuvant chemotherapy in the multi-disciplinary treatment of squamous cell carcinoma of the head and neck. *J Clin Oncol* 1987; 5:10-20.
30. Stell PM, Rawson NS. Adjuvant chemotherapy in head and neck cancer. *Br J Cancer* 1990; 61:779-787.
31. Denham JW, Abbott RL. Concurrent cisplatin, infusional fluorouracil, and conventional fractionated radiation therapy in head and neck cancer: dose-limiting mucosal toxicity. *J Clin Oncol* 1991; 9:458-463.
32. Sanchiz F, Milla A, Torner J. Single fraction per day versus two fractions per day versus radiochemotherapy in the treatment of head and neck cancer. *Int J Radiat Oncol Biol Phys* 1990; 19:1347-1350.
33. Kallman RF. The importance of schedule and drug dose intensity in combinations of modalities. *Int J Radiat Oncol Biol Phys* 1994; 28:761-771.

ADDENDUM B

RADIATION THERAPY FOR CANCER OF THE PIRIFORM SINUS

—

A FAILURE ANALYSIS

American Journal of Clinical Oncology (CCT). 1995;18:502:509.

Ineke J.M. van Mierlo, M.D., Peter C. Levendag, M.D., Ph.D., Wilhelmina M.H. Eijkenboom, M.D.,
Ph.D., Peter P. Jansen, M.D., Cees A. Meeuwis, M.D., Ph.D., Piet J. van Assendelft, M.Sc.,
Wim L.J. van Putten, M.Sc. and Peter J.C.M. Nowak, M.D.

Dr. Daniel den Hoed Cancer Center, Depts. of Radiation Oncology,
Head and Neck Surgery, and Medical Statistics, Rotterdam, The Netherlands.
This work is a co-operative study of the Rotterdam Head and Neck Cooperative Group.

Radiation therapy for cancer of the piriform sinus – a failure analysis

This paper analyzes the results of 109 piriform sinus cancers treated between 1973 and 1984 by surgery and/or external beam radiation therapy (EBRT) in a large comprehensive cancer center, and in particular tries to redefine the role of EBRT in the management of these tumors. At the time the policy was to start with EBRT to a dose of 40 Gy. A good response to a first series was to be continued by EBRT (RT-1); in case of poor responding tumors, the primary and neck were to be operated upon (RT-S). Poor responders unfit for surgery or those refusing surgery were also carried to a full course of EBRT (RT-2). The RT-S, RT-1, and RT-2 actuarial 5-year locoregional relapse-free survival (LR-RFS) and overall survival (OS) were 60%, 40%, and 20% and 40%, 30%, and 20%, respectively. In a multivariate Cox regression analysis the most important prognostic factor appeared to be N stage, with hazard ratios of 1.16 (N1), 2.2 (N2), and 3.3 (N3). The RT-S treatment group fared best (hazard ratio 0.5). The risk of relapse for T3,4 was 1.3 times as high as opposed to T1,2. For stage I/II (19/21 treated by EBRT only), a LR-RFS and OS at 5 years of 60% and 40%, respectively, was observed. This analysis supports data for stage III/IV piriform sinus cancers to be treated by surgery combined with EBRT; in stage I/II there might be a role for EBRT alone. It is speculated that with further sophistication in RT-techniques, the locoregional control rates by EBRT alone could improve.

Keywords: Head and neck cancer, Hypopharynx, Piriform sinus, Radiotherapy, Surgery, Conformal radiotherapy.

1 Introduction

For cancers of the hypopharynx it seems fair to summarize that patients have a grim outlook due to a high incidence of locoregional failure and distant metastasis; 5-year survival rates generally range from 20% to 40% (1,2). Cancers of the piriform sinus constitute the majority of hypopharyngeal tumors and are thought to have the best prognosis, particularly when diagnosed at an early stage. Most patients with piriform sinus cancer unfortunately present with locally advanced tumors. Moreover, approximately 70%-80% of patients have nodal disease at presentation (3-6). Most of the (even recent) oncological literature on the hypopharynx does not discriminate between specific subsites, so detailed reports on cancer of the piriform sinus proper are scarce. Therefore, a retrospective analysis of patients with cancer of the piriform sinus treated in the Dr. Daniel den Hoed Cancer Center (DDHCC) and University Hospital Rotterdam Dijkzigt (UHR-D) was performed. Surgery of the primary site, with or without EBRT, is generally considered to be the mainstay of the treatment. One specific goal of the analysis was to see whether a role for primary EBRT with larynx (voice) preservation could be defined for a subset of patients.

2 Material and Methods

From January 1973 through December 1984, 161 patients with carcinoma of the hypopharynx were treated by the Rotterdam Head and Neck Cooperative Group. The location of the primary tumor was piriform sinus in 130 patients, posterior pharyngeal wall in 22 patients, and postcricoid in 9 cases. We confined our study pop-

ulation to the piriform sinus cancers, treated over the years consistently by a protocol in which the treatment modalities used depended on the response of the primary cancer to a first series of 40 Gy ("RT-selective" protocol). The censor date was January 1, 1993. From the 130 piriform sinus cancer patients, 3 were excluded from further analysis because of distant metastases at presentation. Another 7 patients were excluded because they did not receive radiation therapy (RT) from the start, that is, they were, for reasons not evident from the charts, operated on upfront. Five patients were excluded because of histology other than squamous cell carcinoma. The remaining 115 piriform sinus squamous cell carcinomas form the data set of the present report.

All patients were retrospectively restaged according to the classification rules of the AJCC-1988/UICC-1987 editions (Table 1) (7,8). For the 115 patients, the mean age was 65 (range 30-86)- 93 men, 22 women. Regarding the differentiation grade: 8 were well-differentiated, 43 moderately differentiated, 47 poorly or undifferentiated and for 11 patients the differentiation grade of the cancers was unknown.

Table 1. Piriform sinus cancer 1973-1984 DDHCC/UHR-D

N stage	T stage				Total
	T1	T2	T3	T4	
N0	7	14	22	3	46
N1	1	3	12	6	22
N2a	2	6	7	1	16
N2b	3	5	6	1	15
N2c	1	2	4	1	8
N3	3	1	4	0	8
Total	17	31	55	12	115

During the study period the treatment protocol was to start with EBRT to a dose of 40 Gy (2 Gy per fraction/5 days per week) to the primary tumor and neck by a linear accelerator, using low-energy photons (4-8 MV) and electrons (10 MeV). A second course of EBRT (protocol: total dose 30 Gy) was given in case a good response of the primary tumor (and neck nodes) to the first series of 40 Gy was obtained (RT-1 group; 55 patients). For those tumors considered as poor responders, that is, less than partial response, the primary and neck were to be operated upon (RT-S group; 26 patients).

Those patients refusing surgery or found medically unfit for operation after a poor response to the first series of 40 Gy, were also given a second course of EBRT (RT-2 group; 28 patients). Table 2 presents a stratification of the number of patients according to the different treatment groups. Apparently, 6 tumors were given a low cumulative dose of EBRT (mean dose 34 Gy; range: 21-40 Gy); because of a poor general condition the treatment of these patients had to be terminated at low doses with a residual tumor mass still in situ ("N0Tx": no treatment group) and, subsequently, these patients experienced early death (survival range: 1-6 months). These 6 patients were ultimately excluded from the data set exploring the role of EBRT in

control of cancers in the piriform sinus, leaving 109 full-protocol patients to be analyzed for local control and survival by EBRT alone versus EBRT plus surgery (Table 2).

Table 2. Piriform sinus cancer 1973-1984 DDHCC/UHR-D

Choice of Treatment	RT-I	RT-II	RT-S	NOTx	Total
Good Response	55	—	—	—	55
Refusing Surgery	—	7	—	—	7
Inoperable	—	21	—	—	21
Poor Response	—	—	26	—	26
Inadequate Treatment	—	—	—	6	6
Total	55	28	26	6	115

In analyzing the 109 cases, the primary tumor appeared to have been irradiated with a mean total dose of 65 Gy (range: 50-72 Gy) for the RT-1 group of patients; 64 Gy (range: 40-70 Gy) for the RT-2 group; and 42 Gy (range: 30-70 Gy) for the RT-S group.

In almost every case (104/109) both sides of the neck were electively irradiated by a first series of EBRT. Subsequently, neck nodal disease was treated in the majority of cases by the modality that was used to manage the primary cancer; that is, in 64 of 83 (77%) cases by EBRT and in 19/83 (23%) of the patients by means of a neck dissection for the piriform sinus cancers treated by EBRT only (RT-1/RT-2 groups). In contrast, in all patients of the RT-S group presenting with neck nodes, a neck dissection was performed.

Table 3. Piriform sinus cancer 1973-1984 DDHCC/UHR-D

Cause of Death	RT-I	RT-II	RT-S	Total
Tumor	29	21	9	59
Intercurrent	12	2	4	18
Postoperative Complication	—	—	3	3
Second Primary	2	—	1	3
Unknown	3	1	1	5
Total	46	24	18	88

3 Results

Of 109 piriform sinus cancer patients, 88 ultimately died (81%); that is, 46/55 (84%) of the RT-1 patients, 24/28 (86%) of the RT-2 patients, and 18/26 (69%) of the RT-S patients. The cause of death for all 88 patients is listed in Table 3. The influence of stage on the probability of locoregional relapse-free survival and overall survival at 3, 5, and 10 years is illustrated in Table 4.

Table 5 presents the number of patients per treatment group failing locally, regionally, and with distant metastasis; in Table 6 the type and sequence of relapse are given. Of the relapsing patients only 6/37 (16%) of the RT-1 group, 1/24 (4%) of the RT-2 group, and none (0/11) of the RT-S group survived.

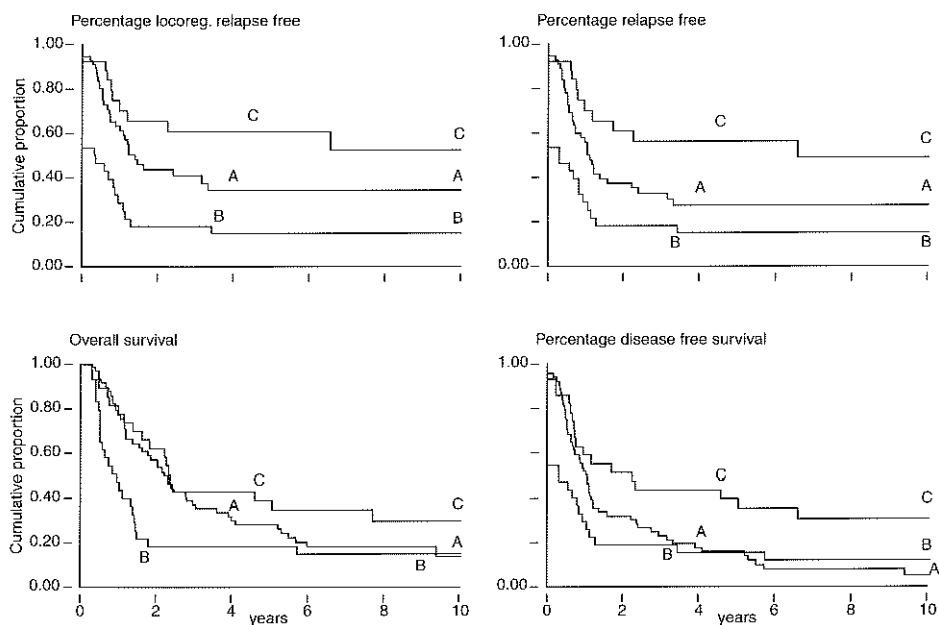


Figure 1. Patients (n=109) with piriform sinus cancers treated between 1973 and 1984 in the DDHCC/UHR-D. Upper left panel: actuarial locoregional relapse-free survival; upper right panel: relapse-free survival; lower left panel: overall survival; lower right panel: disease-free survival. In all panels the survival is presented for each treatment subgroup (RT-1, RT-2, RT-S) separately.

Figure 1 depicts the actuarial locoregional relapse-free survival, the relapse-free survival, the overall survival, and the disease-free survival at 10 years for 109 piriform sinus cancer patients, stratified for the treatment groups RT-1, RT-2, and RT-S. Figure 2 shows similar actuarial survival curves as depicted in Figure 1, now for early-stage piriform sinus cancers (T1,2N0) as opposed to more advanced tumor stages (stage III/IV).

Table 4. Piriform sinus cancer 1973-1984 DDHCC/UHR-D

Tumor Stage	LR-RFS (3-year)	OS (3-year)	LR-RFS (5-year)	OS (5-year)	LRFS (10-year)	OS (10-year)
T1N0	0.625	0.571	0.625	0.429	0.625	
T2N0	0.500	0.643	0.417	0.500	0.417	0.500
Stage I/II	0.559	0.619	0.497	0.476	0.497	0.286
Stage III/IV	0.352	0.261	0.315	0.226	0.280	0.135
Total	0.393	0.330	0.351	0.274	0.324	0.172

4 Discussion

4.1 General Aspects

As has been reported previously, there is a constant force of mortality due to all causes of death during the years of follow-up in cancer of the head and neck. In the

present series this phenomenon is substantiated by the difference between the relapse-free survival and overall survival curves (Figures. 1 and 2), and by the causes of death; that is, 30% (26/88) of the patients died of nontumor related causes (5 unknown, 21 nonprimary tumor-related) (Table 3).

Table 5. Piriform sinus cancer 1973-1984 DDHCC/UHR-D

	Local Failure	Regional Failure	Distant Failure
RT-I	28 (51)	13 (24)	9 (16)
RT-II	21 (75)	13 (46)	4 (14)
RT-S	2 (8)	9 (35)	3 (12)
All	51 (47)	35 (32)	16 (15)

With regard to the treatment-related type of morbidity, the locoregional treatment of piriform sinus cancer by EBRT alone has the advantage over surgery of organ sparing; that is, by preserving the natural swallowing mechanism and speech. However, this could obviously be a trade-off against the chance for cure. In general, given the results reported in the current literature on cancer of piriform sinus proper for the advanced tumor stages, surgery combined with EBRT seems to offer increased locoregional control rates and survival over EBRT alone (3,4). Some centers even emphasize the feasibility of preservation of the larynx and optimal tumor control by a surgical approach for some of the early lesions (9,10). However, in gen-

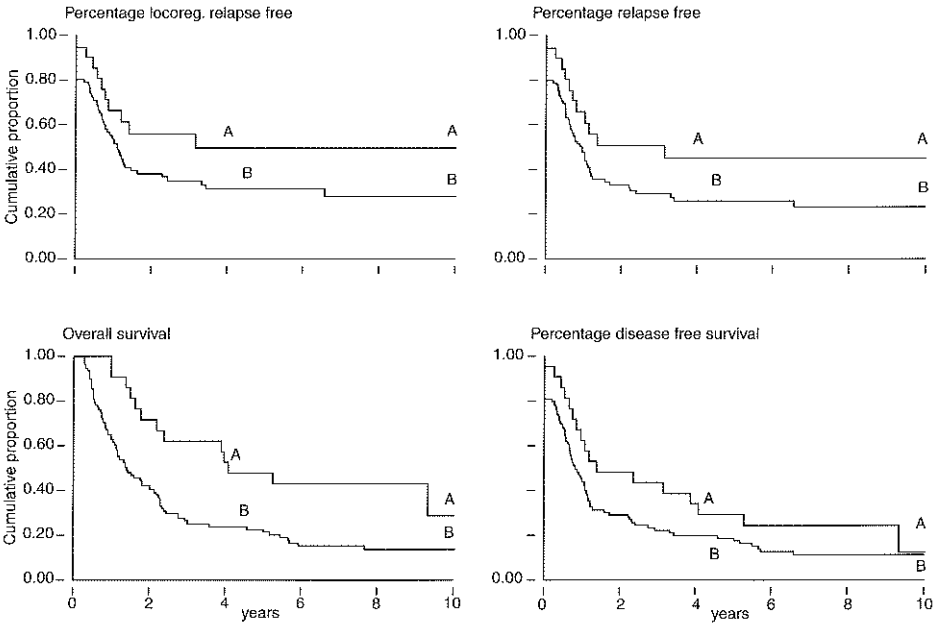


Figure 2. Patients (n=109) with piriform sinus cancers treated between 1973 and 1984 in the DDHCC/UHR-D. Upper left panel: actuarial locoregional relapse-free survival; upper right panel: relapse-free survival; lower left panel: overall survival; lower right panel: disease-free survival. In all panels the survival is presented for early (stage I/II) and advanced tumor stages separately.

eral for the early staged lesions the matter seems to be more controversial, that is, institutional preferences differ between surgery and EBRT alone (9-13). Unfortunately, there is no randomized trial comparing conservation surgery and/or EBRT alone for stage I and II piriform sinus cancer; at best, one can compare the results with the data reported in the current literature. For instance, Marks and colleagues (9) reported local control in 70 out of 80 (88%) piriform sinus cancers treated by preoperative EBRT combined with partial pharyngolaryngectomy; Vandenbrouck and colleagues (10) obtained local control in 16/18 (89%) piriform sinus cancers treated by conservation surgery. With respect to T1 and T2 piriform sinus cancers treated by EBRT alone, Bataini and coworkers (11) achieved local control in 68% (61/90) and in a series reported by Dubois and coworkers (12) 44/60 (73%) of T1/T2 tumors were controlled. In a recent paper by Mendenhall and coworkers (13), a local control rate of 85% (62/73) was observed in T1/T2 piriform sinus lesions treated by EBRT only. Finally, from these data it is apparent that the likelihood of survival for EBRT alone was similar to that after conservation surgery.

Table 6. Piriform sinus cancer 1973-1984 DDHCC/UHR-D

Sequence of Relapse	RT-I	RT-II	RT-S	Total
Local	18	10	1	29
Regional	2	3	6	11
Distant	5	—	1	6
Local → Regional	7	6	1	14
Regional → Local	1	1	—	2
Local → Distant	1	1	—	2
Regional → Distant	1	—	2	3
Distant → Regional	1	—	—	1
Local → Regional → Distant	1	3	—	4
Total	37	24	11	72

4.2 Stage III/IV Piriform Sinus Cancer: Present Series

In our series 24/88 (27%) of the patients with advanced tumor stages were treated by EBRT and surgery (RT-S treatment group); moreover, 24/26 (92%) of the RT-S patients had stage III/IV cancers. For the RT-S treatment group an actuarial locoregional relapse-free survival of about 60% and an overall survival of approximately 40% at 5 years was found (Figure 1). Patients with advanced tumor stages ($n = 38$) and thought to be eligible for EBRT only (good responders, RT-1) had a significantly worse locoregional control rate and survival; that is, a locoregional relapse-free survival of 40% and an overall survival of approximately 20% (Figure 1). A multivariate Cox regression analysis was performed with the endpoints locoregional relapse-free survival, overall survival, and disease-free survival with covariate treatment groups (RT-1, RT-2, and RT-S), T stage, N stage (Table 7). The most important prognostic factor appeared to be N stage, with hazard ratios of 1.16 (N1), 2.2 (N2), and 3.3 (N3). The RT-S treatment group fared best, with a hazard ratio of 0.5. Application of the Cox model (14) showed that the risk of relapse for the T3,4

patients was 1.3 times higher as opposed to the T1,2 patients. So, in conclusion, this analysis supports current literature data for stage III/IV piriform sinus cancers to be treated preferably by surgery combined with EBRT if the aim is optimal chance for control of the primary cancer and given the patient is a suitable candidate indeed for a (major) surgical procedure. It is of relevance, in this respect, that in this series of 88 patients with stage III/IV piriform sinus cancers, 26 poor-responding tumors were considered unsuitable for surgery at the time because of their inoperability *per se*, overall poor medical condition or patient refusal and were, consequently, treated by EBRT (RT-2 group). This selection bias in the treatment options for advanced head and neck tumors favoring EBRT for patients for instance with a low Karnofsky status, is a well-known general phenomenon, and it cannot be excluded that this might have unfavorably influenced the overall treatment results by EBRT alone.

Table 7. Piriform sinus cancer 1973-1984 DDHCC/UHR-D

	Cox model		
	Hazard ratio	se	p-value
RT-I/II	1.654	0.452	0.068
RT-S	0.556	0.204	0.113
N1	1.161	0.428	0.687
N2	2.203	0.618	0.006
N3	3.303	1.557	0.013
T3,4	1.335	0.343	0.264

4.3 Stage I/II Piriform Sinus Cancer: Present Series

In our series, 19 of 21 (91%) of T1,2N0 piriform sinus cancers were treated by EBRT only. The locoregional control (approximately 60% at 5 years) and overall survival (approximately 40% at 5 years) of stage I/II piriform sinus cancers is significantly better as opposed to the results observed in the more advanced tumor stages treated by EBRT, but similar to the best results obtained in the present series, that is, for the patients of the RT-S treatment group (Figures 1 and 2). The survival rates are not dissimilar to those reported in the literature (3,4,9-13). With regard to the control of the primary site: however, some papers did report higher local control rates for T1/T2 piriform sinus cancers with EBRT alone (13).

This sort of comparison, however, is subject to various biases inherent to the evaluation of nonrandomized data. More importantly, given the study period, that is 1973-1984, we feel there are a number of reasons to anticipate on a potential improvement in the results to be obtained, particularly by EBRT:

4.3.1 Neck Control

The impact of neck disease on locoregional control and survival is corroborated by the N stage being the most important prognostic factor in the multivariate Cox regression analysis in our series (hazard ratios 1.161-3.303; Table 7). Overall, a high

regional failure rate was observed in the irradiated patients as well as in the surgically treated patients; 24% in the RT-1, 46% in the RT-2, and 53% in the RT-S patients (Table 5). Since only 20 of 35 nodal relapses were concurrent at some point in time with a local relapse (Table 6), this high neck recurrence rate could not be explained solely by "re-seeding" from a failure at the primary site. We felt that an additional factor might have been, as has been discussed previously (15), the somewhat too low dose of radiation in the electively irradiated necks. Also, during the study period detection of neck nodes was done on clinical palpation. There are currently sufficient reliable data available showing that, with better diagnostic means (e.g., CT/MRI-scanning and ultrasound), more neck nodes can be detected at an earlier date (earlier stage) (16,17). We now routinely use ultrasound (combined with cytological aspirations), and pathologically positive nodes are treated by means of a (bilateral) neck dissection and/or higher (booster) doses of EBRT.

4.3.2 Radiobiological Considerations

There is some debate as to whether the initial tumor response is a good predictor for either failure or control of the irradiated tumors (18-20). Also, there has been some concern expressed in the current literature of accelerated repopulation of clonogenic tumor cells after a lag period of about 4 weeks (21-23). The average split period in our "RT-selective" protocol for piriform sinus cancer was 4-6 weeks. In order to improve the results, we have now abandoned split course regimes in all

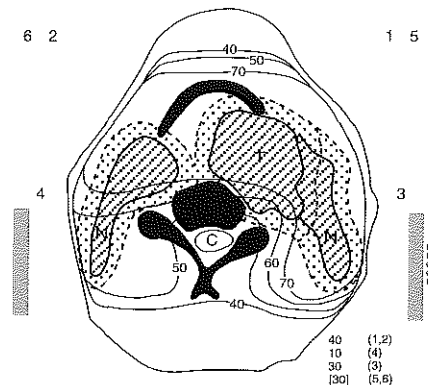


Figure 3. Anatomical data and tumor outline taken from CT slice of patient with piriform sinus cancer. Schematic diagram for treatment technique and dose distributions for piriform sinus cancer patients treated at the DDHCC/UHR-D between 1973 and 1984 by EBRT. Technique: The target volume is radiated by two parallel opposed wedged fields, using 4 MV photons (fields 1 and 2); the lower neck (nodes) by an abutted anterior photon portal (not depicted in the diagram). The posterior part of the piriform sinus lies in close proximity to the vertebra/cord. After a total dose of 40 Gy, the spinal cord is shielded in the 4 MV photon fields and the primary tumor is taken to 70 Gy (fields 5 and 6). An ipsilateral low energy electron field (10 MeV) is added to the parallel opposed (blocked) photon fields to boost the posterior part of the primary tumor to a dose of 70 Gy (field 3); in a number of patients the posterior contralateral neck was carried (electively) to a cumulative dose of 50 Gy (field 4). As can be seen from the diagram, using this technique part of the target volume could have been underdosed, in particular when dealing with bulky lesions.

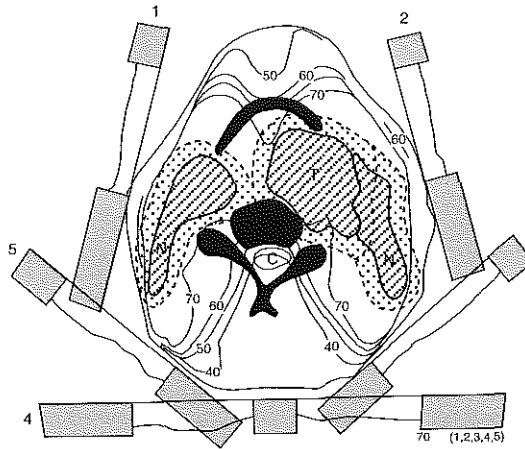


Figure 4. Example of stage I/II piriform sinus cancer treated by EBRT, using 3D conformal radiation therapy techniques. This tumor was hypothetically radiated by a 5-field technique using beam modifiers. As is demonstrated in this schematic diagram, the target volume (primary tumor) can be easily taken to a cumulative dose of 70 Gy without overdosing the normal tissues (compare also Figure 3).

head and neck cancers. Moreover, we no longer use initial tumor responses to EBRT as a means of incriminating potential failures (18).

4.3.3 Radiotherapy Techniques

Over the years a lot of interest has been shown in increasing the tumor control rates by individually tailoring the radiation therapy fractionation regimes, albeit conventional-, hyper- or accelerated fractionation and concomitant boost techniques. Although these individualized fractionation regimes certainly might prove to be of value (24), trying to improve on the EBRT techniques per se should also be underscored (25). The anatomy of the piriform sinus is complicated in the sense that part of the target volume lies in close proximity to the cord and parotid glands. Using a conventional strictly parallel opposed field technique, combining low energy (e.g., 4-8 MV) photons and low energy electrons (e.g., 10 MeV), will have limitations in this respect. For example, let us compare a piriform sinus cancer to be irradiated by conventional EBRT techniques (Figure 3; diagram of actual CT slice of patient with piriform sinus cancer), as opposed to the same tumor mass now treated by three-dimensional conformal EBRT, making use of beam modifiers (Figure 4). The target is defined as primary piriform sinus tumor and neck, including a 0.7 cm margin for microscopic disease and positioning uncertainty. As is demonstrated in the schematic diagrams with the superimposed computed isodose lines, when using simple parallel opposed techniques, dose escalation of the tumor is difficult without the risk of surpassing the tolerance of the cord; xerostomia is inevitable because of the high doses delivered to the (parotid) glands. Moreover, for conventional dose levels (e.g., 70 Gy), part of the target volume could be even underdosed. An improvement in dose distribution is shown in Figure 4, applying multiple beams with beam modifiers, trying to confine the prescribed dose to the target volume only (three-dimen-

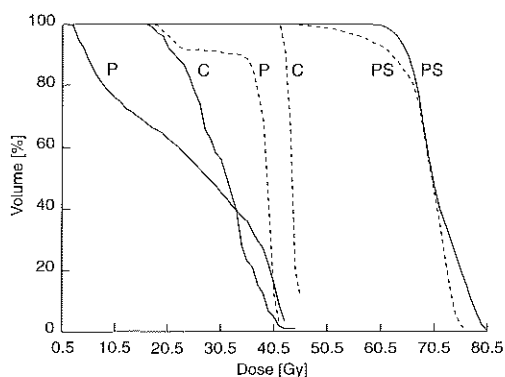


Figure 5. Dose volume histograms for primary piriform sinus cancer, parotid gland (P) and cord (C), comparing conventional treatment technique (Figure 3; stipulated lines) and conformal EBRT using a 5-field technique with beam modifiers (Figure 4; solid lines).

sional conformal therapy). The dose volume histograms given in Figure 5 illustrate that the target volume can now easily be taken to a cumulative dose of 70 Gy without overdosing the normal (critical) tissues.

5 Conclusion

From the present report it is concluded that the majority of piriform sinus cancers have stage III/IV disease and should preferably be treated by surgery combined with EBRT. Given the results obtained in stage I/II piriform sinus cancer treated by with EBRT alone, we feel that EBRT with conservation of the pharynx and larynx should not be discarded as a valid treatment option; moreover, one could even speculate that by improving on the radiation therapy techniques we might be able to achieve substantial higher locoregional control rates with less morbidity in the near future.

Acknowledgments: We gratefully acknowledge Mr. E. Woudstra (Dept. of Clinical Physics) for helping evaluate the 3D computer planning data, and the members of the Rotterdam Head and Neck Cooperative Group for their expertise in patient care (Drs. M.F. de Boer, P.P.M. Knegt, M. Scholtemeyer, H. Spoelstra, L.L. Visch, A. Planting, and S.J.M. Wijthoff). The excellent secretarial work of Mrs. I. Dijkstra in preparing this manuscript is much appreciated.

References

1. Suen JY, Myers EN. Cancer of the Head and Neck. New York: Churchill Livingstone, 1981.
2. Ho CM, Lam KH, Wei WI, Yuen PW, Lam LK. Squamous cell carcinoma of the hypopharynx: analysis of treatment results. *Head Neck* 1993;5:405-12.
3. Tandon DA, Bahadur S, Chatterji TK, Rath GK. Carcinoma of the hypopharynx: results of combined therapy. *Indian J Cancer* 1991;28:131-8.
4. Kleinsasser O, Glanz H, Kimmich T. Zur Behandlung der Karzinome des Sinus piriformis. *HNO* 1989;37:460-4.

5. Wang CC. Carcinoma of the hypopharynx. In: Wang CC, ed. Radiation therapy for head and neck neoplasms. Indications, Techniques and Results. Boston: John Wright PSG, 1983;155-64.
6. Byhardt RW, Cox JD. Patterns of failure and results of preoperative radiation vs radiation alone in carcinoma of the piriform sinus. *Int J Radiat Oncol Biol Phys* 1980;6:1135-41.
7. American Joint Committee on Cancer, Manual for Staging of Cancer. 3rd Ed. Philadelphia: Lippincott, 1988:33-5.
8. UICC TNM Classification of Malignant Tumours. Berlin: Springer-Verlag, 1987.
9. Marks JE, Kurnik B, Powers WE, Ogura JH. Carcinoma of the piriform sinus: An analysis of treatment results and patterns of failure. *Cancer* 1978;41:1008-15.
10. Vandenbrouck C, Eschwege F, De la Rochefordière A, et al. Squamous cell carcinoma of the piriform sinus: Retrospective study of 351 cases treated at the Institute Gustave-Roussy. *Head Neck Surg* 1987;10:4-13.
11. Bataini P, Brugere J, Bernier J, Jaulerry CH, Picot C, Ghossein NA. Results of radical radiotherapeutic treatment of carcinoma of the piriform sinus: Experience of the Institute Curie. *Int J Radiat Oncol Biol Phys* 1982;8:1277-86.
12. Dubois JB, Guerrier B, Di Ruggiero JM, Pourquier H. Cancer of the piriform sinus: Treatment by radiation therapy alone and with surgery. *Radiology* 1986;160:831-6.
13. Mendenhall WM, Parsons JT, Stringer SP, Cassisi NJ, Million RR. Radiotherapy alone or combined with neck dissection for T1T2 carcinoma of the piriform sinus: an alternative to conservation surgery. *Int J Radiat Oncol Biol Phys* 1993;27:1017-27.
14. Cox DR. Regression models and life tables. *J R Stat Soc B* 1972;34:187-220.
15. Levendag PC, Hoekstra CJM, Eijkenboom WMH, Reichgelt BA, Van Putten WLJ. Supraglottic cancer, T1-4N0, treated by radical radiation therapy: problem of neck relapse. *Acta Oncol* 1988;27:253-60.
16. Van den Brekel MWM, Castelijns JA, Croll GA, et al. Magnetic resonance imaging vs palpation of cervical node metastasis. *Arch Otolaryngol Head Neck Surg* 1991;117:666-73.
17. Baatenburg de Jong RJ, Rongen RJ, De Jong PC, Laméris JS, Knegt PPM. Screening for lymphnodes in the neck with ultrasound. *Clin Otolaryngol* 1988;13:5-9.
18. Levendag PC, Ravasz LA, Terhaard CHJ, Hordijk GJ. T3 squamous cell carcinoma of the larynx treated by a split-course radiation protocol. *Am J Clin Oncol* 1993;16:509-18.
19. Terhaard CHJ, Wiggenraad RG, Hordijk GJ, Ravasz LA. Regression after 50 Gy as a selection for therapy in advanced laryngeal cancer. *Int J Radiat Oncol Biol Phys* 1988;15:591-7.
20. Sobil S, Rubin P, Keller B, Poulter C. Tumor persistence as a predictor of outcome after radiotherapy of head and neck cancers. *Int J Radiat Oncol Biol Phys* 1976;1:873-80.
21. Withers HR, Taylor JMG, Maciejewski B. The hazard of accelerated tumor clonogen repopulation during radiotherapy. *Acta Oncol* 1988;27:131-46.
22. Bourhis J, Wilson G, Wibault P, et al. In vivo measurement of the potential doubling time by flow cytometry in oropharyngeal cancer treated by conventional radiotherapy. *Int J Radiat Oncol Biol Phys* 1993;26:793-9.
23. Van Putten WLJ, Van der Sagen MJC, Hoekstra CJM, Levendag PC. Dose, fractionation and overall treatment time in radiation therapy - the effects on local control for cancer of the larynx. *Radiother. Oncol.* 1994;30:97-108.
24. Tucker SL, Chan KS. The selection of patients for accelerated radiotherapy on the basis of tumor growth kinetics and intrinsic radiosensitivity. *Radiother Oncol* 1990;18:197-211.
25. Sailor SL, Sherouse GW, Chaney EL, Rosenman JG, Tepper JE. A comparison of postoperative techniques for carcinomas of the larynx and hypopharynx using 3-D dose distributions. *Int J Radiat Oncol Biol Phys* 1991;21:767-77.

ADDENDUM C

SIMULATION ACCURACY IN RADIOTHERAPY FOR MAXILLARY SINUS TUMORS

International Journal of Radiation Oncology, Biology, and Physics. 1995;32:815-821.

Charles G.J.H. Niël, M.D., Jan P.C. van Santvoort, John R. van Sörnsen de Koste,
Peter J.C.M. Nowak, M.D. and Peter C. Levendag, M.D., Ph.D.

Dr. Daniel den Hoed Cancer Center, Depts. of Radiation Oncology
and Clinical Physics, Rotterdam, The Netherlands

Simulation accuracy in radiotherapy for maxillary sinus tumors

Purpose: To evaluate the accuracy and clinical importance of beam positioning during simulation of radiation treatment for tumors in the maxillary sinus.

Methods and Materials: Five patients were prepared as if they were to be treated for a maxillary sinus tumor. A three-beam computed tomography (CT) scan-based computer plan was made for each patient. The location of the central beam axis of each beam was measured, relative to bony anatomical structures. A simulation was performed using the bony references to position the radiation beams during simulation. After this, the simulation procedure was repeated by the use of a noninvasive external localization frame with a known accuracy and reproducibility within 2 mm margins.

Results: When defining the clinical target volume as the known tumor with a 1 cm margin, three out of five patients would suffer a partial geographical miss throughout the entire radiation treatment due to erroneous beam positioning at the simulation stage when using bony structures as a guide for beam positioning. The influence of these errors is analyzed as normal tissue complication and tumor control probabilities.

Conclusion: When defining a planning target volume, one should consider a margin to correct for possible simulation errors. We advise the use of objective, external (and thus nonanatomical) landmarks as a reference during simulation to reduce this extra margin to a minimum. In case of simulation, using bony structures as a reference, an additional margin should be entered, depending on the simulation accuracy that can be obtained.

Keywords: Maxillary sinus cancer, Radiotherapy, Treatment simulation, Accuracy, Local control, Complication.

1 Introduction

One of the major advances in clinical radiotherapy during the last 10 years has been the introduction of conformal beam therapy. This treatment modality requires a high precision in both preparation and the actual treatment stage. The complexity of radiation therapy for maxillary sinus tumors resembles conformal beam therapy to a certain extent: covering the target volume is largely restricted by the tumor-surrounding normal tissues (14). Moreover, beam positioning during treatment simulation is hampered by the large amount of bony structures that can serve as a landmark, easily leading to a situation in which one cannot see the wood for the trees. Lack of accuracy in radiation treatment preparation for maxillary sinus tumors might therefore be a reason why these tumors recur in a large number of patients (up to 80% of the patients are faced with local recurrence), even after a complete remission after radiotherapy alone or in combination with surgery or regional chemotherapy (the so-called Sato's treatment) (19,20). Indications for the validity of this statement are publications on the influence of the introduction of computed tomography (CT) scanning in radiotherapy planning of maxillary sinus tumors, after which the local control rate and the survival of patients with a maxillary sinus tumor increased significantly (8,9,18,22).

The high number of unexpected radiotherapy-related complications to tumor-surrounding normal tissues is a second argument to consider radiation treatment preparation for maxillary sinus tumors suboptimal. We therefore tried to evaluate

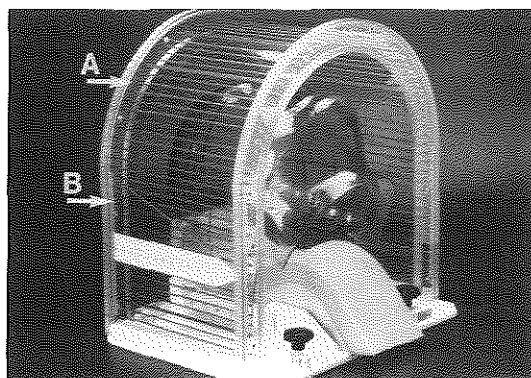


Figure 1. Noninvasive external localization frame with patient fixed in position by a vacuum mask. A: parallel rods; B: Lucite triangle.

the beam positioning accuracy during treatment simulation, one of the most critical steps in radiotherapy, because an error made at this stage will be repeated throughout the entire treatment, largely influencing treatment outcome.

2 Methods and Materials

For the aim of the study, a noninvasive external localization frame was developed (16). This frame was used to compare beam positions as a result of simulation, based on bony anatomical landmarks with beam positioning based on objective, external (and thus nonanatomical) numeric references.

The design of the frame is based on a concept similar to stereotactic frames used routinely in neurosurgery. In contrast to these frames, localization can be performed without computed calculation of coordinates by direct read-out of external numeric references.

The technique of this frame is described elsewhere (16). In brief, it consists of parallel graphite rods, located in the craniocaudal axis and parallel to the table top (Figure 1). These rods are depicted on the CT scan as points, serving as a reference in the anteroposterior and laterolateral direction (Figure 2). At one side of this frame a lucite triangle serves as a reference in the craniocaudal direction; this triangle is seen on the CT scan as a line with a certain length, depending on the location in the craniocaudal direction in which the CT scan is performed (Figures 1 and 2, B). The accuracy and the clinical reproducibility of beam positioning using this frame was found to be within 2 mm margins (16).

Five patients were prepared as if they were treated for a maxillary sinus tumor. During each step of the procedure the patient was immobilized with a vacuum mask to assure reproducible patient positioning in the best achievable way (this is within 2 mm margins under optimal conditions (6,22,25)). CT planning was performed for a three-beam radiation technique, the planning target volume being confined to the maxillary sinus, the tuber maxillae, and the bottom of the orbita, all with a 1 cm margin to cover subclinical disease. CT scans with the noninvasive external localization frame were performed every 5 mm (1). A three-dimensional

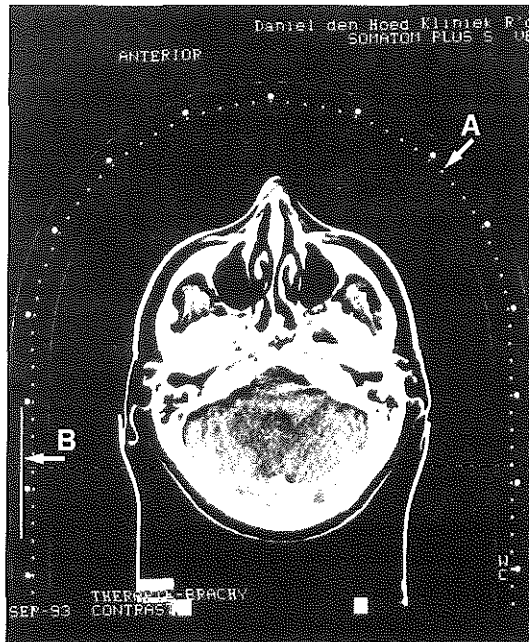


Figure. 2. CT-scan image of immobilized patient with the noninvasive external localization frame. (A) Parallel rods depicted as dots; (B) Lucite triangle depicted as a line.

(3D) treatment plan was made with the Cadplan treatment planning system (2). One anterior and two lateral beams were chosen to adequately cover the target volume and beam blocks were positioned in the beam's eye view to reduce the dose of the surrounding normal tissues to a minimum. This resulted in a homogeneous irradiation of the target volume to a total dose of 70 Gy, with a maximum dose of 20% to

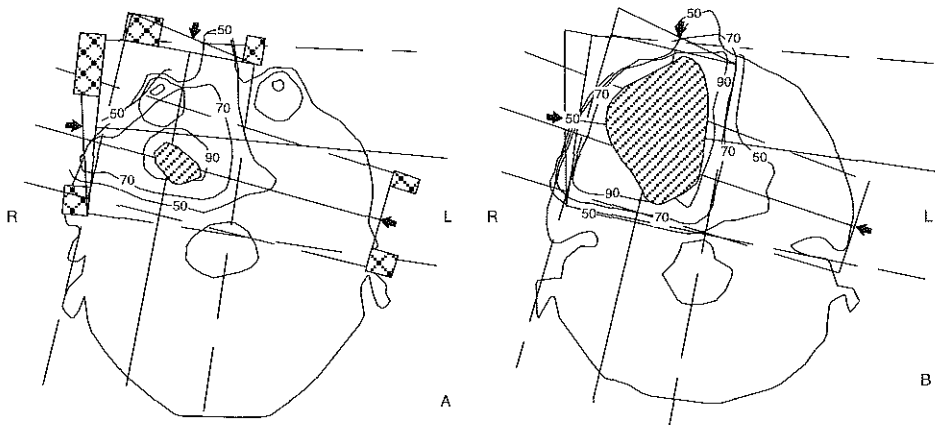


Figure 3. (A) Three-beam computer-assessed 3D treatment plan (Cadplan, Dosetek-Varian); plane through eye lens (70 Gy prescribed dose at 90%, normalization according to ICRU). (B) Three-beam computer-assessed 3D treatment plan (Cadplan, Dosetek-Varian); central plane (70 Gy prescribed dose at 90%, normalization according to ICRU).

the contralateral lens of the eye and of 64% to the spinal cord (Figures 3a and 3b). Each patient was simulated according to his CT-based treatment plan, using the bony structures as a reference for beam positioning during simulation. At this stage the beam portal outlines were indicated on the patient to enable reproducible beam positioning throughout the entire treatment. To avoid introduction of a bias, the simulations were performed by radiation oncologists other than the authors. The non-invasive external localization frame was used to check the accuracy of the simulations. The advantage of this system over the use of radio-opaque catheters mounted on a patient's mask is its ease in use and the addition of references in the craniocaudal direction (24).

The difference between beam positions, resulting from treatment simulation using bony references and beam positions as achieved by using the noninvasive external localization frame, was noted in the laterolateral and craniocaudal direction for the anterior portal, and in the anteroposterior and craniocaudal direction for the right and left lateral portal (all expressed in mm). New dose distributions were calculated, applying these beam positioning errors on the computer plan of one patient, serving as the reference plan.

Table 1. Beam position errors at time of simulation, detected by the noninvasive external localization frame. SD = standard deviation; CC = craniocaudal, AP = anteroposterior, LL = laterolateral; all expressed in mm

Beam	Left		Right		Anterior	
Patient						
no.	CC	AP	CC	AP	CC	LL
1	-8	7	-8	16	-8	3
2	-10	6	-10	-8	-10	10
3	14	3	14	0	14	11
4	-10	5	-10	-2	-10	0
5	13	-5	13	3	13	6
Mean	-0.2	3.2	-0.2	1.8	-0.2	6
SD	11.2	4.3	11.2	8.0	11.2	4.1

A dose volume histogram (DVH) analysis of these dose distributions was performed, together with an analysis of normal tissue complication probability (NTCP) and tumor control probability (TCP) values. The TCPs were calculated from the DVHs according to the clinical response model of Goitein, also described by Munzenrider (5,15). The parameters (dose-response curve for maxillary sinus tumors) for this model were obtained from the data from the literature (2,11,13). The NTCPs were calculated according to the model by Kutcher, using the data of Emami, and fitted as described by Burman (1,3,12).

3 Results

The beam positioning errors made during simulation for maxillary sinus tumors are given for each patient and as an average in Table 1. Although the mean error

made for all patients is low, indicating that these errors occur at random, the individual dislocation of the beams was unexpectedly large. In three out of the five patients (patients 1, 3, and 5) it was found to be more than 1 cm for at least one beam in at least one direction. This also becomes clear from the standard deviation for the errors in the three directions. Because the positioning error is introduced during simulation, the greatest error is the single absolute greatest error in whatever direction and not the mean error per patient in the three directions. It is then clear that three out of five patients will have a systematic error (in at least one direction) introduced of at least 1 cm. These patients would therefore suffer a partial geographical miss throughout the entire treatment when defining the clinical target volume as the known tumor with a 1 cm margin.

The possible clinical value of enhancing simulation accuracy in maxillary sinus tumors was assessed by the DVH, TCP, and NTCP analysis. All five patients were compared with the computer-assessed plan serving as the best achievable clinical result (the intended plan). In ideal circumstances, that is, treatment simulation identical to the computer plan (which can be achieved within 2 mm accuracy by the use of the noninvasive external localization frame), the DVH shows a very steep fall off from 100% to 0% at 70 Gy (Figure 4). The patients in whom simulation was performed using bony landmarks as a reference for beam positioning clearly suffer from a partial geographical miss, as can be seen in their respective target DVH (Figure 4). As expected, the patient with the largest simulation error has the lowest TCP. As an average, the TCP for the five patients was about one-third (27%) of the TCP of the intended plan (78%, Table 2).

Table 2. TCP- and NTCP values when simulated and treated according to treatment plan (intended plan: using the noninvasive external localization frame) or with simulation errors (patient 1-5: simulating by anatomical landmarks).

	TCP	NTCP ipsilateral eye lens	NTCP contralateral eye lens	NTCP spinal cord
intended plan	0.776	1.000	0.072	0.000
patient no. 1	0.413	0.618	0.007	0.000
patient no. 2	0.225	0.016	0.002	0.001
patient no. 3	0.088	1.000	0.997	0.013
patient no. 4	0.472	0.070	0.001	0.000
patient no. 5	0.159	1.000	0.966	0.004
mean (1-5)	0.271			

As to the normal tissues, the contralateral eye lens, when irradiated according to the treatment plan, receives a dose well below its tolerance, which also holds for those patients with the smallest simulation errors. However, in the two patients with the largest beam positioning errors, the contralateral eye lens is irradiated to a considerably higher dose, which is expressed in a large NTCP value (Table 2).

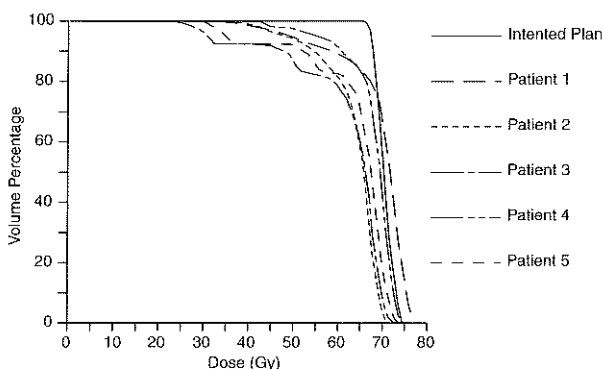


Figure 4. Dose volume histogram for the target volume. Intended plan: simulated and treated according to treatment plan (noninvasive external localization frame). Patient 1-5: treated according to beam position errors of simulation (anatomical landmarks).

In contrast, the right eye lens (which receives the full dose when irradiating according to the computer plan) was found to receive doses well below its tolerance level in the patients with the largest beam positioning errors (Table 2). The spinal cord in all cases was irradiated to a dose well below its tolerance due to the larger distance to the target volume (Table 2).

4 Discussion

Much attention is given to the daily (random) beam positioning accuracy during radiation treatment. This uncertainty factor is accounted for in the planning target volume, defined as the clinical target volume with a margin necessary to avoid a partial geographical miss due to these daily beam or patient positioning errors (ICRU report no. 50). Virtually no information is found, however, about the magnitude and possible clinical relevance of errors made in the process of simulation when bony structures serve as a reference for beam positioning, a method still widely in use. Despite the considerable clinical influence of simulation errors, the reason for this lack of knowledge is unclear. The only publications dealing with the clinical importance of radiation treatment preparation analyze the influence of the type of treatment technique on treatment outcome, but do not address the problem of errors in the transfer from CT to simulator (4,7,17).

After constructing this "missing link" between a planning CT scan and localization x-ray film, we were able to evaluate the possible clinical importance of simulation errors. To study the influence on local control and side effects of potential beam positioning errors at the stage of simulation, we chose maxillary sinus tumors for a number of reasons. First, many radiation treatment techniques exist for these tumors, indicating the complexity of their irradiation. Second, these tumors have a high local recurrence rate, ranging between 20% and 70%, and partly depending on the treatment technique used (10,11,19). The highest local control rates are achieved by multimodality therapy in which high doses of radiation play an impor-

tant role. Any improvement in radiation quality might therefore result in a better treatment outcome, as shown by Kondo and Tsujii (8,9,23). They clearly showed that the introduction of CT scanning in the treatment of maxillary sinus tumors leads to higher local control and survival rates, probably due to a better target delineation. Finally, maxillary sinus tumors were used as a first test site because of the complexity of the treatment simulation procedure, due to the large amount of anatomical structures that may serve as a (mis)lead during simulation. We deliberately did not define an extra margin around the clinical target volume to correct for daily beam positioning errors, because we wanted to evaluate the influence of simulation errors only. This is in contrast to daily practice where a margin is chosen for daily beam and patient positioning errors without taking possible beam-positioning errors during simulation into account.

The results of our analysis are very much according to the clinical results of radiotherapy for maxillary sinus tumors. The beam positioning errors made during simulation were unexpectedly high and, in the DVH and TCP analysis, appear to be of great clinical importance. All patients suffer more or less from a partial geographical tumor miss due to simulation inaccuracy. This is reflected in the mean TCP value, which is about one-third of the maximal TCP (78%) when simulating completely according to the computer-assessed plan. We do, however, like to stress that one cannot give any absolute value to these TCP data because little information exists on a clear dose effect on local control, due to the enormous variation in treatment techniques (2,11,13). Our data show very clearly that simulation beam-positioning errors are of clinical importance and should be taken into account when defining a planning volume if anatomical landmarks are used during simulation. The additional margin that should be chosen for this reason will probably vary according to tumor site and the treatment technique used. For instance, a partial geographical miss due to simulation beam-positioning errors when using anatomical structures as a reference is very unlikely in T1 laryngeal cancer. In contrast, conformal beam therapy for a brain tumor with complex beam settings is more likely to give a significant partial geographical miss when using virtually absent anatomical landmarks as a simulation guide.

With regard to the normal tissues it became clear that the NTCP value of the spinal cord in none of the patients reached above the tolerance level. The contralateral eye lens, however, was shown to be irradiated to a level above tolerance in patients with the largest beam-positioning errors. One might argue that these patients will not develop any lens complication due to a local tumor, which will certainly recur early because these patients were shown to have the largest geographical miss. Interestingly, the ipsilateral eye lens which was planned to be irradiated above its tolerance level (NTCP for the computer plan equaled 1), was apparently spared in two patients, again due to simulation beam-positioning errors. If one takes into account the higher probability for local recurrence after protecting the ipsilateral eye lens by a block, one could seriously question the use of these lens blocks (2,21,23). As a result of our study, it can be concluded that these blocks should be positioned with the highest care, preferably checked daily on a clinical basis.

5 Conclusions

The planning target volume for maxillary sinus tumors should include an additional margin to correct for possible partial geographical misses due to simulation errors caused by the transfer from the CT to the simulator. This error is likely to be smallest when easy to use, objective, and external references (such as our noninvasive external localization frame) serve as a guide for beam positioning during simulation. If anatomical landmarks are used during the entire process of CT scanning, treatment planning, and simulation as a reference, this extra margin will considerably enlarge the treated planning target and thereby the treated volume. As a result, from our study, we advise that the use of anatomical landmarks during simulation be reduced to keep the margin around the clinical tumor volume (defined to account for set-up uncertainties) at a magnitude such that surrounding critical structures can still be spared from high radiation doses.

The possible clinical relevance of simulation errors in tumor sites other than the maxillary sinus is the issue of investigations currently being undertaken at our institute.

Acknowledgements: The authors gratefully acknowledge Ms. Inge Dijkstra for assistance in preparing the manuscript and Dick van Sluis for his never-ending patience in improving the noninvasive external localization frame.

References

1. Burman C, Kutcher GJ, Emami B, Goitein M. Fitting of normal tissue tolerance data to an analytic function. *Int J Radiat Oncol Biol Phys* 1991;21:123-135.
2. Bush SE, Bagshaw MA. Carcinoma of the paranasal sinuses. *Cancer* 1982;50:154-158.
3. Emami B, Lyman J, Brown A, Coia LR, Goitein M, Munzenrider JE, Shank B, Solin LJ, Wesson M. Tolerance of normal tissue to therapeutic irradiation. *Int J Radiat Oncol Biol Phys* 1991;21:109-122.
4. Gaspar LE, Fisher BJ, Macdonald DR, LeBer DV, Halperin EC, Schold Jr. SC, Cairncross JG. Supratentorial malignant glioma: Patterns of recurrence and implications for external beam local treatment. *Int J Radiat Oncol Biol Phys* 1992;24:55-57.
5. Goitein M. The probability of controlling an inhomogeneously irradiated tumour. In: Zink S., ed. *Evaluation of treatment planning for particle beam radiotherapy*. Bethesda: National Cancer Institute; 1987: 1-13.
6. Huizenga H, Levendag PC, De Porre PMZR, Visser AG. Accuracy in radiation field alignment in head and neck cancer: A prospective study. *Radiother Oncol* 1988;11:181-187.
7. Kinzie JJ, Hanks GE, Maclean CJ, Kramer S. Patterns of care study: Hodgkin's disease relapse rates and adequacy of portals. *Cancer* 1983;52:2223-2226.
8. Kondo M, Horiuchi M, Inuyama Y, Dokiya T, Tsutsui T, Iwata Y, Endo M, Hashimoto T, Kunieda E, Hashimoto S. Value of computed tomography for radiation therapy of tumors of the nasal cavity and paranasal sinuses. *Acta Radiol Oncol* 1983;22(Fasc. 1):3-8.
9. Kondo M, Horiuchi M, Shiga H, Inuyama Y, Dokiya T, Takata Y, Yamashita S, Ido K, Ando Y, Iwata Y, Hashimoto S. Computed tomography of malignant tumors of the nasal cavity and paranasal sinuses. *Cancer* 1982;50:226-231.
10. Kondo M, Ogawa K, Inuyama Y, Yamashita S, Tominaga S, Shigematsu N, Nishiguchi I, Hashimoto S. Prognostic factors influencing relapse of squamous cell carcinoma of the

- maxillary sinus. *Cancer* 1985;55:190-196.
11. Korzeniowski S, Reinfuss M, Skolyszewski J. The evaluation of radiotherapy after incomplete surgery in patients with carcinoma of the maxillary sinus. *Int J Radiat Oncol Biol Phys* 1985;11:505-510.
 12. Kutcher GJ, Burman C, Brewster LJ, Goitein M, Mohan R. Histogram reduction method for calculating complication probabilities for three-dimensional treatment planning evaluations. *Int J Radiat Oncol Biol Phys* 1991;21:137-146.
 13. Marks JE, Bedwinek JM, Lee F, Purdy JA, Perez CA. Dose-response analysis for nasopharyngeal carcinoma. *Cancer* 1982;50:1042-1050.
 14. Miralbell R, Crowell C, Suit HD. Potential improvement of three dimension treatment planning and proton therapy in the outcome of maxillary sinus cancer. *Int J Radiat Oncol Biol Phys* 1992;22:305-310.
 15. Munzenrider JE, Brown AP, Chu JCH, Coia LR, Doppke KP, Emami B, Kutcher GJ, Mohan R, Purdy JA, Shank B, Simpson JR, Solin LJ, Urie MM. Numerical scoring of treatment plans. *Int J Radiat Oncol Biol Phys* 1991;21:147-163.
 16. Niël CGJH. A reference frame designed to use external numeric references during simulation for tumours located in the head. *Br J Radiol* 1993;66:927-929.
 17. Perez CA, Stanley KE, Grundy G, Hanson W, Rubin P, Kramer S, Brady LW, Marks JE, Perez-Tamayo R, Brown GS, Concannon JP, Rotman M. Impact of irradiation technique and tumor extent in tumor control and survival of patients with unresectable non-oat cell carcinoma of the lung. *Cancer* 1982;50:1091-1099.
 18. Roa WHY, Hazuka MB, Sandler HM, Martel MK, Thornton AF, Turrisi AT, Urba S, Wolf GT, Lichter AS. Results of primary and adjuvant CT-based 3-dimensional radiotherapy for malignant tumors of the paranasal sinuses. *Int J Radiat Oncol Biol Phys* 1994;28:857-865.
 19. Sakata K, Aoki Y, Karasawa K, Nakagawa K, Hasezawa K, Muta N, Terahara A, Onogi Y, Sasaki Y, Akanuma A. Analysis of the results of combined therapy for maxillary carcinoma. *Cancer* 1993;71:2715-2722.
 20. Sato Y, Morita M, Takahashi H, Watanabe N, Kirikae I. Combined surgery, radiotherapy and regional chemotherapy in carcinoma of the paranasal sinuses. *Cancer* 1970;25:571-579.
 21. Shibuya H, Horiuchi J, Suzuki S, Shioda S, Enomoto S. Maxillary sinus carcinoma: Result of radiation therapy. *Int J Radiat Oncol Biol Phys* 1984;10:1021-1026.
 22. Thornton Jr. AF, Ten Haken RK, Gerhardsson A, Correll M. Three-dimensional motion analysis of an improved head immobilization system for simulation, CT, MRI, and PET imaging. *Radiother Oncol* 1991;20:224-229.
 23. Tsujii H, Kamada T, Arimoto T, Mizoe J, Shirato H, Matsuoka Y, Irie G. The role of radiotherapy in the management of maxillary sinus carcinoma. *Cancer* 1986;57:2261-2266.
 24. Tsujii H, Kamada T, Matsuoka Y, Takamura A, Akazawa T, Irie G. The value of treatment planning using CT and an immobilizing shell in radiotherapy for paranasal sinus carcinomas. *Int J Radiat Oncol Biol Phys* 1989;16:243-249.
 25. Verhey LJ, Goitein M, McNulp J, Munzenrider JE, Suit HD. Precise positioning of patients for radiation therapy. *Int J Radiat Oncol Biol Phys* 1982;8:289-294.

ADDENDUM D

TREATMENT PORTALS FOR ELECTIVE RADIOTHERAPY OF THE NECK — AN INVENTORY IN THE NETHERLANDS

Radiotherapy and Oncology. 1997;43:81-86.

Peter Nowak, Erik van Dieren, John van Sörnsen de Koste,
Henry van der Est, Ben Heijmen, Peter Levendag

Department of Radiation Oncology, Dr. Daniel den Hoed Cancer Center/University Hospital
Rotterdam-Dijkzigt, Groene Hilledijk 301, 3075 EA, Rotterdam, The Netherlands

Treatment portals for elective radiotherapy of the neck – an inventory in The Netherlands

Purpose: To assess the variation in and the three-dimensional dosimetric consequences of treatment portals for elective neck irradiation.

Materials and Methods: Radiation oncologists (n=16) from all major Head and Neck Co-operative Groups in The Netherlands (n=11) were asked to delineate treatment portals on a lateral and an anterior simulation film in case of elective neck irradiation for a T3N0 tumor of the supraglottic larynx and a T2N0 tumor of the mobile tongue. In addition, they had to define their target, i.e. which parts of the neck nodal regions they would choose to irradiate electively for these particular tumor sites. Subsequently, treatment portals were compared and evaluated using CT-data and a 3-dimensional (3D) treatment planning system.

Results: Significant variations were found in the in the shapes and sizes of the applied treatment techniques and portals. Also, among radiation oncologists who elected to irradiate the same lymph node regions, a significant variation in the delineated treatment portals was observed. As a consequence, substantial variations in treated volumes and in calculated normal tissue complication probabilities (NTCPs) for the parotid- and submandibular glands were observed.

Conclusion: For the tumor sites studied there appears to be lack of standardization in the areas of the neck to be irradiated electively. The observed differences may have consequences for the ultimate failure rate and particularly with regard to the side effects, e.g. the degree of xerostomia. It is argued that in the near future a more precise three-dimensional definition on CT of the lymph node regions in the neck might allow for a better standardization of the treatment portals and, in addition, for the development and application of conformal radiotherapy techniques for optimal sparing of the critical normal tissues (e.g. parotid- and submandibular glands) with maximum tumor control probability.

Keywords: Head and neck, Radiotherapy, Treatment portals, Elective radiation

1 Introduction

Elective irradiation of the N0 neck has shown to be effective in eliminating sub-clinical disease (1,6-9). Unfortunately, this treatment is not without morbidity; that is, xerostomia is usually experienced because of (partial) inclusion of the (major) salivary glands in the treatment portals (10).

The purpose of the present study was to assess the variation in the routinely applied treatment portals in case of elective neck irradiation. This was done through a nationwide inventory. To study the 3D consequences of the observed variation in treatment portals, the portals were compared and evaluated using CT-scans and a 3D treatment planning system.

In a recent study, Leslie and Dische showed that the radiation-induced reduction in pre-treatment parotid salivary flow is dependent on the percentage of parotid gland volume irradiated (5). For this reason, in this study special attention is also given to the potential consequences of the observed variations in the cranial and ventral boundaries of the applied lateral parallel opposed portals.

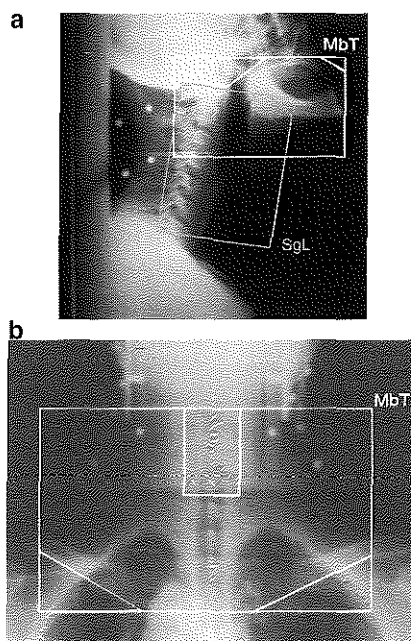


Figure 1. Right lateral (a) and anterior (b) simulation film with the portals of the first responding radiation oncologist for a T3N0 supraglottic larynx carcinoma (SgL) and a T2N0 mobile tongue carcinoma (MbT).

2 Materials and Methods

This study is based on a commonly used radiation technique in head and neck cancer, that is, the use of lateral parallel opposed portals with or without an abutted low-anterior radiation field. For this purpose, right lateral- and anterior simulation films and a set of CT-slices of a patient, who was previously treated in our department, were used. Both the simulation films and the CT-scans were made in treatment position. The films were taken using a focus-to-film distance of 145 cm; CT slices were obtained from the base of skull down to the clavicles, using a slice distance of 5 mm.

Copies of the simulation films were sent to 16 experienced head and neck radiation oncologists in 11 departments of radiation oncology in The Netherlands. In an accompanying letter the radiation oncologists were asked to participate in a small survey regarding the size and shape of neck portals used for two different tumor sites, supposing that the local treatment policy was to electively irradiate (parts of) the neck. So, the question posed was really two-fold: firstly, to delineate the treatment portals covering neck (and primary tumor), assuming that this patient had a T3N0 carcinoma of the supraglottic larynx or a T2N0 carcinoma of the mobile tongue. Secondly, to indicate which parts of the neck, i.e. high- (upper)-, mid-, lower-jugular, and posterior neck lymph node regions they intended to irradiate electively for these two clinical indications. As the investigation was focused at studying the consequences of 'routine' radiotherapy treatment techniques com-

monly used in any radiation therapy department treating head and neck cancer patients, participating radiation oncologists were not given access to the CT-data of the patient in treatment position at the time of delineating the treatment portals.

All treatment portals were imported in the 3D planning system CADPLAN (Varian-Dosetek, Finland). Dose distributions were calculated using the CT-data of the patient in treatment position, beam data of a 6 MV photon beam and a pre-scribed dose of 46 Gy. The dose applied by the lateral parallel opposed portals was prescribed to the midplane of the patient; in case of an anterior portal for irradiation of the lower part of the neck, this dose was prescribed at a depth of 3 cm. Dose-volume histograms (DVHs) for the body outline were generated to calculate treated volumes, defined as the volumes absorbing more than 95% of the prescribed dose (3). In addition, using the DVHs of the parotid and submandibular glands, NTCPs were calculated (2,4). For calculation of the NTCPs of the submandibular

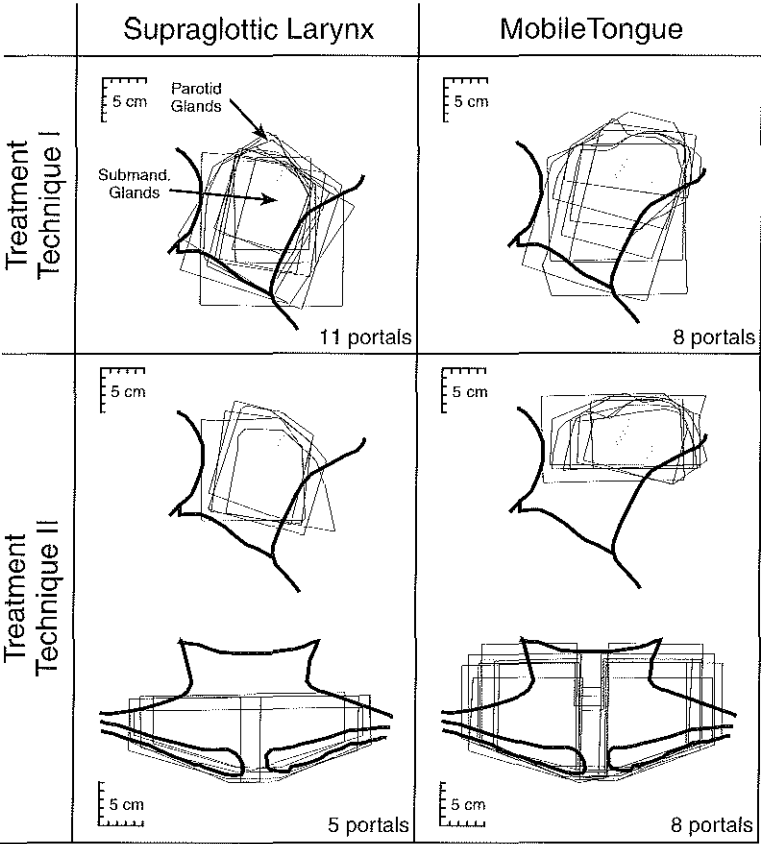


Figure 2. The delineated treatment portals of all participating radiation oncologists superimposed in beam's eye view on the patient anatomy, i.e. the patient outline and the submandibular and parotid glands for the lateral portals and the patient outline and the clavicles for the anterior portals. Technique I: lateral parallel opposed portals only. Technique II: lateral parallel opposed portals in combination with an anterior portal. The scale (5 cm) relates to a distance of 100 cm from the focus.

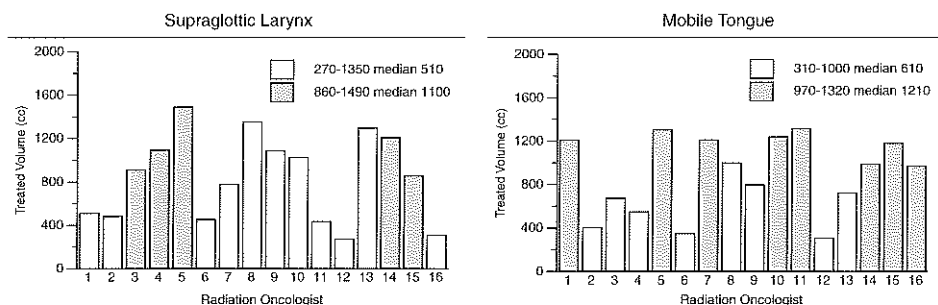


Figure 3. Treated volumes, i.e. volumes absorbing more than 95% of the prescribed dose for Techniques I (open bars) and Technique II (closed bars), in combination with minimum, maximum and median values.

glands (not specified in the parameter list of Burman et al.), the same parameters as used for the parotid glands were implemented (2).

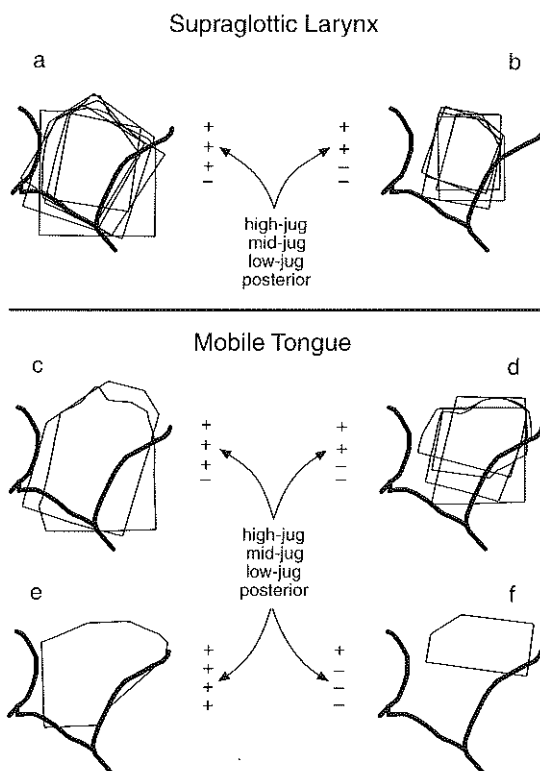


Figure 4. Lateral parallel opposed treatment portals of Figure 2 (Technique I only), grouped by similar treatment intention (see also Table 1). In each panel, the inclusion (+) or exclusion (-) of high-, mid-, lower-jugular, and posterior lymph node regions is indicated. The scale (5 cm) relates to a distance of 100 cm from the focus.

3 Results

As an example of the generally used treatment portals, in Figure 1, the delineated portals of the first responding radiation oncologist are shown. In this case, for the T3N0 supraglottic larynx carcinoma (SgL), only lateral parallel opposed portals are used (Technique I). For the T2N0 mobile tongue carcinoma (MbT), lateral parallel opposed portals are used in combination with an anterior portal for the lower part of the neck with shielding of the larynx (Technique II).

In Figure 2, the treatment portals of all participating radiation oncologists, subdivided according to treatment site and applied treatment technique, are shown in beam's eye view. For both techniques and sites, a large variation in size and shape of the portals can be observed.

The treated volumes resulting from the volumetric calculations are displayed in Figure 3. A substantial range in the treated volumes is observed: for the supraglottic larynx carcinoma a range varying from 270 to 1490 cm³, for the mobile tongue a range varying from 310 to 1320 cm³. Table 1 shows, for all radiation oncologists combined, the target they selected to treat for the two studied tumor sites. For the supraglottic larynx carcinoma, all radiation oncologists apparently elected to irradiate the high- and mid-jugular neck region, with 10 out of 16 irradiating the lower jugular region as well. However, none of the radiation oncologists chose to treat the posterior neck nodes. For the mobile tongue carcinoma a larger variation was found; that is, only the high-jugular nodes (x1), or the high- and mid-jugular nodes (x5), or the high-, mid- and lower-jugular nodes (x8), or all jugular lymph node regions, the posterior nodes inclusive (x2), were irradiated. The high- and mid-jugular nodes were treated by lateral parallel opposed fields; for the irradiation of the

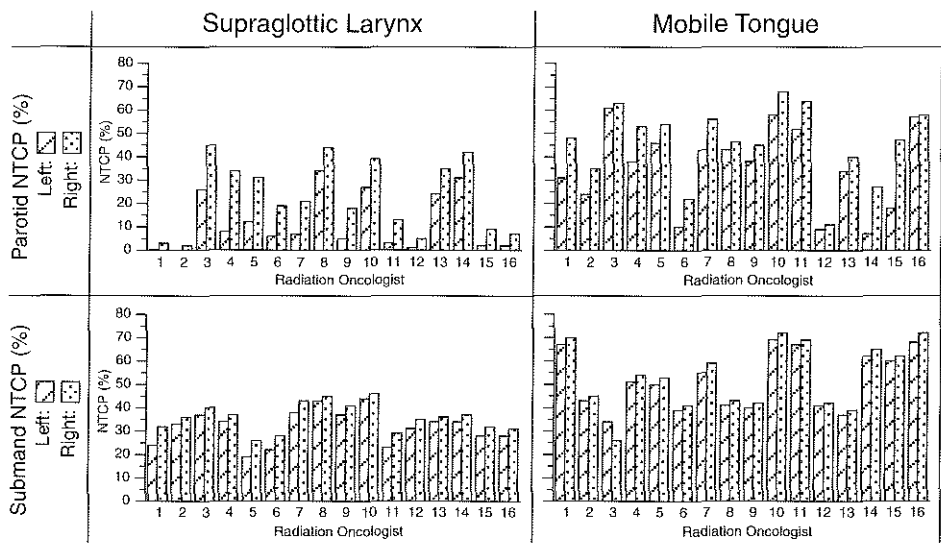


Figure 5. Left and right parotid and submandibular gland NTCPs for a prescribed dose of 46 Gy to the neck.

lower jugular neck nodes, for both primary sites either Technique I or Technique II was apparently used.

In Figure 4 the lateral parallel opposed portals are depicted in case of supraglottic laryngeal carcinoma (panels a and b) or mobile tongue carcinoma (panels c-f) for radiation oncologists using Technique I. The portals were grouped according to the target volume the radiation oncologists had elected to irradiate (Table 1). As is clearly shown by panels a-d, the portals still demonstrate a large variation in shape and size, that is even when the radiation oncologists selected similar targets.

Table 1. Inventory of selected target volumes. An inventory of selected target volumes by 16 radiation oncologists, in case of elective irradiation of T3N0 supraglottic laryngeal carcinoma and T2N0 mobile tongue carcinoma. The radiation oncologists are numbered according to arrival date of response. The proposed treatment technique is indicated with I or II (Technique I: lateral parallel opposed portals only; Technique II: lateral parallel opposed portals in combination with an anterior portal). The intention of the radiation oncologists to irradiate/not to irradiate the four defined lymph node areas (high-, mid-, lower jugular, and posterior) is indicated with + or -.

Carcinoma	Radiation oncologist															
	1	2	3	4	5	6	7	8	9	10	11	12	13	14	15	16
Supraglottic Larynx (T3N0)																
Treatment technique	I	I	II	II	II	I	I	I	I	I	I	I	I	II	II	I
High-jugular	+	+	+	+	+	+	+	+	+	+	+	+	+	+	+	+
Mid-jugular	+	+	+	+	+	+	+	+	+	+	+	+	+	+	+	+
Low-jugular	-	+	+	-	+	-	+	+	+	+	-	-	+	+	+	-
Posterior	-	-	-	-	-	-	-	-	-	-	-	-	-	-	-	-
Mobile Tongue (T2N0)																
Treatment technique	II	I	I	I	II	I	II	I	I	II	II	I	I	II	II	II
High-jugular	+	+	+	+	+	+	+	+	+	+	+	+	+	+	+	+
Mid-jugular	+	+	-	+	+	+	+	+	+	+	+	+	+	+	+	+
Low-jugular	+	-	-	-	+	-	+	+	+	+	+	-	+	+	+	-
Posterior	+	-	-	-	-	-	-	-	+	-	-	-	-	-	-	-

In Figure 2, a substantial variation in the position of the boundaries of the treatment portals at the level of the major salivary glands is seen. Since parotid glands exhibit a large volume effect, a large variation in calculated salivary gland NTCP is found (Figure 5) (2,5). Similar types of observations can be made for the sub-mandibular glands (Figure 5). The NTCPs for the T3N0 supraglottic larynx are on average lower (0%-50%) than for the T2N0 mobile tongue (20-70%).

4 Discussion and conclusions

In this study, large variations in applied treatment portals for elective irradiation of the neck in cancer of the supraglottic larynx or mobile tongue have been found.

To some extent, this stems from apparent disagreement as to which parts of the neck (high-, mid- and lower-jugular, and posterior) are to be irradiated. However, importantly, there are also major variations in the shape and size of the lateral parallel opposed portals selected to treat similar lymph node regions, that is, the anticipated precise location of the high-, mid- and/or lower-jugular lymph node regions seems uncertain. This could result in large variations in the morbidity of the treatment, e.g. degree of xerostomia. In addition, a mismatch between target and treated volume obviously may result, in case of a geographical miss, in an increased failure rate.

Therefore, a standardization of the target volume seems warranted. This applies both to the lymph node regions to be irradiated for a particular primary tumor site in the head and neck, as well as to the exact location (boundaries) of these regions. We feel that the development of a three-dimensional CT target volume definition, based on the already established surgical definitions for lymph node levels I-VI, might solve part of this problem (11,12). Firstly, it allows for an optimal design of treatment portals, provided agreement exists on the lymph node regions to be treated. Secondly, a three-dimensional target volume allows for the development and evaluation of more conformal radiotherapy (CRT) techniques for (elective) neck irradiation. Hence, it may be possible to substantially reduce the occurrence and/or severity of xerostomia resulting from elective radiotherapy of the neck, while maintaining a high tumor control rate. In fact, the establishment of CT definitions of the lymph node regions and development of 3D CRT techniques of the neck is the subject of an ongoing study in our institute.

Acknowledgements: The authors sincerely appreciate the kind co-operation of the radiation oncologists L.E.C.M. Blank, (Academic Medical Center, Amsterdam), F.R. Burlage and W.V. Dolsma (University Hospital Groningen), W.M.H. Eijkenboom and P.P. Jansen (Dr. Daniel den Hoed Cancer Center/University Hospital Rotterdam-Dijkzigt), J.J. de Jager and J.M.A. de Jong (Radiotherapeutic Institute Limburg, Heerlen), J.H.A.M. Kaanders and L.A.M. Pop (Catholic University Hospital, Nijmegen), R.B. Keus and V.J. de Ru (Netherlands Cancer Institute/Antoni van Leeuwenhoek Hospital, Amsterdam), F. Smit (University Hospital Utrecht), C.H.J. Terhaard (Medisch Spectrum Twente, Enschede), P.R. Timmer (Sophia Hospital, Zwolle), R.E. Tjho-Heslinga (University Hospital Leiden), J.M. Tabak (Zeeuws Radiotherapeutic Institute, Vlissingen).

References

1. Barkley HT, Fletcher GH, Jesse RH and Lindberg RD. Management of cervical lymphnode metastases in squamous cell carcinoma of the tonsillar fossa, base of tongue, supraglottic larynx, and hypopharynx. *Am J Surg* 1972;124:462-467.
2. Burman CM, Kutcher GJ, Emami B and Goitein M. Fitting of normal tissue tolerance data to an analytic function. *Int J Radiat Oncol Biol Phys* 1991;21:123-135.
3. International Commission on Radiation Units and Measurements. Prescribing, Recording, and Reporting Photon Beam Therapy (ICRU Report 50). 1993.
4. Kutcher GJ, Burman CM, Brewster LJ, Goitein M and Mohan R. Histogram reduction method for calculating complication probabilities for three-dimensional treatment planning evaluations. *Int J Radiat Oncol Biol Phys* 1991;21:137-146.

5. Leslie MD and Dische S. The early changes in salivary gland function during and after radiotherapy given for head & neck cancer. *Radiother Oncol* 1994;30:26-32.
6. Levendag PC, Sessions RB, Vikram B, Strong EW, Shah JP, Spiro RH and Gerold F. The problem of neck relapse in early stage supraglottic larynx cancer. *Cancer* 1989;63:345-348.
7. Lindberg RD. Distribution of cervical lymph node metastases from squamous cell carcinoma of the upper respiratory and digestive tracts. *Cancer* 1972;29:1446-1449.
8. Mendenhall WM, Million RR and Cassisi NJ. Elective neck irradiation in squamous cell carcinoma of the head and neck. *Head Neck Surg* 1980;3:15-20.
9. Million RR, Cassisi NJ, Mancuso AA, Stringer SP, Mendenhall WM and Parsons, JT. Management of the neck for squamous cell carcinoma. In: *Management of Head and Neck Cancer, A Multidisciplinary Approach*, pp. 75-142. Editors: RR Million and NJ Cassisi. JB Lippincott, Philadelphia PA, 1994.
10. Parsons JT. The effects of radiation on normal tissues of the head and neck. In: *Management of Head and Neck Cancer, A Multidisciplinary Approach*, pp. 245-290. Editors: RR Million and NJ Cassisi. JB Lippincott, Philadelphia PA, 1994.
11. Robbins KT, Medina JE, Wolfe GT, Levine PA, Sessions RB and Pruet CW. Standardizing neck dissection terminology. *Arch Otolaryngol Head Neck Surg* 1991;117:601-605.
12. Shah JP, Strong EW, Spiro RH and Vikram B. Neck dissection: current status and future possibilities. *Clin Bull* 1981;11:25-33.

ABBREVIATIONS

Abbreviations

3D	three-dimensional
AP	antero-posterior
BEV	beam's eye view
C	cord
CC	cranio-caudal
CC-RT	continuous course radiation therapy
CD-i	compact disc interactive
CRT	conformal radiation therapy
CT	computed tomography
CTV	clinical target volume
DVH	dose volume histogram
GTV	gross tumor volume
ICRU	international commission on radiation units
IV	irradiated volume
LL	latero-lateral
MeV	megaelectronvolt
MRI	magnetic resonance imaging
MT	mobile tongue
MV	megavolt
N, N0	TNM classification
ND	neck dissection
NP	nasopharynx
NTCP	normal tissue complication probability
NTD	normalized treatment dose
P	parotid gland
PS	piriform sinus
PTV	planning target volume
PTV-a	planning target volume adjusted
S	submandibular gland
SC	spinal cord
SC-RT	split course radiation therapy
SD	standard deviation
SL	supraglottic larynx
T, T2, T3	TNM classification
TCP	tumor control probability
TV	treated volume
US	ultrasound
USFNAC	ultrasound fine needle aspiration cytology

SUMMARY

SUMMARY
—
SAMENVATTING

Summary

The curability of patients with tumors in the head and neck is dependent, among other factors, on the presence of lymph node metastases in the neck, i.e. the N-stage of the disease. If the lymph nodes are not clinically palpable or detectable by diagnostic means such as CT, MRI scanning or ultrasound investigation (N0 neck), the potential for subsequent development of lymph node metastasis dictates whether the neck should be treated electively. This thesis deals with radiation therapy as a single modality treatment for the N0 neck.

The major side effect of elective neck irradiation is the dry mouth syndrome (xerostomia) due to damage to the salivary glands, with resulting dental caries, swallowing disorders and speech disturbances. In many institutions, elective neck irradiation is the preferred treatment for patients with tumors in the head and neck when the probability of subclinical disease is considered to exceed 10-20%. It is of utmost importance, therefore, to try and reduce the side-effects of radiation therapy.

With the introduction of CT planning systems and the development of 3D conformal radiation therapy, it has become feasible to deliver adequate doses of radiation to the target (neck) whilst, at the same time, saving (parts of) the salivary glands from doses exceeding tolerance. A prerequisite for such techniques is the need for an exact knowledge of the target, i.e. the elective neck, which has to be depicted on every planning CT slice.

The main goal of this thesis was to develop and present a 3D CT definition of the clinical target volume of the clinically negative neck and also demonstrate that this definition allows the development of conformal (3D) radiotherapy techniques which adequately cover the primary tumor and the neck, whilst sparing the major salivary glands. An additional goal was the creation of an interactive compact disc (CD-i) for confirmation of the CT target definition, for studying isodose distributions of 3D radiotherapy techniques, and for educational purposes.

Chapters 2 and 3 describe the background of this study. In Chapter 2, clinical aspects of lymph node involvement of the neck in head and neck tumors are summarized. The different diagnostic methods to detect these lymph nodes are shown, as are the ways to treat the neck electively. It is concluded, as mentioned earlier, that elective treatment of the N0 neck is mandatory when the risk of subclinical disease in the neck is substantial. Fundamental aspects of radiotherapy (e.g. the ICRU-50 recommendations for target definition, dose-response relationships for the primary tumor site and the N0 neck, side effects of elective neck irradiation) are also discussed. A number of basic principles and the expected benefits of conformal radiotherapy are described. A dose-response relationship has been shown for many tumors of the head and neck, i.e., suboptimal doses of radiotherapy are detrimental for clinical outcome. Certain primary tumors, e.g. piriform sinus tumors, can only be adequately irradiated using conformal radiotherapy techniques. A prerequisite for the clinical use of these sophisticated conformal techniques is good quality assurance. The importance of verification of patient positioning with portal imaging techniques, in order to minimize patient setup errors during a treatment course is stressed. Some of the subjects in this chapter are further elaborated on in the first three addenda of this thesis. Chapter 3 describes the conventional techniques of

elective radiotherapy of a T2N0 mobile tongue cancer and a T3N0 supraglottic larynx cancer. In this summary of a nationwide study in The Netherlands, it was shown that there was a lack of standardization as to which areas of the neck had to be treated electively for these tumor sites. There was disagreement as to which anatomical regions had to be treated and also with respect to the delineation of the (2D) borders of these anatomical regions. Addendum D gives a full overview the study.

In Chapter 4, the 3D definition of the target of the elective neck on CT is given. As the regional control rates for elective treatment of the neck are comparable for surgery and radiotherapy, the target for both modalities should be similar. Thus, the well established level definition of the Memorial Sloan-Kettering group served as a backbone for the CT target definition. Two anatomical studies were performed to translate soft tissue landmarks, given in a surgical (rotated) position of the head, into easily recognized borders on transversal CT slices. Small adjustments had to be made, mainly because of the different treatment positions of the head. All six levels were translated into six regions. The borders of these regions had to be available on all CT slices. Moreover, the way in which the definition had been accomplished had to be accessible. These demands could be fulfilled by the development of the "Definition Target" and the "Magnified Target" modules on the CD-i.

In Chapter 5, conventional and conformal radiotherapy techniques are compared for two primary tumor sites, i.e. an early-stage nasopharynx and an early-stage supraglottic larynx cancer without detectable neck nodes. Using the definition of the CT target of Chapter 4, the target of the primary tumor and the neck regions to be treated for both sites were delineated on CT. The conventional treatment technique consists of two lateral parallel opposed fields with (nasopharynx) or without (supraglottic larynx) an abutted anterior field. A six-field conformal radiotherapy technique was developed for both primary tumors. Some constraints were imposed upon the conformal technique: firstly, it should be feasible in a busy radiotherapy department. Secondly, the coverage of the target should be comparable or superior to the conventional technique. Finally, the major salivary glands should be spared in such a way that a clinical benefit is expected. Dose-distributions, dose-volume histograms, tumor control probabilities and normal tissue complication probabilities for the conventional and conformal radiotherapy techniques were computed. It was possible to evaluate all data and this was accomplished by the implementation of the "Beam's Eye View" and the "Radiation Therapy" modules on the CD-i. It is concluded that xerostomia can be reduced or avoided with conformal radiotherapy.

The CD-i is obviously a very important element in this thesis as the answers to the questions addressed in the thesis have been implemented on CD-i. Chapter 6 shows the manner in which the data were incorporated on CD-i, how the 3D CT target definition can be verified, and how the data in Chapters 4 and 5 can be studied. As matching of the CT, MRI and anatomical data was performed in the second anatomical study (Chapter 4), MRI data are also available. In addition, frontal and sagittal reconstructions were made for the CT and MRI slices, showing both the regions of the neck and isodose distributions. The CD-i concludes with the "Rationale" slides, which give an overview of the goals of this study and the "Materials and Methods" slides, which describe how the data in Chapters 4 and 5 were accumulated.

A CT target definition for elective irradiation of the neck has been developed and incorporated into a user-friendly CD-i. The work performed for this thesis indicates that a reduction in radiation morbidity (in particular, the dry mouth syndrome) is feasible. This CD-i (thesis) will hopefully provide a strong foundation for the conduct of clinical trials of conformal radiotherapy in head and neck cancer.

Samenvatting

De genezing van patiënten met tumoren in het hoofd-halsgebied hangt, naast andere factoren, af van de aanwezigheid van lymfekliermetastasen in de hals, d.w.z. van het N-stadium van de ziekte. Indien de lymfeklieren klinisch niet palpabel of detecteerbaar zijn met behulp van diagnostische middelen, zoals CT, MRI scanning of echografisch onderzoek (N0 hals), bepaalt de kans op het ontstaan van lymfekliermetastasen of de hals electief behandeld dient te worden. Dit proefschrift gaat over radiotherapie van de hals (N0) als enige behandelingsmodaliteit.

De belangrijkste bijwerking van electieve bestraling van de hals is het "droge mond syndroom" (xerostomie) ten gevolge van beschadiging van de speekselklieren, met als gevolg tandbederf, slikstoornissen en spraakstoornissen. In veel instituten is electieve bestraling van de hals de voorkeursbehandeling, indien de kans op subklinische ziekte groter geschat wordt dan 10-20%. Het is daarom van het grootste belang te trachten de bijwerkingen van bestraling te verminderen.

Met de introductie van CT planningssystemen en de ontwikkeling van 3D conformatie-radiotherapie is het haalbaar geworden het doelvolumen adequaat te bestralen, terwijl tegelijkertijd de dosis op (een deel van) de speekselklieren de tolerantiedosis niet te boven gaat. Voor zulke technieken is een exacte kennis van het doelvolumen, d.w.z. de electieve hals, vereist, en dient dit op iedere plannings-CT-coupe afgebeeld te worden.

Het voornaamste doel van dit proefschrift was de ontwikkeling en presentatie van een 3D CT definitie van het klinische doelvolumen (clinical target volume) van de klinisch negatieve hals, alsook om aan te tonen dat het met deze definitie mogelijk is conformatie (3D)-radiotherapietechnieken te ontwikkelen, die de primaire tumor en de hals adequaat bestralen, met sparing van de grote speekselklieren. De creatie van een interactieve compact disc (CD-i) was een extra doel, om de CT-definitie van het doelvolumen te bevestigen, isodoseverdelingen van 3D-radiotherapietechnieken te bestuderen, en als leermiddel.

De hoofdstukken 2 en 3 beschrijven de achtergrond van deze studie. In hoofdstuk 2 worden de klinische aspecten van halslymfeklieren bij hoofd-halstumoren samengevat. De verschillende diagnostische middelen om deze lymfeklieren te detecteren worden getoond, evenals de manieren om de hals electief te behandelen. De conclusie luidt, zoals eerder vermeld, dat electieve behandeling van de N0 hals aangewezen is, indien de kans op subklinische ziekte substantieel is. Fundamentele aspecten van de radiotherapie worden besproken (bijv. de ICRU-50 aanbevelingen voor de definitie van het doelvolumen, dosis-responsrelaties voor de primaire tumor en de N0 hals, bijwerkingen van electieve bestraling van de hals), evenals een aantal basisprincipes en de verwachte voordelen van conformatie-radiotherapie. Een dosis-responsrelatie is aangetoond voor vele tumorsoorten in het hoofd-halsgebied, d.w.z. niet-optimale bestralingsdoses hebben een nadelige invloed op het klinische resultaat. Bepaalde tumoren, zoals tumoren uitgaande van de sinus piriforme, kunnen alleen met conformatie-radiotherapietechnieken afdoende worden bestraald. Goede kwaliteitsbewaking is een noodzakelijke voorwaarde voor het klinisch gebruik van deze geperfectioneerde conformatietechnieken. Het belang van controle van de patiëntpositionering met behulp van portal

imaging technieken, om instellingsfouten gedurende de bestralingen te voorkomen, wordt onderstreept. Op sommige van deze onderwerpen wordt verder ingegaan in de eerste drie bijlagen bij dit proefschrift. Hoofdstuk 3 geeft een beschrijving van de conventionele technieken bij de electieve bestraling van een T2N0 carcinoom uitgaande van het beweeglijke deel van de tong en van een T3N0 carcinoom uitgaande van het bovenste gedeelte van het strottehoofd. In deze samenvatting van een in Nederland uitgevoerde nationale studie werd aangetoond dat bij deze tumorlocaties niet standaard was vastgelegd welke gebieden in de hals electief behandeld dienen te worden. Er was geen overeenstemming over de te behandelen anatomische gebieden, noch over de begrenzing van deze gebieden. Bijlage D geeft een volledig overzicht van de studie.

In hoofdstuk 4 wordt de 3D-definitie van het doelvolumen van de electieve hals op CT gegeven. Aangezien de controlepercentages voor electieve behandeling van de hals voor chirurgie en radiotherapie vergelijkbaar zijn, dient het doelvolumen voor beide behandelingsmodaliteiten gelijk te zijn. Derhalve heeft de gevestigde "level"-definitie van de Memorial Sloan-Kettering groep als basis voor het doelvolumen op CT gediend. Om markeringen in de weke delen, weergegeven in een chirurgische (gedraaide) positie van het hoofd, te vertalen naar gemakkelijk te herkennen grenzen op transversale (dwarse) CT-opnamen, werden twee anatomiestudies verricht. Met name de verschillende behandelingsposities van het hoofd maakten kleine aanpassingen noodzakelijk. Alle zes "levels" werden vertaald naar zes regio's ("regions"). De grenzen van deze regio's moesten op alle CT-opnames beschikbaar zijn. Bovendien moest de manier waarop de definitie tot stand was gekomen, begrijpelijk zijn. Aan deze voorwaarden kon worden voldaan door het ontwikkelen van de modules "Definition Target" en "Magnified Target" op de CD-i.

In hoofdstuk 5 worden conventionele en conformatie-radiotherapietechnieken vergeleken voor twee primaire tumorlocaties, nl. een carcinoom uitgaande van de neuskeelholte en een carcinoom uitgaande van het bovenste deel van het strottehoofd zonder detecteerbare halslymfeklieren (beide in een vroeg stadium van de ziekte). Gebruikmakend van de CT-definitie van het doelvolumen uit hoofdstuk 4, werden het doelvolumen van de primaire tumor en de te behandelen gebieden in de hals voor beide zijden vastgelegd op CT. De conventionele bestralingstechniek bestaat uit twee laterale, parallel opponerende bundels met (neuskeelholte) en zonder (strottehoofd) een aangrenzend voorste veld. Voor beide primaire tumoren werd een zes-velden conformatie-radiotherapietechniek ontwikkeld. De conformatietechniek moest aan een aantal voorwaarden voldoen: ten eerste moet de techniek uitvoerbaar zijn binnen een drukke radiotherapie-afdeling. Ten tweede moest de behandeling van het doelvolumen gelijkwaardig zijn aan of zelfs beter dan de conventionele techniek. Tenslotte moesten de grote speekselklieren zodanig gespaard worden dat een goed klinisch resultaat verwacht kan worden. Voor zowel de conventionele als de conformatie-radiotherapietechnieken werden dosisdistributies, dosis-volumehistogrammen, kansen op tumorcontrole en op normale-weefselcomplicaties berekend. Alle gegevens dienden geëvalueerd te kunnen worden, hetgeen mogelijk was door te voorzien in de modules "Beam's Eye View" en "Radiation Therapy" op CD-i. De conclusie luidt dat xerostomie met conformatie-radiotherapie verminderd of zelfs vermeden kan worden.

De CD-i is duidelijk een zeer belangrijk onderdeel van dit proefschrift, aangezien de antwoorden op de vragen in dit proefschrift op de CD-i zijn terug te vinden. Hoofdstuk 6 toont de wijze waarop de gegevens zijn verwerkt op CD-i, hoe de 3D CT-definitie van het doelvolumen kan worden geverifieerd, en hoe de gegevens van hoofdstukken 4 en 5 kunnen worden bestudeerd. Aangezien de CT-, MRI- en anatomische gegevens in de tweede anatomiestudie werden gekoppeld (hoofdstuk 4), zijn ook MRI-gegevens beschikbaar. Bovendien werden er frontale en sagittale reconstructies gemaakt van de CT- en MRI-opnames, die zowel de te behandelen regio's in de hals als de isodoseverdelingen laten zien. De CD-i laat tenslotte de dia's "Rationale" zien, die een overzicht geven van de doelen van deze studie en de dia's "Materials and Methods", die beschrijven hoe de gegevens in hoofdstukken 4 en 5 werden verzameld.

Een CT-definitie van het doelvolumen voor electieve bestraling van de hals werd ontwikkeld en op een gebruikersvriendelijke CD-i verwerkt. Het werk dat ten behoeve van dit proefschrift werd verricht, laat zien dat een vermindering van de stralingsbijwerkingen (met name van het "droge mond syndroom") haalbaar is. Hopelijk zal deze CD-i (dit proefschrift) een sterke basis vormen voor het uitvoeren van klinische studies met conformatie-radiotherapie bij kanker in het hoofd-halsgebied.

ACKNOWLEDGMENTS

Acknowledgments

This thesis is part of an on-going research project at the Daniel den Hoed Cancer Center / University Hospital Rotterdam-Dijkzigt on the development of conformal radiotherapy of cancer in the head and neck.

I am grateful to all members of the head and neck conformal radiotherapy group. Many thanks are expressed to: Peter Levendag, a stimulating promotor and project leader, with whom I had “heavy” discussions regarding the CT target definition; Erik van Dieren, who processed most of the images on the CD-i and developed many treatment plans; John van Sörnsen de Koste, who was involved in the anatomical studies and developed many treatment plans; Henrie van der Est, for developing many treatment plans; Oda Wijers, for testing and discussing the CT target definition; Ben Heijmen, for the many discussions.

I would like to thank the members of the promotion committee for reviewing the manuscript, particularly, professor van der Klauw for his valuable suggestions for improving the CD-i and on his critical review of the manuscript.

I would like to acknowledge my colleagues who provided crucial support in the following aspects. For the anatomical studies: Cees [preparaat] Meeuwis, Cees [Black en Decker] Entius, Hans [flitsend] Vuik, Theo [the mask] Klein; for the CT and MRI imaging: Rene [Hein] Kruijt, Arie [tomo] Munne, Peter [magnetisch] Kappert, Deni Kraus; for testing the CT target definition: Charles [tekenaar] Niël; for the development of the CD-i: Andre [C++] Rasenberg, Marcel [330 m/s] Maassen, Yvonne [in the picture] Mullink; for linguistic corrections of this thesis: Suresh [E-E] Senan; for the secretarial work: Pauline [fotomodel] Roodenburg, Wendy [rechter hand] Smit, Inge [E-N] Dijkstra; for allowing me to spend time on this thesis: the radiation oncologists of the Daniel den Hoed Cancer Center / University Hospital Rotterdam-Dijkzigt.

Last but not least, I would like to thank Jacoba for her neverending support.

CURRICULUM VITAE

Curriculum Vitae

Peter J.C.M. Nowak was born on January 7th, 1953 in Sittard, The Netherlands. After high school ('Gymnasium β ') in Heerlen, he studied physics, chemistry and mathematics at the University of Amsterdam from 1971 until 1977. He graduated cum laude ('doctoraal examen') on November 9th, 1977 in experimental physics on the subject of 'Rotational predissociation of molecular ions' (project leader: Prof. J. Los, Ph.D.). From 1974 to 1978 he worked at the FOM-institute ('Fundamental Research on Matter') for atomic and molecular physics in Amsterdam (chairman: Prof. J. Kistemaker, Ph.D.).

In 1978 he commenced his study in medicine at the University of Amsterdam and graduated ('artsexamen') on February 2nd, 1986. Prior to his residency in radiation oncology, he worked from September 1988 until November 1989 at the faculty of radiobiology in Groningen (chairman: Prof. A.W.T. Konings, Ph.D.). From 1989 to 1994, he was resident in radiation oncology at the Dr. Daniel den Hoed Cancer Center in Rotterdam (chairman: Prof. P.C. Levendag, M.D. Ph.D.). During this period he followed a fellowship of five months in stereotactic radiotherapy/radiosurgery at the department of radiation oncology of the University of San Francisco (UCSF, chairman: Prof. T. Phillips, M.D. Ph.D.).

Since May 1st, 1994 he has held the appointment of radiation oncologist at the University Hospital Rotterdam/Daniel den Hoed Cancer Center.

